JMR

JOURNAL OF MARITIME RESEARCH

Spanish Society of Maritime Research

VOL.II N.1

APRIL 2005

JMR
JOURNAL OF MARITIME RESEARCH

UNIVERSITY OF CANTABRIA

Escuela Técnica Superior de Náutica
c/ Gamazo nº1, 39004 SANTANDER
Telfno (942) 201362; Fax (942) 201303
e-mail: info.jmr@unican.es
http://www.jmr.unican.es

Layout: JMR

Printed bay: Gráficas Calima

ISSN: 1697-4840

D. Legal: SA-368-2004

CONTENTS

Journal of Maritime Research, Vol. II. No. 1, pp. 3–4, 2005

ISSN: 1697-4840

The crew-members of the future

Today's society is immersed in a process of automatisation of tasks which were traditionally assigned to human beings. This automatisation affects all stages of the process, from theory to design and construction. Perhaps the diversity of the fields which it takes in is so great because of the transversal nature of automatisation, allowing its application in all of these fields. In any case, the degree of maturity attained at present in this discipline is great indeed. Furthermore, its potential for development is apparently endless. There are also economic motives which drive and promote this process. One of the most strategically important activities in business production is undoubtedly the development of technology, since this improves the efficiency of companies and lowers their costs.

Perhaps the continuous development of research into artificial intelligence and other parallel fields will allow us to come ever closer to the visions proposed by science fiction. For technological and economic reasons, some people think that the future may arrive at any moment, while some others think that it is already here. People talk about the smaller crews of the ships of the future but there already exist ships that cross the oceans operated by only six crew members. What will the ship of the future be like? Of course, everything would seem to point to the fact that it will be totally automated, but how many crew members will it have?

I recently read a manual from a course in Oxford which referred to the future of life on board ship. Its author, probably with some irony, made it clear how the ship of the future would be manned:

The crew was made up of just two members. A captain and a dog. The captain's work was to feed the dog (one might add, to formalise all the paperwork on commercial aspects, safety and quality). The dog's work was to bite the captain whenever he touched any piece of machinery.

The ways in which science can alter the relation between capital and work, as we know them today, would seem to have no limits. Everything is possible, the problem is when? It is very difficult to predict when automisation will reach the point where a man will be able to share his work with his most faithful friend. Whatever the case, the range of possibilities is enormous and means constantly taking on new challenges. In this sense, the scientific community is constantly responding to these challenges, developing lines of research in different spatial and sectorial areas.

The first organisation that should be mentioned in this context is, of course, the Institute of Electrical and Electronic Engineers (IEEE), an organisation present in some 170 countries, dedicated to theoretical and empirical advances in electrical, electronic and information engineering.
A secondly organisation that plays an immensely important role is the Ocean Engineering Society (OES), which helps to achieve the aims of the IEEE in the maritime environment, collaborating in advances in the theory, practice and accessibility of oceanographic engineering. This society currently includes an emerging and highly promising group of researchers from the Spanish Chapter of the OES.

In this context, Spanish researchers in the area of "Automisation in the Marine Sector" and others belonging to the Spanish division of the OES have contributed decisively to the elaboration of the present issue of our review.

The Journal of Maritime Research, always with the aim of contributing to the advancement, development and diffusion of research in the maritime sector thus embarks on a new adventure with the present special issue on "Naval Automisation", We hope to continue to constitute a meeting point to discuss the maritime sector from a multidisciplinary viewpoint. We believe that, on this first voyage, the aims have been achieved thanks mainly to the illusion and hard work of all of those involved in it.

Carlos A. Pérez Labajos
Editor

Journal of Maritime Research, Vol. II. No. 1, pp. 5-7, 2005

ISSN: 1697-4840

Automation in marine systems

This special issue on automation in marine systems includes 6 papers of different groups that took part in the thematic network AUTOMAR (Automation in the maritime sector). AUTOMAR is a special action of the Ministry of Science and Education in order to form groups from different institutions (universities and research centers) whose members are interested in control theory, robotics, and artificial intelligence and their applications to maritime activities.

Before introducing the papers in this Special Issue it is useful to briefly describe the background to AUTOMAR. As stated above, the main sponsor of AUTOMAR was the Ministry of Science and Education of Spain. Under the auspices of CEA, the Spanish committee of IFAC (International Federation of Automatic Control), a workshop on Automation and Marine Systems was held on November 24, 2004 at the CSIC ("Consejo Superior de Investigaciones Científicas", Spanish Council for Scientific Research). This workshop was conceived as a meeting place for professionals from universities and all branches of industry who are interested in research and development as well as technological innovation in the maritime sector. The conference represents the culmination of a series of previous meetings held in Santander, Barcelona, El Ferrol and Cádiz. A book (Aranda et al., 2004) was published with a collection of chapters about the works of each group. In the meeting, we planned a special issue in relation with this workshop.

The aim of this issue is to present a panoramic vision of the activities of the research groups working in Spain in the field of Automation and Control of

Naval and Marine Systems at the present time. Our goal is to diffuse information about their work to all actors in this strategic sector in order to promote further research and cooperation not only within Spain but also with groups from the rest of Europe.

Six papers about robots, modelling, simulation and control was chosen for this issue.

The first paper, Armada et al. "On the Design and development of climbing and walking robots for the maritime industries" gives an overview of the development of mobile robots (climbing and walking) with examples taken from the maritime industries applications, coming mostly from the experience of the Industrial Automation Institute of the Spanish Council for Scientific Research (IAI-CSIC).

The second paper, Antich et al. "A PFM-based control architecture for a visually guided underwater cable tracker to achieve navigation in troublesome scenarios" shows a architecture of control based on Potential Field Methods for visually guiding an Autonomous Underwater Vehicle to detect and track a cable or pipeline laid on the seabed is presented. A simulation environment with a hydrodynamic model of the real GARBI robot has been used.

In "An analysis of models identification methods for high speed crafts" (Aranda et al.) two different approaches of system identification has been proposed in order to analysis and identify models for the heave, pitch and roll dynamics of a high speed craft. The study is focused on a ship advancing at constant mean forward speed with arbitrary heading in a train of regular sinusoidal waves.

The four paper, "Application of a Robust QFT Linear Control Method to the Course Changing Manoeuvering of a Ship" (Rueda et al.) describes a robust controller for the control of the changing of a ship's course by the QFT methodology.

The next paper, Ferreiro et al., "Trends on modelling techniques applied on ship's propulsion system monitoring" shows some aspects about modelling techniques using analytical redundancy usually applied in fault detection, fault isolation, decision making and system recovery in order to achieve fault tolerant control system.

The final paper, Lopez-Piñeiro et al., "Simulation of passengers movement on ship emergencies. Tools for IMO regulations fulfilment" shows the conceptual design, models and user oriented software tools development inside the SIFBUP project. A summary of the main ship evacuation problems, related regulations and different numerical model types for the study of passengers movements are presented.

This special issue gives a representative sample of the breadth of applications and research in the area of automation in marine systems. We would like to express gratitude to the authors and the reviewers for their efforts in making this special issue possible.

Jesús M. De la Cruz
Chairman IEEE-OES Spanish Chapter

Joaquín Aranda
Secretary IEEE-OES Spanish Chapter

Francisco J. Velasco
Tecnical Commitee Coordinator IEEE-OES Spanish Chapter

JMR

Journal of Maritime Research, Vol. II. No. 1, pp. 9–32, 2005

ISSN: 1697-4840

ON THE DESIGN AND DEVELOPMENT OF CLIMBING AND WALKING ROBOTS FOR THE MARITIME INDUSTRIES

M. Armada[1], M. Prieto[1], T. Akinfiev[1], R. Fernández[1], P. González[1], E. García[1], H. Montes[1], S. Nabulsi[1], R. Ponticelli[1], J. Sarria[1], J. Estremera[1], S. Ros[1], J. Grieco[2] and G. Fernandez[2]

ABSTRACT

Modern robotic systems are increasingly powerful in terms of sensor fusion and mobility. Present technological progress allows advanced robots to cope progressively much better also with complex environments such as those which are frequently found in the maritime industries. An overview of the development of mobile robots (climbing and walking) is presented with examples taken from some research projects carried out by the Industrial Automation Institute of the Spanish Council for Scientific Research.

Keywords: Automation, shipbuilding, welding, hull cleaning, climbing and walking robots.

INTRODUCTION

The Automatic Control Department of the Industrial Automation Institute (IAI-CSIC) has been carrying out research and development projects in the field of robotic systems for more than twenty five years. Since late seventies this activity began with the realisation of industrial robots, what provided the research team with a wide experience and reputation in robot kinematics, dynamics, mechanical design, and control systems. After some successful developments in that field, the depart-

1 Instituto de Automática Industrial - CSIC, Arganda del Rey, Madrid, Spain (armada@iai.csic.es)

2 Instituto de Ingeniería, Grupo de Mecatrónica, Caracas, Venezuela

ment focused its interest in the area of robots for hostile/hazardous environments. In these kind of environments it is necessary to carry out a variety of tasks (inspection, manipulation, welding, grinding, etc.), what implies human operators are exposed to hard working conditions. Also there are a great number of potential applications that cannot be performed directly by human operators because of difficulties in reaching working positions in a proper and safe way. This situation yields, in a natural way, to the utilisation of remotely controlled devices, where tele-robots can be considered as the most advanced and promising solutions. Doing so a number of advantages will come: improved working conditions, improved safety, automation of repetitive tasks, and opening the possibility of providing innovative solutions to emerging applications.

However, although many applications can be solved by means of an appropriate tele-manipulator, equipped with the right tools and with the concurrence of the human operator skills, many others cannot be solved in this way due to working position difficult access. The problem of accessing to more or less remote job sites presents major difficulties and prevents automation. There are, reported in the literature, interesting solutions to this situation, for example very long reach manipulators. Other, not less interesting approach is to provide a transport mean for the tele-manipulator. Such a transport mean includes wheeled or tracked vehicles, and more recently, legged-machines (climbing or walking).

Nowadays shipbuilding industry is being forced to adapt its production to new technical specifications, shorter delivery time and new safety regulations, so that the ships have to be built faster, more economically and under better environmental condition for operators. New robotic systems are improving these features. Especially, robot manipulators are helping to enhance the quality of welding, decrease arc time, and avoid operators be exposed to fume concentration. However, current robotic systems cannot accomplish some industrial applications, especially those related with mobility in complex environments. These scenarios appear in some stages of the ship construction such as are the operations in the dry dock, and also in the ship repairing yards in what respects ship cleaning and inspection. In this chapter some solutions are presented dealing with specially tailored climbing and walking robots for the maritime industries. These robotic systems have been mostly developed in the framework of European funded projects.

In the field of shipbuilding there are three main stages in the ship erection process:

— Block's construction in the workshop.
— Transportation of blocks to the dry dock or to the slip-way using cranes and especial vehicles.
— Connection of consecutive blocks in the dry dock or slip-way.

The first activity consists of the construction and assembly of huge ship blocks. This work is performed in highly automated workshops with a relatively

good productivity, which is being increased by current research in this area. After the transportation of the blocks, which is performed in the second stage, the third involves joining two consecutive blocks by welding together all the longitudinal reinforcements and all the vertical bulkheads.

For environmental safety, most ships, especially tankers and bulk carriers are built with a double bottom and double hull so the cargo will not spill out if the hull is breached. This double structure forms cells all over the ship's hull. There are two important welding problems in ship erection: butt-welding in position along the near-flat external hull surface, and butt/fillet welding for joining double hull cells. In the last years IAI-CSIC has been involved in several projects dealing with welding automation in shipbuilding. Three main results are briefly reported in this work: one six-legged and one four-legged climbing robots for butt-welding of ship hull skin, and one robotic system for welding inside the double hull vertical cells (ROWER 2). All robots have been equipped with industrial welding units and special sensors for seam tracking. A fourth climbing robot, this time underwater, intended for sea adherence cleaning and hull inspection will be the subject of the last part of this chapter.

REST 1 CLIMBING ROBOT

The REST 1 climbing robot has six reptile-type legs with three degrees of freedom each one, actuated by dc motors through appropriate gearing. The leg kinematics is of *scara* type, with two rotational articulations and a prismatic one that holds at its end the foot. Feet at the end of legs are provided with special grasping devices based on electromagnets, securing the robot to ferromagnetic-material walls with intrinsic safety. Some degree of compliance has been provided to the feet, by means of an extra passive degree of freedom, so that the robot can adapt itself to a certain extent of surface unevenness. The climbing robot carries on board his control system that consists on an industrial PC that serves as a master for a bunch of slave processors that controls in real time the 18-degrees of freedom. One of the main features is the combination of 6 low-cost/high-performance digital control and 6 power electronic cards (one per leg, each one providing control for 3 joints), specifically developed for this project, and that are the responsible of the just mentioned control of each one of the 18 degrees of freedom of the robot.

The main specifications of the REST 1 climbing robot are:

— Leg number: 6
— Degrees of freedom: 18
— Body frame length: 1100 mm
— Body frame width: 600 mm.
— Robot weight: 220 Kg.
— Robot payload: up to 100 Kg.

Different gaits and control algorithms has been implemented and evaluated. A detail on algorithm preparation is presented in next chapter sections.

The problem of climbing

The displacement of a climbing robot is the result of a co-ordinate motion of its legs. This motion is defined by some climbing gait that reflects specifications such as speed, direction etc. There are two phases clearly differentiated in the contribution of each leg to the robot motion. During the support phase every leg should be able to exert a certain force over the climbing surface, in order to provide the necessary forces to the body allowing moving it according to a predetermined path. Later on, during the transfer phase, the leg should displace toward its next support point in order to re-establish the sequence of motion. Each phase imposes a set of requirements to the leg operation. So, during the support phase the leg must have a great capability of force generation, while in the transfer phase the main requirement is the return speed.

The speed and force demand are straight related with the task to be carried out by the climbing robot as well as by the robot location on its environment. Once a task has been defined, the path is established and must be followed by the robot in its working space. The gait will define the state transitions for every leg. Nevertheless, the leg trajectory during the support phase is determined by the body trajectory. There are an infinite number of these trajectories that can be used to obtain the desired robot motion. In order to simplify this selection some authors do the assumptions that: (1) the reachable range of each foot is a rectangular prism, and the feet ranges take up symmetric positions and, (2) each trajectory symmetrically passes the centre C_i of the plane that is the horizontal projection of the reachable area [1,2]. These assumptions, which are based only on the leg mobility, work well for a walking machine on a regular terrain but there are not appropriate for a climbing machine.

One of the big distinctions among the walking and climbing robots reside in the influence of the gravity forces into the robot operation. Depending on the climbing direction, It could be generated some violation of the torque availability conditions associated with the robot's motors. For climbing robots a more reasonable approach towards the selection of foot trajectories should be based on a torque and speed optimisation process along the leg trajectory. The trajectory optimisation problem has been studied widely in the robotics literature [3,4]; generally, the initial and final points are known and the problem is to determine the optimum trajectory that joins both points according with some criterion. The problem exposed in this paper is different since the kind of trajectory is known (i.e. a straight line) while it should be decided its location in the work space, that is to determine the initial position of the leg so that the path is carried out with minimum cost. In this paper we

use a torque optimisation approach and a minimum leg velocity criterion in order to select the optimum climbing trajectories during the leg support phase. Later on, we review the influence of the torque restriction over the workspace. Finally, we determine the greatest stroke allowed as a function of the climbing direction.

Leg placement. An optimum approach

In climbing robot the acceleration force/ support force ratio is very small. For that reason, in this paper a static force approach is used in order to find the best place for the legs during the support phase.

Defining the objective function

Consider a climbing robot, which is hanging on the wall. Let F_i the force applied by the *ith* leg in such a way that the robot centre of gravity remains in equilibrium. The static support torque is given by,

$$\hat{o}_i = J_i\,(q_i)^T \cdot F_i \tag{1}$$

Lets ψ (x,y) the cost function considering the energy of a leg in support phase positioned in coordinates x,y in its workspace, then it can be defined as,

$$Ø(x,y) = \hat{o}^T \cdot \hat{o} = F^T \cdot J \cdot J^T \cdot F \tag{2}$$

where JJ^T is given by,

$$JJ^T = \begin{bmatrix} (l_1 s_1 + l_2 s_{12})^2 + (l_2 s_{12})^2 & -(l_1 s_1 + l_2 s_{12})(l_1 c_1 + l_2 c_{12}) - l_2^2 c_{12} s_{12} & 0 \\ -(l_1 s_1 + l_2 s_{12})(l_1 c_1 + l_2 c_{12}) - l_2^2 c_{12} s_{12} & (l_1 c_1 + l_2 c_{12})^2 + (l_2 c_{12})^2 & 0 \\ 0 & 0 & 1 \end{bmatrix} \tag{3}$$

for a SCARA type leg. Thus, the objective function can be stated as,

$$\begin{aligned} \Psi(x,y) = &\left[(l_1 s_1)^2 + 2(l_2 s_{12})^2 + 2 l_1 l_2 s_1 s_{12}\right] F_X^2 + \left[(l_1 c_1)^2 + 2(l_2 c_{12})^2 + 2 l_1 l_2 c_1 c_{12}\right] F_Y^2 - \\ &2\left[l_2^2 s_{12} c_{12} + l_1 l_2 s_{12} c_1 + l_1 l_2 s_1 c_{12} + l_1^2 s_1 c_1\right] F_X F_Y + F_Z^2 \end{aligned} \tag{4}$$

Finally, using the kinematic equations for a SCARA leg it is obtained,

$$\Psi(x,y) = \left[y^2 + l_2^2 s_{12}^2\right] F_X^2 + \left[x^2 + l_2^2 c_{12}^2\right] F_Y^2 - 2 \cdot \left[x \cdot y + l_2^2 s_{12} c_{12}\right] F_X F_Y + F_Z^2 \tag{5}$$

Vertical climbing motion

The objective function varies not only with the x,y coordinates of the leg but also with the F force which in turn depends in the climbing gait. This suggests that for every climbing gait an optimum path will exist that minimise the actuator torque for the leg. In order to solving the foot placement problem it should be necessary to establish it certain considerations. Of the forces that provide support and motion to the climbing robot, the higher contribution belongs to the vertical force. A first approach to the foot positioning problem could be to consider only this force so then the objective function is given by,

$$\Psi(x,y)=\left[x^2+l_2^2c_{12}^2\right]F_Y^2 \tag{6}$$

Consider the support phase time T_a and the leg stroke R. The objective function associated with a x(t), y(t) trajectory could be obtained evaluating the equation (6) along the path. Therefore the trajectory objective function is given by,

$$\Psi_{TRAY}(x_c,y_c,T_a)=F_Y^2\cdot\int_0^{T_a}\left(x(t)^2+l_2^2c_{12}(t)^2\right)\,dt \tag{7}$$

where,

$$c_{12}(t)=\frac{x(t)\cdot(l_1-D(t)\cdot l_2)-y(t)\cdot l_2\cdot\sqrt{1-D(t)^2}}{x(t)^2+y(t)^2} \tag{7b}$$

$$D(t)=\frac{x(t)^2+y(t)^2-l_1^2-l_2^2}{-2\cdot l_1\cdot l_2} \tag{7c}$$

Including the constraints

Some constraints must be considered in the optimisation process because of the leg structure and the environment in which the robot moves.

Figure 1 show the workspace for the front leg of an hexapod robot during vertical climbing and different constraints for and specific task (welding on a ship hull). For this task, the environment constraints can be defined as,

$$-0.18 < x(t) < 0.280 \tag{8}$$

The structural constraints are due to physical limitation of the leg joints. For the REST robot these are: hip joint (± 90º), knee joint (± 130º), link length (250mm).

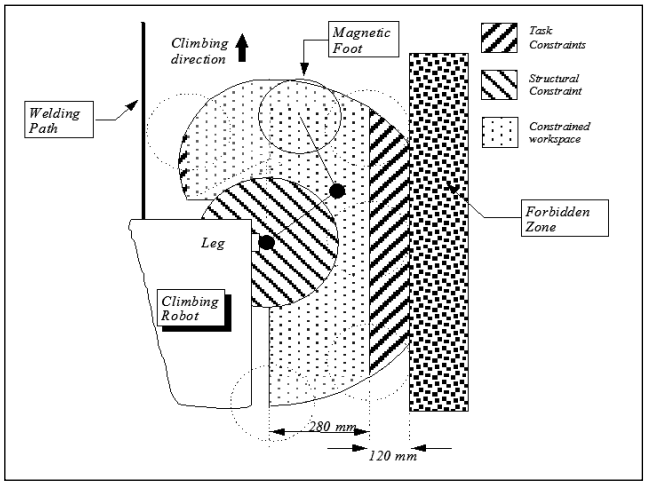

Figure 1 Workspace and structural and task constraints for a hexapod robot

Getting the location for the optimum leg placement

Once the constraints are established and the leg path (i.e. a straight line motion) is defined, then the foot placement problem can be formulated as a non linear optimisation problem defined as,

$$\underset{x_c\ ,y_c}{\text{minimize}}\ \Psi\left(x_c\ ,y_c\ ,R,T_a\ \right)=\int_0^{T_a}\left(x(t)^2+l_2^2 c_{12}\ (t)^2\ \right)dt$$

subject to:

$$\begin{aligned}
&x^2+y^2<L^2\\
&-2.27\,\text{rad}<\tan^{-1}\left(\frac{\sqrt{1-D^2}}{D}\right)<2.27\,\text{rad}\\
&-\frac{\pi}{2}<\tan^{-1}\left(\frac{y}{x}\right)-\tan^{-1}\left(\frac{\sqrt{1-D^2}}{1-D}\right)<\frac{\pi}{2}\\
&-0.18<x<0.280
\end{aligned}\qquad(9)$$

This is solved numerically using the Optimisation Toolbox of MATLAB [5].

Numerical results

In a climbing robot using a periodic continuous gait the robot velocity is

$$V = \frac{R}{\beta \cdot T} \tag{10}$$

so, keeping the ratio βT constant (the robot support forces depend on the duty factor) its possible to increase the velocity changing the leg stroke. Nevertheless, different legs stroke have different positions of the contact point for the legs that gets minimum actuator torque.

Figure 2 show the constraint workspace and the objective function for a leg stroke of R=0.2 mts. and (x,y) trajectory centre.

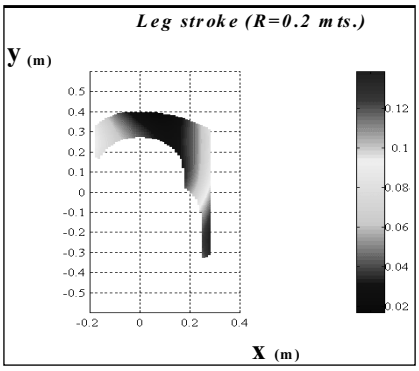

Figure 2 Objective function for a front leg with a stroke of 0.2 m.

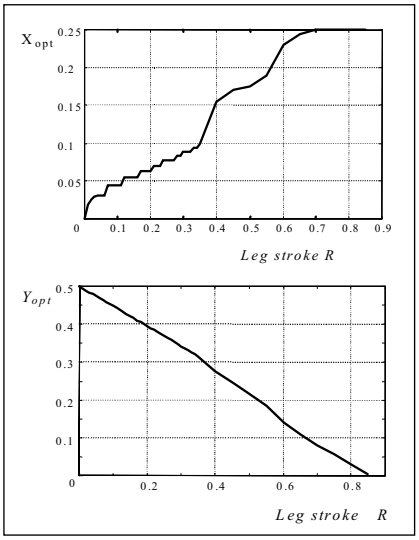

Figure 3 Optimum leg contact position during vertical climbing.

In order to study the dependency of the optimum foot contact position with the leg stroke, it was necessary to run many simulations for different strokes. Figure 3 show the locations of the optimum foot contact position as a function of the leg stroke.

Omnidirectional climbing.

In omnidirectional climbing mode the robot can ascend in any direction. This section deal with the foot placement optimisation problem when a climbing robot moves following a straight line and the robot's longitudinal axis set a particular angle α with respect to the vertical climbing.

If two walking robot move following a straight line, over a regular terrain, and use the same gait parameter, changing only the walking directions, they will have the same power requirements. However, this is not true for climbing robots due to gravity force. This suggests that the optimum foot placement depend not only on the leg stroke but also on the climbing angle.

Figure 4 show a climbing robot with an α angle motion direction. Let F_{Ti} be the support force for the *ith* leg and let F_m be the acceleration force so the robot can follow the desired trajectory. The

acceleration force can be considered proportional to the support force so $Fmi \approx \kappa F_{Ti}$. Thereby, the *ith* foot force is given by,

$$\begin{aligned} F_x &= F_{Ti} \cdot sen\acute{a} \\ F_y &= F_{Ti} \cdot cos\acute{a} + F_{mi} \end{aligned} \tag{11}$$

Using eq. 11 and eq.5 the objective function is,

$$\Psi(x,y,\alpha,\kappa) = \left\{ \begin{array}{c} \left[y^2 + l_2^2 s_{12}^2\right] \cdot sen(\alpha)^2 + \left[x^2 + l_2^2 c_{12}^2\right] \cdot [cos(\alpha) + \kappa]^2 - \\ 2 \cdot \left[x \cdot y + l_2^2 s_{12} c_{12}\right] sen(\alpha) \cdot [cos(\alpha) + \kappa] \end{array} \right\} \cdot F_{Ti}^2 \tag{12}$$

For a continuos climbing gait with constant velocity the objective function it is simplified by the condition $\kappa=0$.

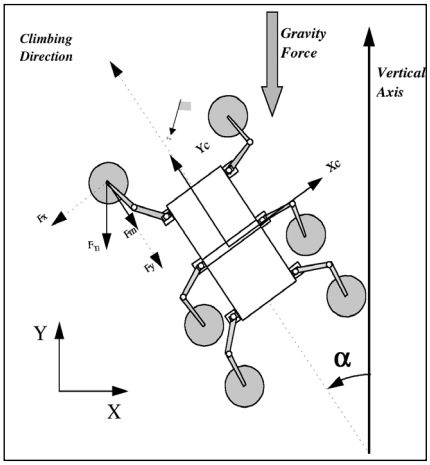

Figure 4 Diagonal climbing robot

Let T_a the support time and R the leg stroke then, the motion cost can be obtained minimising the objective function along the trajectory { $x(t) = X_c$, $y(t) = Y_c + R/2 - Rt$ } with coordinate value (X_c, Y_c) for the trajectory centre. This can be formulated as a non-linear optimisation problem defined as,

$$\underset{x_c\ ,\ y_c}{\text{minimise}}\ \Psi_{Traj}\left(x_c\ ,y_c\ ,\acute{a}\ ,R\ ,T_a\right) = \int_0^{T_a} \Psi\left(x,y,\acute{a},\kappa=0\right) dt$$

subject to:

$$x^2 + y^2 < L^2$$

$$-2.27\,\text{rad} < \tan^{-1}\left(\frac{\sqrt{1-D^2}}{D}\right) < 2.27\,\text{rad}$$

$$-\frac{\pi}{2} < \tan^{-1}\left(\frac{y}{x}\right) - \tan^{-1}\left(\frac{\sqrt{1-D^2}}{1-D}\right) < \frac{\pi}{2} \qquad (13)$$

Numerical results

Some simulations have been carried out in order to find the optimum contact point for different climbing directions. All the solutions are based in a leg stroke *R*=0.25 mts. The robot symmetry permits simplify the problem and solutions for leg pairs (1-6) and (2-5) are the same. Figure 5 shows the optimal coordinates for the trajectory centre for legs 1-2-5-6 as a function of the climbing angle. The discontinuity presented for α = 0.669 rad is related with the structural restrictions.

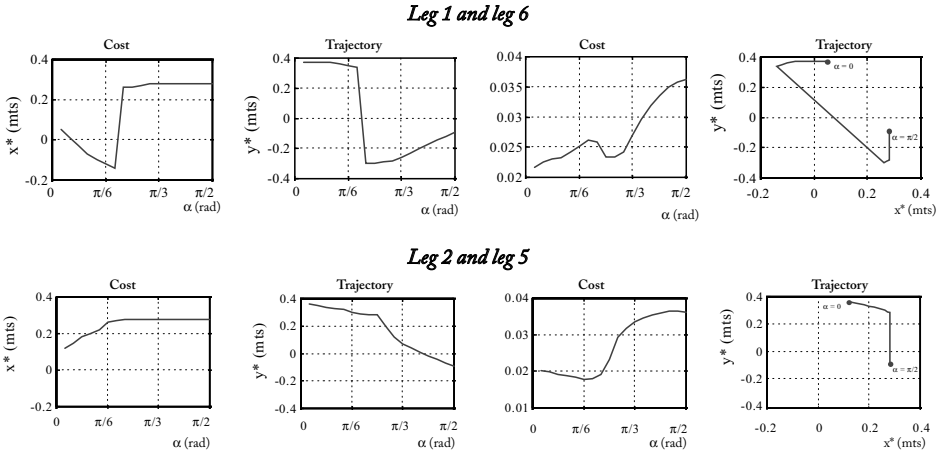

Figure 5 Optimal position for an SCARA type leg of an Hexapod robot

Figure 6 shows the optimal positions for the central legs 3-4 of the hexapod REST.

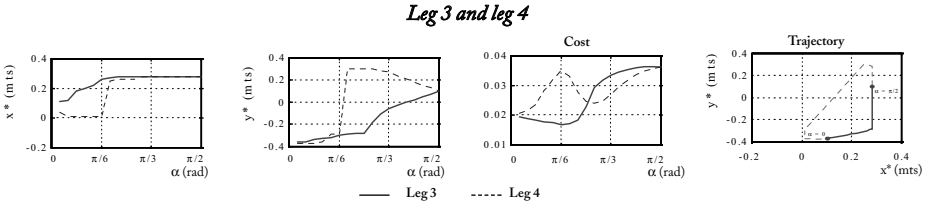

Figure 6 Optimal position for an SCARA type leg of an Hexapod robot. Legs 3-4

Figure 7 shows the climbing sequence for an hexapod robot using optimal foot placement solution for a climbing angle α = 0.61 *rad* with a leg stroke R = 0.25 *mts*. It can be seen the difference between a climbing robot with optimal contact position and a walking robot using standard leg positioning. In this figure the climbing robot use a Sawing Gait [6] with leg motion sequence {6-3-2-5-4-1}.

Finally, using SIDIREST [7] a comparison between the requirements for a horizontal climbing mode and a vertical climbing mode has been carried out. Figure 8 shows the simulation results for a front leg of the REST hexapod [6] using a wave gait with β=5/6, R=0.3 m and a cycle time T_c=12 sec. Figure 8 is an example of duality between the kinematic differential equations (velocity) and static equation (force).

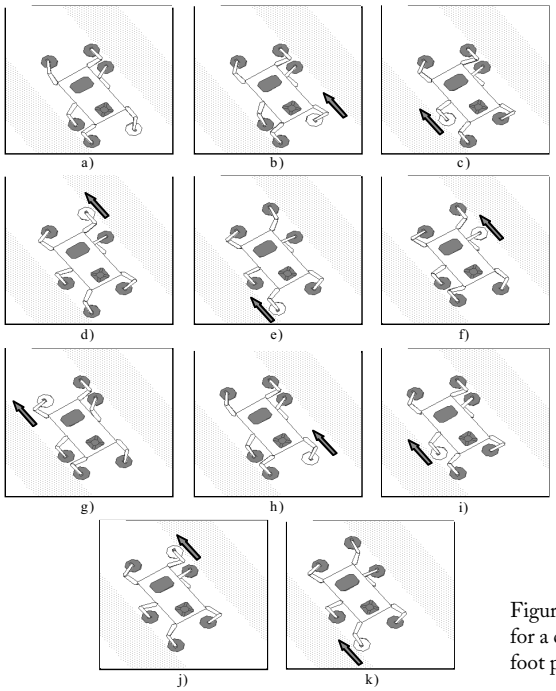

Figure 7 (left) Motion sequence for a climbing robot using optimal foot placement.

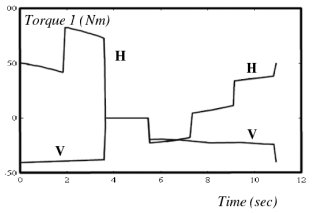

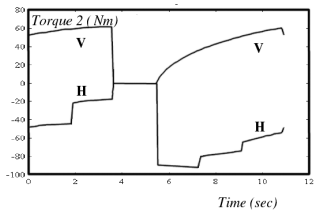

TORQUE AND VELOCITY REQUIREMENT FOR HORIZONTAL AND VERTICAL CLIMBING USING OPTIMAL POSITIONS (LEG 2)

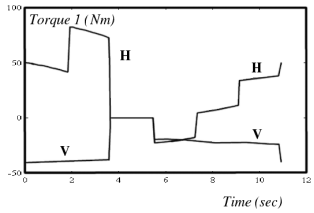

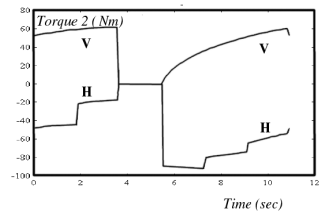

Figure 8
SIDIREST simulation for horizontal and vertical climbing.

Additionally to the torque requirement sometimes is necessary to consider the actuator velocity in order to keep tracked the desired trajectory. The velocity depends on the climbing gait. During the support phase the leg and robot velocity are the same and it is determined for the task while during the leg return phase the leg velocity and the robot velocity follow the relation,

$$V_{leg} = \frac{\beta}{1-\beta} \bullet V_{body} \tag{14}$$

If a duty factor β=11/12 is used, then the leg velocity is 11 times greater than the robot velocity. In this case the velocity must be taking in account in order to satisfy the requirement. The next section deal with the multicriteria optimisation based on torque and velocity requirement.

Multi-objective Optimisation

Consider a climbing robot, which is hanging on the wall. Let $\dot{x}_i$ the tip velocity of the *ith* leg during the return phase. The joint velocity are given by,

$$\dot{q}_i = J_i(q_i)^{-1} \cdot \dot{x}_i \tag{15}$$

Lets Γ (x,y) the cost function for a coordinate point (x,y) in the leg's workspace considering the velocity at the foot, then it can be defined as,

$$(x,y) = \dot{q}_i^{\,T} \cdot \dot{q}_i = \dot{x}_i^{\,T} \cdot \left(J_i(q_i) \cdot J_i(q_i)^T \right)^{-1} \cdot \dot{x}_i \tag{16}$$

where $(JJ^T)^{-1}$ is,

$$\left(JJ^T\right)^{-1} = \frac{1}{l_2^2 \cdot (y \cdot c_{12} - x \cdot s_{12})^2} \cdot \begin{bmatrix} x^2 + (l_2 c_{12})^2 & x \cdot y + l_2^2 c_{12} s_{12} & 0 \\ x \cdot y + l_2^2 c_{12} s_{12} & y^2 + (l_2 s_{12})^2 & 0 \\ 0 & 0 & l_2^2 \cdot (y \cdot c_{12} - x \cdot s_{12})^2 \end{bmatrix} \tag{17}$$

and $\dot{x}_i = [\, \dot{x}_{xi} \; \dot{x}_{yi} \; \dot{x}_{zi} \,]^T$.

During the return phase the leg follow the trajectory given by $x_i(t)$ and $\dot{x}_i(t)$ which depend on gait parameter.

Defining the objective function

Using a similar procedure of the previous section and considering the eq. 17, the objective function, evaluated on point (x,y) of the return trajectory, can be stated as,

$$\Gamma(x,y)=\frac{\left[y^2+l_2^2 s_{12}^2\right]}{l_2^2\cdot(y\cdot c_{12}-x\cdot s_{12})^2}V_y^2(x,y) \tag{18}$$

An important attribute of this functional is its not dependency with the climbing direction. Considering the return phase time T_r, the leg stroke R and a constant velocity V_r., then, the objective function could be obtained evaluating the equation (18) along the path. Therefore the trajectory objective function is given by,

$$\Gamma_{TRAY}(x_c,y_c,T_r)=V_y^2\cdot\int_0^{T_r}\frac{\left[y(t)^2+l_2^2 s_{12}(t)^2\right]}{l_2^2\cdot(y(t)\cdot c_{12}(t)-x(t)\cdot s_{12}(t))^2}dt \tag{19}$$

Therefore, considering the objective functions ψ (x,y) and Γ (x,y) the multi-criteria optimisation problem can be defined as,

$$\text{Let}\quad \Omega=[\,\Psi_{TRAY}(x_c,y_c,R,T_a)\;\Gamma_{TRAY}(x_c,y_c,R,T_r)\,]$$

$$\underset{x_c,y_c}{\text{minimize}}\;\Omega(x_c,y_c,R,T_a,T_r)$$

subject to:

$$\begin{aligned}
&x^2+y^2<L^2\\
&-2.27\,\text{rad}<\tan^{-1}\left(\frac{\sqrt{1-D^2}}{D}\right)<2.27\,\text{rad}\\
&-\frac{\pi}{2}<\tan^{-1}\left(\frac{y}{x}\right)-\tan^{-1}\left(\frac{\sqrt{1-D^2}}{1-D}\right)<\frac{\pi}{2}\\
&-0.18<x<0.280
\end{aligned} \tag{20}$$

There are many methods to resolve a multi-objective optimisation problem. In this paper it is used a weighted sum strategy to convert the multi-criteria optimisation of the Ω vector into a scalar one by means of weight associated with each objective. Thus, the multi-criteria optimisation can be defined as,

$$\begin{aligned}
&\underset{x_c,y_c}{\textit{minimize}}\quad \tilde{\Omega}=\alpha_1\cdot\Psi_{TRAJ}(x_c,y_c,R,T_a)+\alpha_2\cdot\Gamma_{TRAJ}(x_c,y_c,R,T_r)\\
&\textit{subject to constraint Eq}\quad 20
\end{aligned} \tag{21}$$

Numerical results for multi-objective optimisation

In this section it is considered the same importance for torque and velocity objective. This is established doing $\alpha_1 = \alpha_2 = 0.5$. Those interested readers can see [8] for a general selection of (α_1 , α_2) based on climbing parameters.

The optimisation was carried out for different leg strokes, from 0.01m to 0.8 m. Figure 9 shows the optimum foot contact point for the REST robot during vertical climbing as a function of the leg stroke. It can be see that for a big leg stroke the multi-criteria optimisation converge to the torque optimisation due to restriction in the workspace. For a small leg stroke, R<0.5m, there are fewer motion restrictions. In order to have a general rule to get the foot placement positions an approximated solution was obtained using a fitting least square ninth degree polynomial.

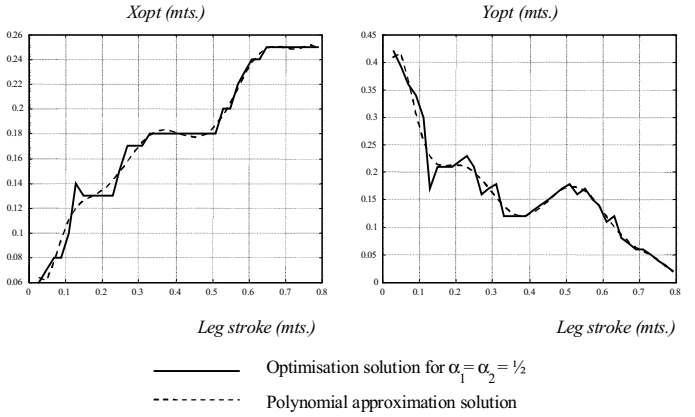

Figure 9 Optimum foot placement for a multi objective optimisation. Vertical climbing

Influence of the climbing direction on the leg stroke

Determination of the maximum leg stroke

Let us consider a climbing robot moving on a direction forming an angle α. The effective leg workspace varies in accordance with its configuration, with the direction angle and with the support force. In order to estimate the climbing stroke - $R_{\max}$ - is required to calculate the maximum stroke- $R^i_{\max}$ – that it is associated to robot leg *i*; taking in account that all supporting legs must use the same stroke during the locomotion cycle, then $R_{\max}$ is determined by $min\{R^i_{\max}\}$.

Due leg configuration affects directly to $R_{\max}$, then it is possible to determine the n-legs configuration that permits to obtain the maximum value for $R_{\max}$. Let F_i the feet support phase force, and let be τ_{imax} the maximum torque that can be generated by the *i th* leg actuators. The support trajectory centre is given by the x_c, y_c point. The stroke is *r*. Determination of $R^i_{\max}$ can be posed as:

$$R^{i}_{max} = \max_{x_a, y_a, r} r$$

subject to:

$$\begin{aligned} &a)\ x_a^2 + (y_a - \omega \cdot r)^2 < L^2 \\ &b)\ -\frac{13\pi}{18} < q_{2i}(x_a, y_a - \omega \cdot r) < \frac{13\pi}{18} \\ &c)\ -\frac{\pi}{2} < q_{1i}(x_a, y_a - \omega \cdot r) < \frac{\pi}{2} \\ &d)\ J_i(x_a, y_a - \omega \cdot r) \cdot F_i(\alpha) < \tau_{i\,max} \end{aligned} \qquad (22)$$

$$\forall \omega \in [0,1]$$

where a), b) and c) are leg kinematic restrictions, while d) represents the associated restriction to the maximum torque allowed through the trajectory. Once determined the values of R^i_{max} for each leg it can be determined R_{max} such,

$$R_{max} = min\left\{R^i_{max}\right\} \qquad i = 1,2,...,n \qquad (23)$$

Optimisation results

Leg	Configuration A			Configuration B			Stroke Max.
	P_x(cm)	P_y(cm)	R(cm)	P_x(cm)	P_y(cm)	R(cm)	
1	3.47 -24.35	26.75 -35.75	20.2 14.62	-24.58	12.13	16.97	14.62-16.97 20.20
3	-2.5 -24.35	25 -35.75	16.24 14.62	-24.58	12.13	16.97	14.62-16.24 16.97
5	-2.5 -24.35	25 -35.75	16.24 14.62	-24.58 16.17	12.13 -12.7	16.97 14.49	14.62-16.24 16.97
2	24.58 -16.17	-12.13 12.7	16.97 14.49	2.5 24.35	-25 35.75	16.24 14.62	14.62-16.24 16.97
4	24.58	-12.13	16.97	2.5 24.35	-25 35.75	16.24 14.62	14.62-16.24 16.97
6	24.58	-12.13	16.97	-3.47 24.35	-26.75 35.75	20.2 14.62	14.62-16.97 20.20

Table 1 Maximum leg stroke depending on the leg disposition.

Two different leg configurations have been study. The configuration A represents an "elbow down" leg configuration referred to the first quadrant while configuration B exhibits an "elbow up" disposition referred to the same quadrant. Table 1 presents the obtained results for each leg in the REST robot.

Previous results exhibit how the maximum leg stroke, to be employed during the climbing motion with angle $\alpha=\pi/3$, is R_{max}=16cm. This distance can be reached with any of the possible leg configurations, as it is shown in the Table 1.

Rmax variation with the climbing angle

Figure 10 represented the variation of maximum leg stroke depending with the climbing angle. It can be seen a strong discontinuity, close to 30º. Starting from this angle the leg's workspace consist of two separated areas reducing the maximum stroke.

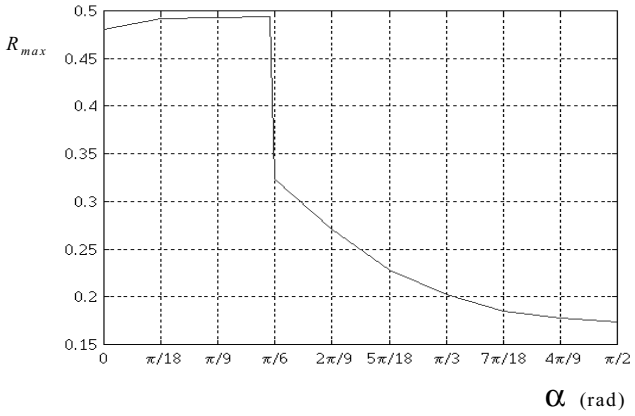

Figure 10 Leg stroke variation with climbing angle

As a summary of this previous sections, the optimum foot placement problem for a climbing robot has been formulated as a non-linear optimisation problem subject to kinematic and environment constraints. The technique permit to select the optimal placement from an energetically point of view. The diagonal climbing has been studied and different foot positions have been established for climbing direction ranging from vertical to horizontal. A multi objective optimisation is proposed in order to consider the velocity requirements during climbing tasks. Finally, the influence of climbing direction in the maximum leg stroke was presented.

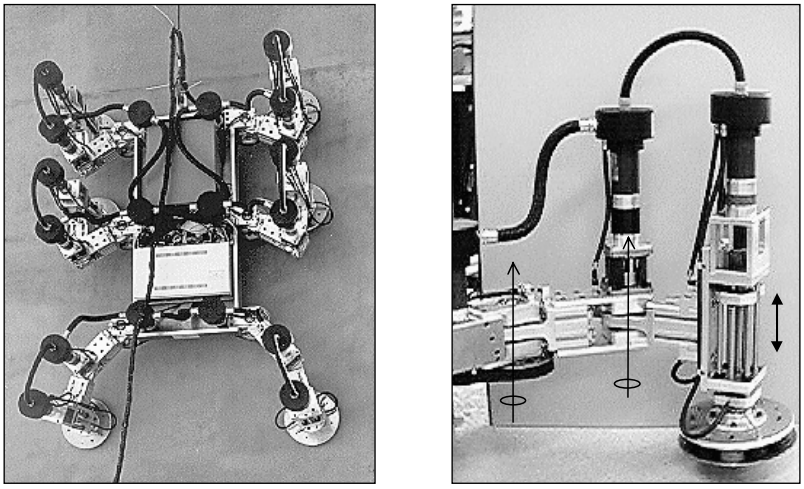

Figure 11 REST 1 climbing robot under experimental testing on a ship hull.

Figure 11 left illustrates the experimental testing of REST 1 six-legged climbing robot on a ship hull, right side shows a detail of the scara type legs.

REST 2 CLIMBING ROBOT

Following REST 1, a second prototype of climbing robot that moves continuously along the wall, named REST 2 has been constructed. It uses a variation of the well known wave gait in order to obtain fast continuous movement on softly undulated terrain together with foothold selection to handle obstacles and irregularities during climbing. The robot uses electromagnets to attach itself to ferromagnetic walls and has four legs (12 degrees of freedom) that resemble properties from sliding frames and true legged climbers. The novel leg design and geometrical configuration allows for fully overlapping workspaces. As a result of this novel leg and robot design, it was possible to achieve a much better payload to weight ratio, increased velocity, better inertial properties and reduced energy consumption. Our approach to reliability was to simplify the robot structurally and to support modularity of parts and connections.

REST 2 has been designed to carry on a light manipulator for butt welding. The robot weights less than 50 Kgs. Figures 12 and 13 show a comparison of both climbing machines.

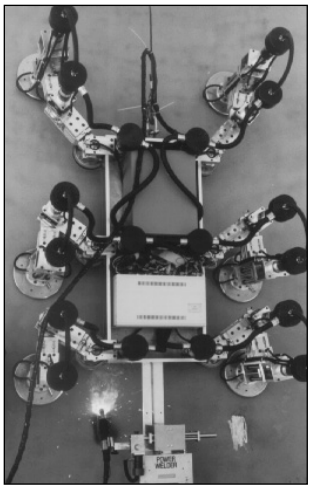

Figure 12. REST 1 climbing robot welding ship hull

Figure 13. REST 2 climbing robot during testing

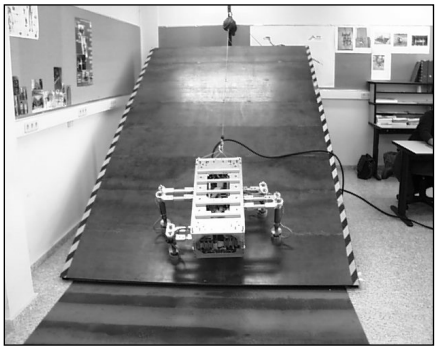

ROWER 2

A second development (after ROWER 1) was intended for contributing the problem of welding automation inside the double-bottom vertical cells. So further developments yielded to ROWER 2 (Figure 14), where a light manipulator is moved in the vertical direction for welding the double hull vertical cells.

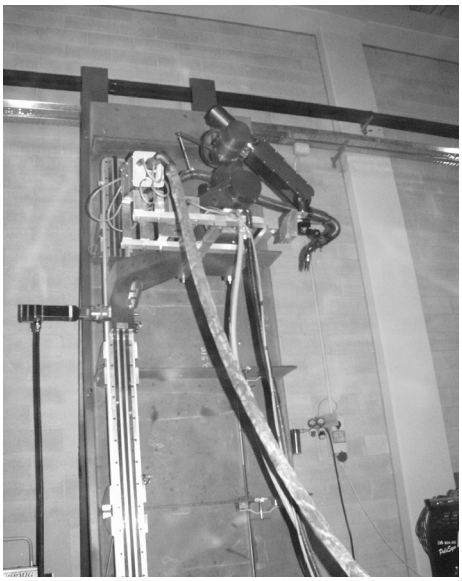

Figure 14. ROWER 2 system.

AURORA UNDERWATER CLIMBING ROBOT

It is well known that all kind of ship's underwater hull become overgrown with sea adherence (weed, barnacles) very fast. This means raise of fuel consumption, and freeing atmosphere an extra amount of CO_2 (incrementing greenhouse effect) and of sulphur dioxide (acid rain), apart from deterioration of ability of ship's control. This situation becomes important even after six months of ship activity. For recovery of ship's required operational performance, it is necessary for Ship-Repairing and Conversion Industries to dry dock a ship and proceeds to cleaning. This procedure is very time consuming and of high cost, but it is the only available solution nowadays for SRYs. On the other hand, this cleaning activity is the first to be done when a ship needs maintenance and/or some repairing, being the last the main activity of SRYs. So hull treatment is required and, at present time, is done manually in dry-dock using different adapted methods like grit blasting or water jet, and it has to be noticed that, in itself, it is a very contaminant operation (dust contains always painting particles), it is harmful for human operators health and it is a very uncomfortable job.

To provide a solution to these problems an EC funded project (G3RD-CT-000-00246) was organised: AURORA (Auxiliary Climbing Robot for Underwater Ship Hull Cleaning of Sea Adherence and Surveying). The project partnership brings together 7 partners with complementary roles: the Industrial Automation Institute (IAI-CSIC) which is the Project co-ordinator, two ship-repairing yards, T. Kalogeridis&Co. Inc. and Unión Naval de Barcelona, Algosystems S.A., the Division of Robotics, Department of Mechanical Engineering, from Lund University, SAIND, manufacturer and vendor of equipment for shipyards, and Riga Technical University.

AURORA scenario consists in the underwater hull that after some time of ship operation is plenty of marine incrustations, where a new kind of underwater climbing robot equipped with special tools should perform cleaning and surveying tasks. That scenario presents large dimensions and exhibits some areas of very difficult reach-ability and poses some additional technical difficulties. As it has been conceived the underwater climbing robot control is a human-in-the-loop process. Human-Machine Interface (HMI) design takes this into consideration whether

using direct control or supervised control. This interface includes a control command set used to select the machine trajectory and a graphic representation used to get information about the robot and its environment. Figure 15 shows the concept of AURORA project and some view of the teleoperation station. Figure 16 shows overall system architecture. The system has demonstrated excellent performance.

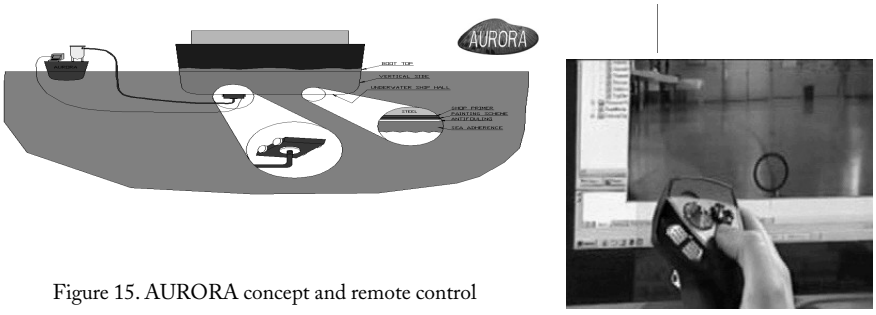

Figure 15. AURORA concept and remote control

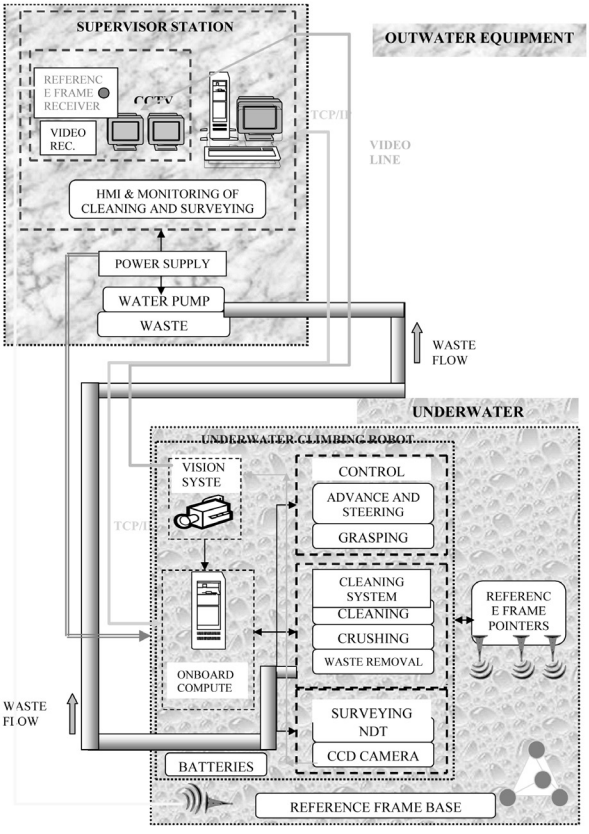

Figure 16. AURORA architecture.

CONCLUSIONS

Some achievements in the field of climbing robots related to the maritime industries in the last years have been presented. Most of the systems have being conceived to solve practical problems, but a lot of research is underlying and there are still many open questions.

ACKNOWLEDGEMENTS

The REST climbing robot has been developed entirely in the IAI under the project PACE PR 212 SACON funded partially by ESPRIT and by the CDTI-MINER of Spain. The authors want to acknowledge also the other two project partners AESA and SAIND for their co-operation. REST-2 was developed with CICYT funding under TAP 1999-0993 "SACON-2". ROWER 1 and ROWER 2 have been funded by BRITE/EURAM and GROWTH; other partners where TECNOMARE, FINCANTIERI, ENVC, CELSIUS, LUND University and AESA. IAI-CSIC is a member of the ROBMAR and CLAWAR Thematic Networks, where and important activity dealing with advanced concepts, technologies and applications of climbing and walking robots is being carried out. AURORA project was funded also by the CE under GROWTH programme under contract G3RD-CT-000-00246 (partners LUND, SAIND, ALGOSYSTEMS, Riga Technical University, Kalogeridis I&T, Unión Naval de Barcelona). Author's acknowledgement is extended to all the partners of the mentioned projects and to the European Commission.

REFERENCES

[1] **Zhang, C. and Song, S.M.** "Gaits and Geometry of a Walking Chair for the Disabled". J. of Terramechanics. Vol.26, Nº3/4 1989.

[2] **Lee, J.K. and Song, S.M.** "Path Planning and Gait of Walking Machine in an Obstacle-Strewn Environment". J. Rob. Syst., Vol.8, Nº 6. 1991.

[3] **Kawato, M., Uno, Y. and Suzuki, R.** "Formation and Control of Optimal Trajectory in Human Multijoint Arm Movement". Biological Cybernetics. Vol. 61. 1989.

[4] **Zefran, M., Kumar, V. and Yun X.** "Optimal Trajectories and Force Distribution for Cooperating Arms". Proc. IEEE Int. Conf. Rob. Autom. pp.1005-1012. San Diego 1994.

[5] **Grace, A.** "Optimization Toolbox User's Guide". The MathWorks Inc. Mass. USA. 1994.

[6] **Grieco, J.C.; Prieto, M.**; Armada, M.; González de Santos, P. "A Six-Legged Climbing Robot for High Payloads". 6th IEEE Conference on Control Applications ICCA'98. Trieste, Italy. September 1-4, 1998.

[7] **Grieco, J.C., Armada, M., González de Santos, P. and Guerrero, A.** "Computer-Aided-Design of a Climbing Robot for Harsh Environment". IFAC Workshop on Human-Oriented Design of Advanced Rob. Syst. DARS 95. Vienna, Austria. September 1995.

[8] **Grieco, J.C.;** "Robots escaladores. Consideraciones acerca del diseño, estabilidad y estrategias de control.". Tesis Doctoral. Universidad de Valladolid, Spain. 1997.

ACERCA DEL DISEÑO Y DESARROLLO DE ROBOTS CAMINANTES Y ESCALADORES PARA LA INDUSTRIA MARÍTIMA

RESUMEN

Los sistemas robóticos modernos son cada vez más potentes en términos de fusión sensorial y de movilidad. El progreso tecnológico actual hace posible que robots avanzados hagan frente a entornos complejos como los que se encuentran frecuentemente en la industria marítima. En este artículo se presenta una descripción de diversos robots móviles (caminantes y escaladores) con ejemplos tomados de algunos proyectos desarrollados por el Instituto de Automática Industrial del Consejo Superior de Investigaciones Científicas de España (IAI-CSIC).

METODOLOGIA

El Departamento de Control Automático del Instituto de Automática Industrial ha venido realizando investigaciones para el desarrollo de proyectos en el campo de la robótica por más de veinticinco años. Desde los años setenta esta actividad empezó con la realización de robots industriales, lo que proporcionado una vasta experiencia y reputación en cinemática, dinámica, diseño mecánico y sistemas de control. Después de algunos desarrollos exitosos en este campo, el departamento ha enfocado su interés en el área de robots para ambientes hostiles y peligrosos. En este tipo de ambientes es necesario realizar gran variedad de tareas (supervisión, manipulación, soldadura, etc.), lo que implica que los operarios humanos tengan que estar expuestos a condiciones de trabajos extremadamente duras. También hay un gran número de aplicaciones potenciales que no son posibles de realizar por los operadores humanos debido a la dificultad de llegar a alcanzar algunas posiciones de trabajo de forma segura. Esta situación implica, de forma natural, el uso de dispositivos controlados de manera remota, en donde se pueden considerar los tele-robots como la solución más avanzada y prometedora. De esta manera se tendrán las siguientes ventajas: se mejorarán las condiciones de trabajo, se mejorarán los sistemas de seguridad, se automatizarán las tareas repetitivas y se abrirán posibilidades para proveer de distintas soluciones para nuevas aplicaciones.

Sin embargo, aunque hay muchas aplicaciones que se pueden solucionar con el uso de un tele-manipulador apropiado, equipado con las herramientas necesarias y con la destreza de un operador, muchos de estos trabajos son pueden ser solucionados mediante este sistema debido a la dificultad de acceso a la zona deseada. El problema del acceso en lugares de trabajo remotos presenta mayores dificultades y

previene la automatización. Hay publicaciones en las que se muestran soluciones interesantes a este problema, por ejemplo el uso de manipuladores de largo alcance. Algunas otras soluciones, no menos interesantes, consisten en proveer de un transporte a los manipuladores tele-operados. Este transporte incluye vehículos con ruedas o vehículos con orugas, y más reciente maquinas con patas (caminantes o escaladoras).

Actualmente la industria de construcción naval está siendo forzada a adaptarse a nuevas especificaciones técnicas, menores tiempos de entrega y nuevas regulaciones de seguridad, de esta forma los buques se deben construir más rápido, con menor coste y con mejores condiciones de trabajo para los operarios. Los nuevos sistemas robóticos están mejorando estas características. Especialmente, los robots manipuladores están ayudando aumentar la calidad de la soldadura, disminuyendo el tiempo de arco y evitando que los operarios estén expuestos a la concentración de gases nocivos. Sin embargo, los sistemas robóticos actuales no pueden realizar algunas aplicaciones industriales, especialmente las que están relacionadas con la movilidad en ambientes complejos. Estos casos se presentan en algunas etapas de la construcción de buques sobre todo en las actividades realizadas en dique seco y también en la reparación de buques en lo que respecta a la limpieza y la inspección. En esta publicación se presentan como soluciones robots escaladores y caminadores especialmente adaptados para la industria marítima. La mayoría de estos trabajos han sido desarrollados bajo la financiación de proyectos Europeos.

Hay tres etapas principales para la construcción de un buque en el campo de fabricación marítima:

— Construcción de los bloques en los talleres de pre-fabricación.
— Transporte de los bloques al dique seco utilizando grandes grúas o vehículos especiales.
— Unión de los bloques.

La primera actividad consiste en la construcción y ensamblaje que los enormes bloques de los buques. Este trabajo se realiza en talleres especializados con una productividad relativamente buena, que se ha visto incrementada por desarrollos realizados en este campo. Después de transportar los bloques, lo que es realizado en un segundo plano, la tercera etapa incluye la unión de dos bloques consecutivos mediante la soldadura de todos los refuerzos longitudinales y todos los tabiques herméticos.

Por seguridad medioambiental, la mayoría de los buques, especialmente petroleros y otros, son construidos con doble casco, y así se evita el derrame de la carga si la parte externa sufre algún daño. Esta doble estructura forma celdas alrededor de todo el casco. Hay dos problemas importantes para soldar en la fabricación de buques: el empalme de la soldadura en posiciones a lo largo de planos cercanos a la superfie del casco y en las uniones de las celdas del doble fondo de los cascos. En los últimos años el IAI-CSIC ha estado involucrado en varios proyectos para la automa-

tización de la soldadura en la fabricación de buques. El resultado principal de tres proyectos acerca de este trabajo son presentados en esta publicación: un robot escalador hexápodo y uno cuadrúpedo para la soldadura del casco de los buques y un sistema robótico para soldar las celdas verticales del casco del buque (ROWER 2). Todos estos robots han sido equipados con sistemas de soldadura industrial y sensores especiales para supervisar la soldadura. El cuarto robot escalador, en este caso submarino, ha sido desarrollado para la limpieza de adherencias y la inspección del casco con el buque a flote, es presentado al final del artículo.

CONCLUSIONES

Se han presentado algunos logros que han sido alcanzados en el área de robots caminantes y escaladores para la industria marítima. La mayoría de los sistemas han sido concebidos para resolver problemas prácticos, pero todavía hay una gran cantidad de esfuerzo requerido para la obtención de soluciones realmente prácticas, y todavía hay muchas preguntas por responder.

El robot escalador REST ha sido creado completamente en el IAI bajo el auspicio del proyecto PACE PR 212 SACON financiado parcialmente por ESPIRIT y por CDTI-MINER de España. Los autores quieren expresar sus agradecimientos a los colaboradores del proyecto AESA y SAIND por su cooperación. REST-2 ha sido financiado por CICYT bajo el proyecto TAP 1999-0993 “SACON-2”. ROWER 1 y ROWER 2 han sido financiados por BRITE/EURAM y GROWTH. AURORA ha sido financiado por la Comunidad Europea en el programa GROWTH bajo el contrato G3RD-CT-000-00246.

Journal of Maritime Research, Vol. II. No. 1, pp. 33-50, 2005

ISSN: 1697-4840

A PFM-BASED CONTROL ARCHITECTURE FOR A VISUALLY GUIDED UNDERWATER CABLE TRACKER TO ACHIEVE NAVIGATION IN TROUBLESOME SCENARIOS

J. Antich[1] , A. Ortiz[2] and G. Oliver[3]

ABSTRACT

Nowadays, the surveillance and inspection of underwater installations, such as power or telecommunication cables and pipelines, are carried out by trained operators who, from the surface, control a Remotely Operated Vehicle (ROV) with cameras mounted over it. This is a tedious, time-consuming and expensive task, prone to errors mainly because of loss of attention or fatigue of the operator and also due to the typical low quality of seabed images. In this study, a control architecture based on Potential Field Methods (PFM) for visually guiding an Autonomous Underwater Vehicle (AUV) to detect and track a cable, or pipeline, laid on the seabed is presented. Additionally, a solution to the typical trapping problem linked to this kind of control systems is proposed. The efficiency of the solution is evaluated and compared against other popular strategies appearing in the literature. A 3D simulation environment which incorporates the hydrodynamic model of a real underwater vehicle called GARBI has been used with this purpose.

Key words: Autonomous Underwater Vehicles, Obstacle Avoidance, Local Path Planning, Vision-based Pipeline Tracking.

[1] Profesor Ayudante de Escuela Universitaria, Universidad de las Islas Baleares, (javi.antich@uib.es), Telf. 971172911, Fax 971173003, Escuela Politécnica Superior. Ctra. Valldemossa km 7.5, 07071 Palma de Mallorca, Spain.

[2] Profesor Titular de Escuela Universitaria, Universidad de las Islas Baleares (alberto.ortiz@uib.es) Telf. 971172992, Fax 971173003, Escuela Politécnica Superior. Ctra. Valldemossa km 7.5, 07071 Palma de Mallorca, Spain.

[3] Profesor Titular de Universidad, Universidad de les Illes Balears (goliver@uib.es), Telf. 971173201, Fax 971173003, Escuela Politécnica Superior. Ctra. Valldemossa km 7.5, 07071 Palma de Mallorca, Spain.

INTRODUCTION

The feasibility of an underwater installation can only be guaranteed by means of a suitable inspection programme. This programme must provide the company with information about potential hazardous situations or damages caused by the mobility of the seabed, corrosion, or human activities such as marine traffic or fishing. Nowadays, the surveillance and inspection of these installations are carried out using video cameras attached to ROVs normally controlled by operators from a support ship. Obviously, this is a tedious task because the operator has to concentrate for a long time in front of a console, which makes the task highly prone to errors mainly due to loss of attention and fatigue. Besides, undersea images possess some peculiar characteristics which increase the complexity of the operation: blurring, low contrast, non-uniform illumination and lack of stability due to the motion of the vehicle, just to cite some of them. Therefore, the automation of any part of this process can constitute an important improvement in the maintenance of such installations with regard to errors, time and monetary costs.

To this end, an automatic system for autonomously locating and tracking a cable/pipeline on the basis of visual feedback is presented and discussed in this paper. For a start, the rigidity and shape of the underwater cable is exploited by a computer vision algorithm to discriminate the cable from the surrounding environment even in very noisy images. A suitable control architecture makes then use of the output of the vision system to make the AUV track the cable. Behaviours and PFM are in the heart of the proposed architecture. Besides, it integrates a novel reactive obstacle avoidance/navigation strategy to escape from both local and global trapping situations. A 3D OpenGL-based simulator incorporating the dynamics model of a real underwater vehicle has been used to validate the proposal.

The rest of the paper is organized as follows: the vision system is briefly described in section 2; section 3 presents the control architecture, while the navigational approach is discussed in section 4; and, finally, the last section gives some conclusions and future work.

THE VISION SYSTEM

Brief Description

Artificial objects usually present distinguishing features in natural environments. In the case of the cable, given its rigidity and shape, strong alignments of contour pixels can be expected near its sides. The vision system exploits this fact to find the cable in the images.

To this end, every image is first segmented by means of a classification algorithm working over an (intensity, intensity gradient) space. Next, from the region contours, alignments of contour pixels are determined and analysed. If among those alignments there is strong evidence of the location of the cable (mainly two align-

ments with a great number of pixels lined up and with a high degree of parallelism, even without discounting the perspective effect), then the cable is considered to have been located and its parameters are computed. Otherwise, the image is discarded and the next one is analysed.

Once the cable has been detected, its location and orientation in the next image are predicted by means of a Kalman filter, which allows reducing the pixels to be processed to a small ROI (Region Of Interest). In this way, the computation time is considerably lowered together with the probability of misinterpretations of similar features appearing in the image.

When tracking the cable, a low or null evidence of its presence in the ROI can be obtained. In such a case, a transient failure counter is increased after discarding the image. If this anomalous situation continues throughout too many images, then it is attributed to a failure in the prediction of the ROI, resulting in two special actions: the Kalman filter is reset and the ROI is widened to the whole image.

Detailed information about the different steps of the system can be found in (Antich and Ortiz, 2003).

Presentation of Some Results

The vision system has been tested using sequences from a video tape obtained in several tracking sessions of various real cables with an ROV driven from the surface. These cables were installed several years ago, so that the images do not present highly contrasted cables over a sandy seabed; on the contrary, these cables are partially covered in algae or sand, and are surrounded by algae and rocks, making thus the sequences highly realistic. The mean success rate that has been achieved is about 90% for a frame rate of more than 40 frames/second on average.

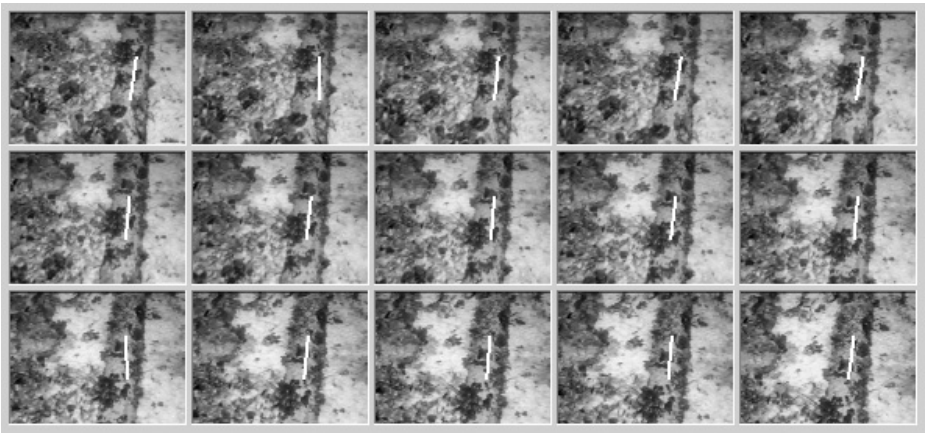

Figure 1 shows results for an excerpt of one of the testing sequences.

A BEHAVIOUR-BASED CONTROL ARCHITECTURE

Framework

Robot control is the process of taking information about the environment, through the sensors of the robot, processing it as necessary to decide how to act, and then executing those actions by means of the available effectors to achieve the set of goals corresponding to a user-specified mission. Nowadays, there is a small number of fundamentally different classes of robot control methodologies (see (Ridao et al., 1999) (Valavanis et al., 1997), among many others) which are usually embodied in particular control architectures and that can be roughly classified as: deliberative/hierarchical, behavioural/reactive, and hybrid. However, only the two last ones are suitable to deal with complex, non-structured, and changing worlds, like the majority of underwater environments. This paper proposes a complete behavioural control architecture based on Motor Schemas with 3D Potential Fields to control the navigation of the underwater cable tracker. Simplicity and modularity have been the key factors to choose this approach.

In this context, behaviours are the basic building blocks to carry out robotic actions, representing each of them the reaction to a stimulus. Behavioural responses are all coded as 3D vectors whose orientation denotes the direction to be followed by the vehicle while the magnitude expresses the strength of the response against other behavioural commands. The vectors generated by the architecture's active behaviours are asynchronously channelled into a coordination mechanism that combines them in order to obtain the final control system response.

Mission Stages and Sensory Equipment

Several stages are distinguished within a cable-tracking mission: diving, sweeping, tracking and homing. In the first one, the AUV, after having been released from the support ship, goes down until a certain distance to the seabed is reached. The second and third stages comprise, respectively, searching for the cable in a predefined exploration area and tracking it once found. Finally, the vehicle returns to the starting point after having achieved the limits of the exploration area while tracking the cable.

The control architecture assumes the existence of three different kinds of sensors to carry out cable-tracking missions: forward and side-looking sonars, a compass and a camera. Furthermore, the position of the vehicle is estimated by means of an acoustic positioning system of the so-called Long Base Line (LBL) type.

Behaviour Description

Taking into account the aforementioned general way of action for the AUV, the reactive control layer of the vehicle was split into five primitive behaviours.

Some of them appear in the classical literature about behavioural architectures, but others are specific of this application. They all are described in the following:

— *Stay on region* prevents the AUV from straying from the area to be explored. The behaviour is exclusively activated when the vehicle is close to the limits of the exploration area. In such a case, a vector that moves the vehicle away from those limits is generated, being its magnitude directly related to the corresponding distance: the closer to the limits, the larger the magnitude.

— *Avoid obstacles* allows the vehicle to avoid navigational barriers such as rocks, algae or, even, other possible cooperating vehicles. In this case, a vector in the opposite direction to the obstacles is generated. The magnitude of the vector is again variable, now according to the distance that separates the AUV from the obstacles ahead.

— *Cable detection and tracking* moves the vehicle strategically through the exploration area in search of a sufficient evidence of the presence of the cable. Specifically, after having acquired the working depth through a vertical path from the surface, the AUV executes the sweeping stage performing a zigzag movement on the exploration area until the cable is found. Although other more optimised strategies could have been devised, it is important to notice that it has been assumed a total lack of information about the location of the cable, so that there are no many more alternatives but an exhaustive or near-exhaustive search.

Once the cable has been detected, the tracking stage starts. At this point, the AUV can be oriented in any one of the two possible —and opposite— directions to start tracking the cable. The particular choice is based on a predefined parameter which establishes a certain range of preferred orientations.

Along the tracking, two different tasks are sequentially executed: the first one tries to keep the cable oriented vertically in the field of view (FOV), while the second task intends to maintain the cable in the central area of the FOV. In this way, improvements in both the cable visual detection and the longitude and smoothness of the vehicle's path are expected.

As can be easily anticipated, anomalous situations can arise in a real application. In particular, the cable can disappear from the images because the AUV's course has drifted apart from the actual cable location. In such cases, a suitable recovery mechanism is activated, consisting in making the behaviour return to its internal search state, where the vehicle acquires again the zigzag movement. However, now the area to be explored is reduced using the vehicle's trajectory during the past tracking stage (see figure 2). This trajectory is fitted by a straight line and a new search zone is determined computing the intersection between such line and the limits of the exploration area. Note that the dimensions of the new exploration area can be readjusted according to the AUV's manoeuvrability.

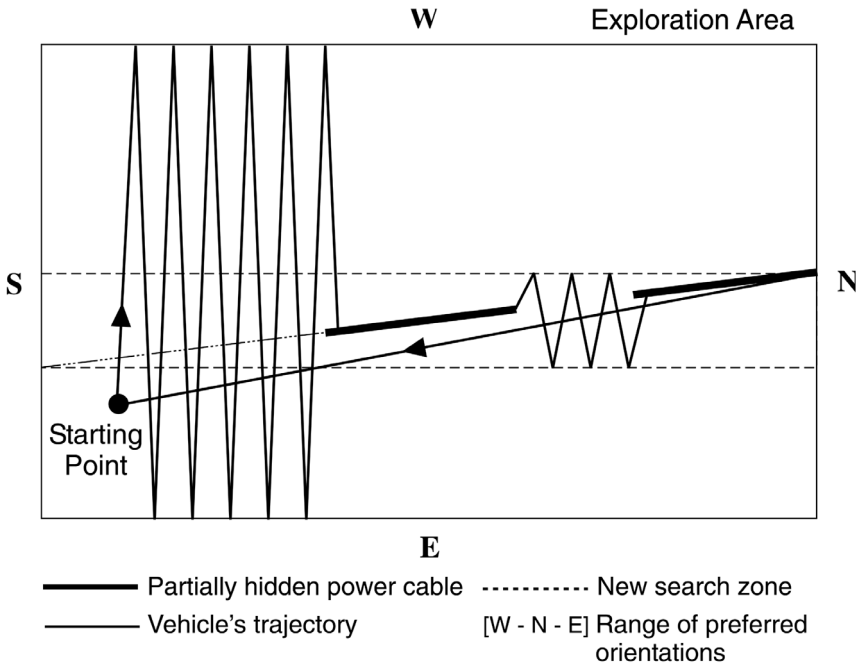

Figure 2. AUV's trajectory for a typical mission

— *Keep distance to seabed* tries to maintain the distance to the seabed constant in order to keep the apparent width of the cable in the images also constant. In this way, the vision subsystem can assume that the separation between both sides of the cable does not vary, and use this information to reduce its probability of failure. Sonars or, in case they cannot bring accurate enough measures, the acoustic positioning system, are expected to supply the required distance to the seabed.
— *Go home*, finally, makes the vehicle go to the mission start point. Two different steps are carried out: first, the AUV approaches to the starting point keeping a certain distance to the seabed; afterwards, it goes up until the sea surface is reached. In both cases, the magnitude of the output vector is proportional to the proximity to the intermediate/final goals considered.

A Hybrid Coordination Mechanism

As it has been said, the output vectors generated by the architecture's active behaviours are asynchronously channelled into a coordination mechanism which is responsible for obtaining the final control system response. Such mechanisms are typically classified into two groups: competitive or cooperative. In the former, the control of the robot is given to one behaviour until the next execution cycle. On the

contrary, the latter combines recommendations from multiple behaviours to form a single control action which represents their consensus. Both strategies offer advantages and disadvantages. On the one hand, competitive methods provide good robustness but non-optimal paths from the point of view of their smoothness and length. Cooperative methods, on the other hand, present the opposite features.

After the previous analysis, it seems obvious that a hybrid methodology that is able to make the most of both coordination strategies is desirable. With this aim, a new concept called *activity level* has been introduced. It represents the urgency of a behaviour for taking the control of the robot in a certain moment, expressed by a real value within the interval [0,1]. Additionally, the hybrid coordinator assigns, in a dynamic way, priorities low and high to the behaviours according to whether they generate an activity level above or below a user-defined value. Moreover, a different threshold can be established for each behaviour. Once the prioritisation process has finished, the coordinator acts competitively between the aforementioned priority levels and cooperatively inside them.

Some comparative data between the cooperative and the hybrid approaches, obtained by simulation, are provided in figure 3. More precisely, the figure shows the resistance of a vehicle to collide when it is trapped into a box-shaped canyon and the goal point is beyond the walls. During the experiment, the gain of a GoTo-type behaviour was progressively increased keeping constant the weight of the basic obstacle avoidance primitive, whose activity level, for the hybrid case, was inversely proportional to the distance to the nearest obstacle detected. As can be observed in the figure, the hybrid coordination mechanism managed to avoid collisions for the length of all the simulations, while the cooperative version led to a collision almost all the times.

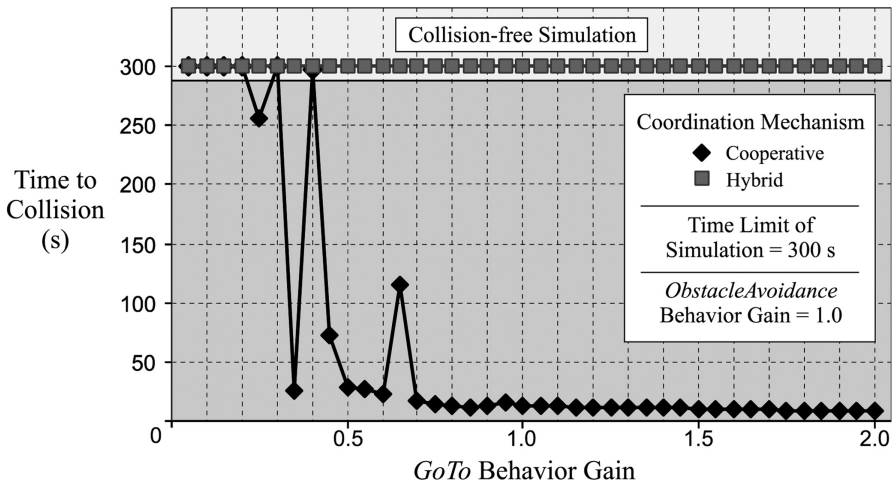

Figure 3. A comparison between a cooperative and a hybrid coordination mechanism

Identified Shortcomings

In robotic navigation, potential field methods are a well-known solution for dealing with unknown and dynamic scenarios by taking into account the reality of the environment during the robot motion. The characteristic elegance and simplicity of the approach when representing and successfully solving a path-planning problem in real-time explains its extensive application in this field. However, substantial shortcomings have been identified as problems inherent to this principle (Koren and Borenstein, 1991). *Getting stuck in local minima* is the best-known and most often-cited problem with PFMs. Consequently, several obstacle configurations may lead to undesirable trapping situations. Figure 4 shows, by way of example, how the underwater cable tracker is unable to escape from a U-shaped canyon. This result was obtained by using a 3D simulation environment named $NEMO_{CAT}$ (Antich and Ortiz, 2004 (a)) which incorporates the dynamic model of a real underwater vehicle called GARBI, designed and built by the Computer Vision and Robotics research group of the University of Girona (Spain), making thus the simulations more realistic.

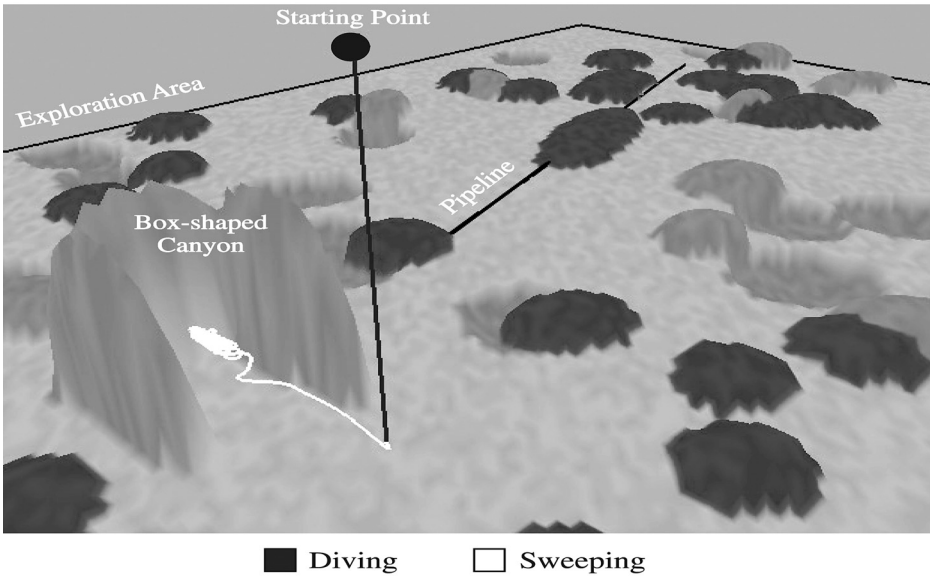

Figure 4. The AUV, after the diving stage, is trapped into a box-shaped canyon

In the next section, a new component will be added to the control architecture in order to solve the aforementioned problem.

A NEW NAVIGATIONAL APPROACH

A navigation strategy called *Random T²* will be explained now. It gives an efficient solution to the trapping problem by applying two new concepts: *Traversability* and *Tenacity*. Figure 5 shows the new navigation module integrated in the framework of the previously described behaviour-based control architecture. It mainly consists of a filtering process which makes the robot take a different direction to the one suggested by the coordination mechanism in case it is not appropriate for the present configuration of surrounding obstacles. The details are given in the following, together with a comparative study on the path length performance of the proposal for a series of experiments.

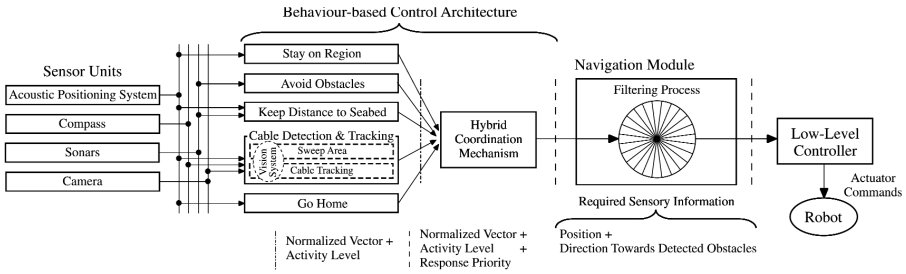

Figure 5. Complete underwater cable tracker's control system

The Filtering Process

The appropriate alteration of the direction of the motion vector generated by the coordination mechanism pertaining to the control architecture is the main concern of the filtering process. Such change is carried out according to the *traversability* and *tenacity* concepts. The former suggests banning those directions where an obstacle has been detected, choosing an obstacle-free direction close to the desired one. The latter, on the other hand, determines the way how that selection process has to be done. Essentially, a criterion of avoiding abrupt changes in the robot heading is applied.

As can be observed in figure 6(a), the space of directions around the robot is divided into K identical angular regions, and obstacles detection information for each region is stored in a suitable data structure, which also registers the approximate obstacles location. This information has to be kept updated as the robot moves, even when no new obstacles are detected in the environment (see figure 6(b)). Finally, in this context, a region is said to be *banned* when at least one obstacle is known to be in the range of directions which consists of.

After receiving the output of the reactive control system, its viability is studied on the basis of the traversability principle. Changes are required only if the

direction of the motion vector belongs to a banned region. In such a case, two alternative directions are obtained (see figure 6(c)) and a decision has to be made. In this work, this decision is taken in a random way the first time. Afterwards, the tenacity principle is applied by choosing between the two options the region closest to the one taken the last time.

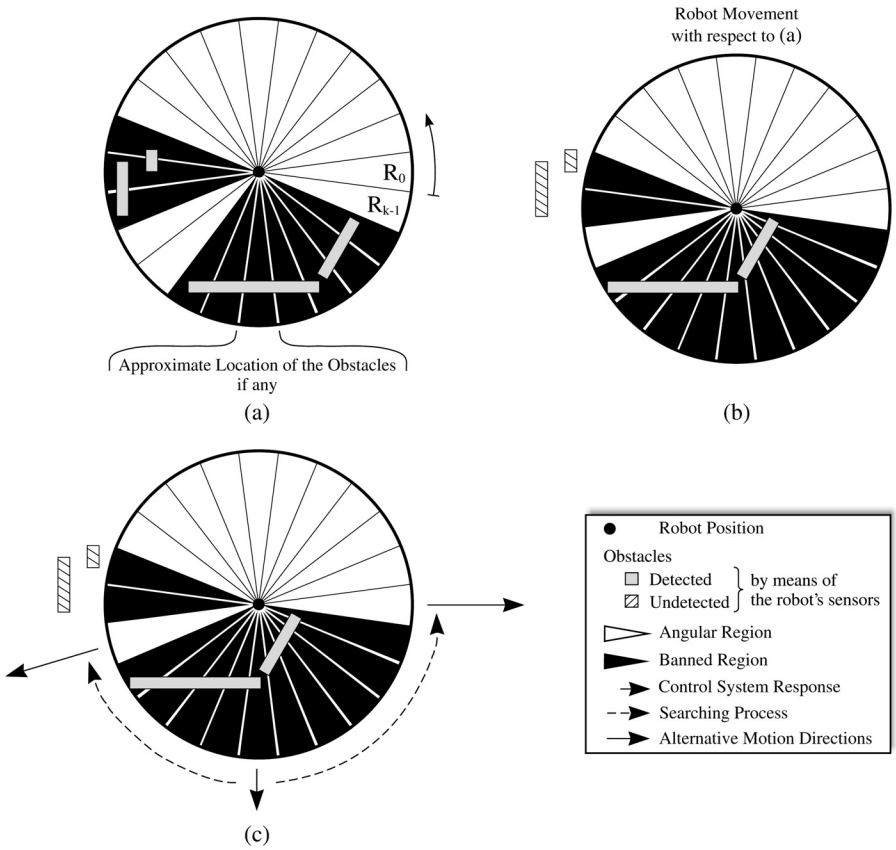

Figure 6. Implementation of the traversability concept: (a) division of the space of directions around the robot; (b) maintaining the region data coherence while navigating; (c) selection of two apparent obstacle-free motion directions

The application of all these steps results in a global system behaviour that can be summarized in two points:

— When the robot is navigating far from obstacles, it heads for its current goal which will be defined by either the *cable detection and tracking* or the *go home* behaviours depending on the mission stage. During this period of time, the filtering process remains inactive.

— After the detection of an obstacle, on the other hand, the robot follows its contour in a certain randomly-chosen direction until a way out is found. The repeated input of motion vectors linked to non-banned regions indicates the end of a presumed trapping situation. In such a case, the filter is reset loosing thus all the previously kept information.

By way of example, figure 7 shows how a robot is able to escape from a U-shaped canyon by applying the described process.

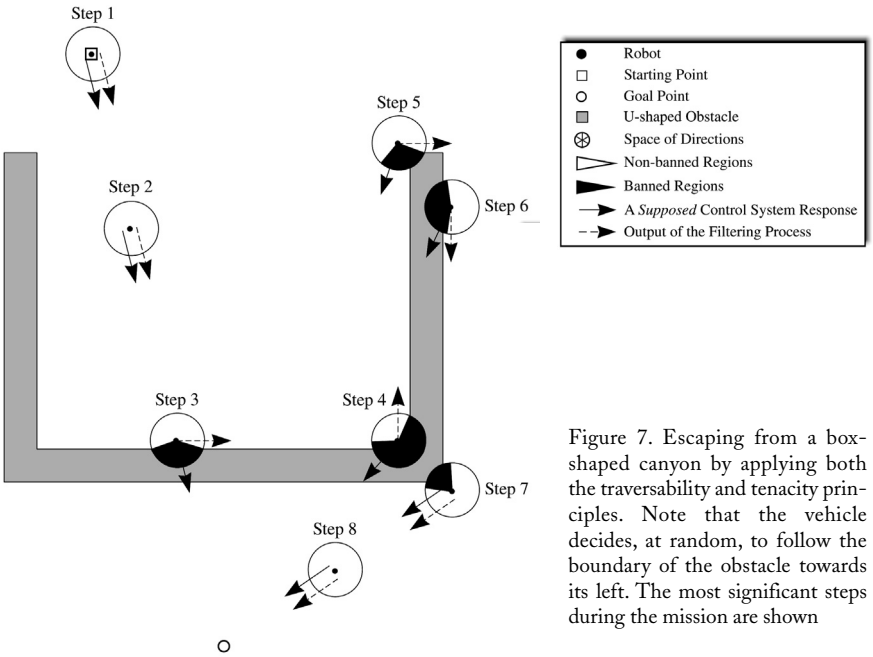

Figure 7. Escaping from a box-shaped canyon by applying both the traversability and tenacity principles. Note that the vehicle decides, at random, to follow the boundary of the obstacle towards its left. The most significant steps during the mission are shown

It is important to note how relatively easy this strategy detects potentially deadlock situations, mainly due to environment concavities, which may result in a cyclic behaviour. These are characterized by a space of directions fully, or almost fully, banned. In this kind of cases, contrary to other approaches, the robot tenaciously continues following the obstacle boundary rejecting an apparently correct but, in general, wrong path towards the goal.

In this way, the proposed navigation module solves the best-known and most often-cited problem of PFMs: trapping situations due to local minima. However, some other interesting properties stem from the application of the aforementioned principles. On the one hand, oscillations in both the presence of obstacles and in narrow corridors are significantly reduced owing to the restricted motion of the robot in directions where obstacles have not been detected. Better stability results are obtained when the robot is, additionally, forced to follow the obstacle contour in

only one direction by filtering sudden robot heading changes suggested by the reactive control layer. As a consequence, these robots are certainly suitable to navigate in cluttered environments with closely spaced obstacles.

A Comparative Study

In the following, a comparative study on the performance of the navigation strategy proposed is presented and discussed. The comparison is carried out from the point of view of a single criterion which is the length of the path between the starting and the goal points. The other algorithms considered in the study are: *Avoiding the Past*, *Learning Momentum* (LM), and *Micronavigation* (mNAV). A brief description of each of them is given next:

— *Avoiding the Past* makes the robot avoid recently visited locations by maintaining and utilizing a local spatial memory (Balch and Arkin, 1993).

— *LM* adjusts the behavioural parameters of a reactive control system at runtime depending on which one of several predefined situations the robot is in (Lee and Arkin, 2001).

— *μNAV* is a PFM-based approach which provides the robot with a hierarchy of simple behaviours designed for smooth obstacle avoidance and for escaping from concavities (Scalzo et al., 2003).

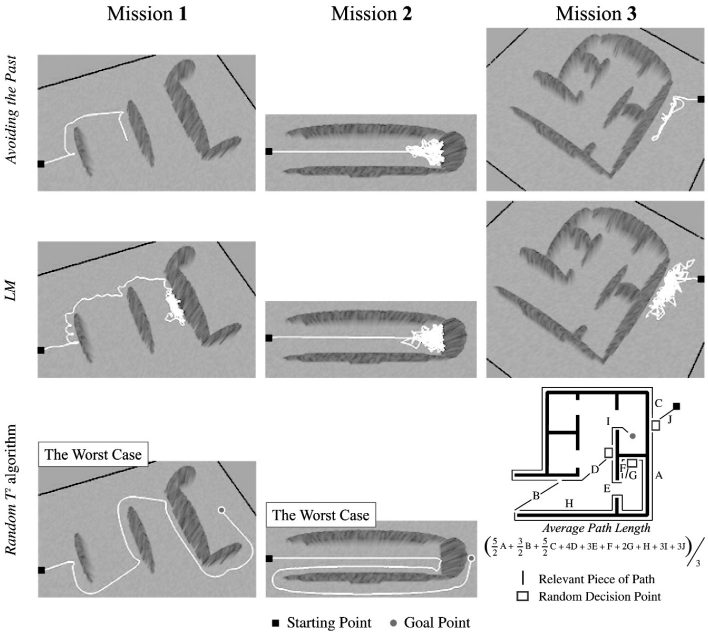

Figure 8. From top to bottom, paths generated by the Avoiding the Past, LM, and Random T2 approaches in NEMOCAT. Note that due to the non-deterministic behaviour of our strategy, different results can be obtained in different runs of the simulator. Only one, the worst, is shown in the figure whenever possible. A stochastic analysis about the average length of the AUV's path is presented when such worst case cannot be computed due to its infinite extent (see the details about this in (Antich and Ortiz, 2004 (b))

$NEMO_{CAT}$ was used again to measure the path length of the two first navigational approaches as well as *Random T²* under a simplified framework where a behaviour of the control architecture, *cable detection and tracking* or *go home*, was supposed to establish the only goal point considered for each mission. As can be observed in figure 8, three environments were defined. In the first one, walls/rocks of different length impede the progress of the vehicle towards its goal. The second environment, on the other hand, corresponds to a very deep box-shaped canyon. Finally, the third one appeared in (Ranganathan and Koenig, 2003), where a control system with deliberative capabilities was employed to solve it. *Avoiding the Past* and *LM* strategies were not able to successfully carry out any of the previously described missions, which shows their poor effectiveness to escape from large trapping areas. In both cases, the simulation was stopped after a travel time twice that of *Random T²*.

In order to continue with the study, a robot programming environment based on the AuRA (Arkin and Balch, 1997) architecture called *MissionLab* (Mackenzie et al., 1997) was also used. The latest release of this software (version 6.0) integrates the *mNAV* algorithm implemented by one of its authors. Different tests with increasing complexity were performed in MissionLab, simulating a holonomic robot equipped with several range finders, and wheel encoders to compute its position by means of dead-reckoning. As can be verified in (Scalzo et al., 2003), such experiments are a representative sample of the whole power of the *mNAV* strategy for a typical behaviour hierarchy. Each environment was then accurately reproduced in $NEMO_T$ and successfully solved by *Random T²*. The results obtained are shown in figure 9. Besides, table 1 compares the performance of both strategies from the viewpoint of the resultant path length.

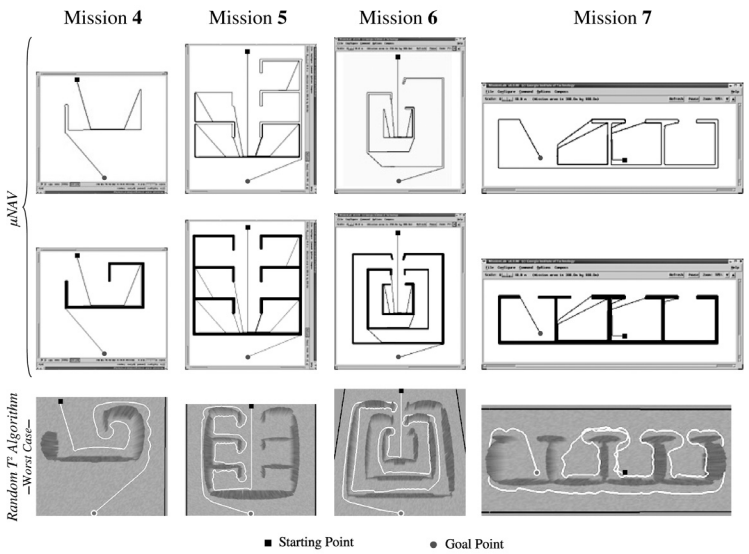

Figure 9. Simulation results for the *μNAV* (top -walls removed- and middle) and Random T² (bottom) algorithms by using MissionLab and $NEMO_{CAT}$, respectively

Mission	Algorithm Type		Improvement (%)	$\frac{\mu NAV}{Random\ T^2}$
	Random T^2 (average[1])	μNAV		
4	286.83	384.20	25.34	1.34
5	883.47	4180.41	78.87	4.73
6	1586.71	2489.40	36.26	1.57
7	675.42	1316.40	48.69	1.95
Total	3432.43	8370.41	58.99	2.40 (average)

Table 1. Comparing the path lengths (m) of Random T^2 and the μNAV strategies

As can be observed, our proposal produced, on average, trajectories between the starting and goal points 2.4 times shorter than *μNAV*. The difference derives from the fact that *μNAV* allows the robot, in general, to head for the goal as soon as it is faced without any immediate obstacle in the way, while *Random* T^2 limits the applicability of such rule to situations where a concavity is not detected.

The reader is referred to (Antich and Ortiz, 2004 (b)) for a more extensive comparative study using both simulation and real results. Specifically, a representative member of the popular Bug family of robot motion planning algorithms called *Bug2* is, in addition, taken into account.

CONCLUSIONS AND FUTURE WORK

A behaviour-based control architecture for visually guiding an AUV to detect and track a cable, or pipeline, laid on the seabed has been presented. A novel strategy to avoid the typical trapping problem associated with this kind of control systems has been proposed as the main contribution to this work. The approach called *Random* T^2 provides a solution in both local and global level by using a reduced amount of memory and computational resources. *Random* T^2 has been compared against other well-known algorithms sharing the same goal (*Avoiding the Past*, *Learning Momentum*, and *Micronavigation*). The length of the resulting paths has been used as the figure of merit. Our proposal generated, on average, trajectories 2.4 times shorter. These results were obtained by means of an underwater simulation environment named $NEMO_{CAT}$. In the near future, experimentation at sea with our SeaLion robot (see figure 10) will be carried out. An extension to three dimensions will also be addressed in the future to take advantage of the larger number of DOFs of underwater robots against land robots.

[1] In order to compute this value, all the possible paths between the starting and the goal points together with their corresponding probabilities of happening have been considered for each mission.

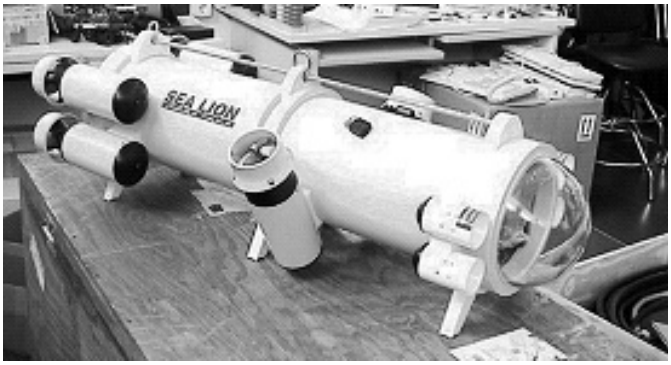

Figure 10. Torpedo-like robot belonging to our research group SRV

ACKNOWLEDGEMENTS

This study has been partially supported by project CICYT-DPI2001-2311-C03-02 and FEDER funds. Its authors wish to thank the Georgia Tech Research Corporation for the free distribution of the software *MissionLab*.

REFERENCES

Antich, J. and Ortiz, A. (2003) Underwater Cable Tracking by Visual Feedback, *Proceedings of the 1st iberian conference on Pattern Recognition and Image Analysis*, 4-6 June, Mallorca, Spain, pp. 53-61.

Antich, J. and Ortiz, A. (2004 (a)) An Underwater Simulation Environment for Testing Autonomous Robot Control Architectures, *Proceedings of the IFAC conference on Control Applications in Marine Systems*, 7-9 July, Ancona, Italy, pp. 509-514.

Antich, J. and Ortiz, A. (2004 (b)) *T²: An Approach to Robotic Navigation in Unknown and Dynamic Environments*. Technical Report A-3-2004. University of the Balearic Islands, Spain.

Arkin, R. and Balch, T. (1997) AuRA: Principles and Practice in Review. *Journal of Experimental and Theoretical Artificial Intelligence 9 (2), 175-189*.

Balch, T. and Arkin, R. (1993) Avoiding the Past: a Simple but Effective Strategy for Reactive Navigation, *Proceedings of the International Conference on Robotics and Automation*, vol. 1, pp. 678?685.

Koren, Y. and Borenstein, J. (1991) Potential Field Methods and their Inherent Limitations for Mobile Robot Navigation, *Proceedings of the International Conference on Robotics and Automation*, vol. 2, pp. 1398-1404.

Lee, J. and Arkin, R. (2001) Learning Momentum: Integration and Experimentation, *Proceedings of the International Conference on Robotics and Automation*, vol. 2, pp. 1975-1980.

Mackenzie, D. and Arkin, R. and Cameron, J. (1997) Multiagent Mission Specification and Execution. *Autonomous Robots 4 (1), 29-52*.

Ranganathan, A. and Koenig, S. (2003) A Reactive Robot Architecture with Planning on Demand, *Proceedings of the International Conference on Intelligent Robots and Systems*, vol. 2, pp. 1462-1468.

Ridao, P. and Batlle, J. and Amat, J. and Roberts, G. N. (1999) Recent Trends in Control Architectures for Autonomous Underwater Vehicles. *International Journal of Systems Science 30 (9), 1033-1056*.

Scalzo, A. and Sgorbissa, A. and Zaccaria, R. (2003) mNAV: a Minimalist Approach to Navigation, *Proceedings of the International Conference on Robotics and Automation*, vol. 2, pp. 2018?-2023.

Valavanis, K. and Gracanin, D. and Matijasevic, M. and Kolluru, R. and Demetriou, G. (1997) Control Architectures for Autonomous Underwater Vehicles. *IEEE Control Systems Magazine 17, 48-64*.

UN SISTEMA DE CONTROL REACTIVO BASADO EN CAMPOS DE POTENCIAL PARA UN VEHÍCULO CAPAZ DE DETECTAR Y SEGUIR VISUALMENTE CABLES SUBMARINOS EN ESCENARIOS COMPLEJOS

La operabilidad de una instalación submarina ¾cables de transporte de energía eléctrica o de telecomunicaciones y/o tuberías¾ puede sólo ser garantizada a través de un programa de inspección capaz de proporcionar a tiempo información sobre condiciones de peligro potenciales o daños causados por la movilidad del suelo oceánico, la corrosión o actividades humanas tales como el tráfico marino y la pesca. Hoy en día, estas tareas de vigilancia e inspección son realizadas por operadores que desde la superficie de un barco controlan un ROV (Remotely Operated Vehicle) sobre el que se han montado cámaras de vídeo. Evidentemente, ésta es una tarea tediosa en la que el operador debe permanecer largos periodos de tiempo concentrado en frente de una consola, favoreciendo todo ello la aparición de errores cuyo origen es, principalmente, la pérdida de atención y la fatiga. Además, las peculiares características de las imágenes obtenidas del fondo marino ¾*blurring*, bajo contraste, iluminación no uniforme, etc.¾ dificultan aún más la ya compleja operación. Por tanto, la automatización de cualquier parte de este proceso puede constituir una importante mejora en el mantenimiento de este tipo de instalaciones, no sólo en cuanto a la reducción del tiempo de inspección y de los errores, sino también de los costes asociados.

Con este objetivo, en este artículo, se propone un sistema de control para realizar el guiado de un AUV (Autonomous Underwater Vehicle) capaz de detectar y seguir autónomamente un cable/tubería sobre la base de retroalimentación visual. Dicho sistema incorpora, adicionalmente, una novedosa estrategia de evitación de obstáculos/navegación que permite al vehículo escapar rápidamente de cualquier situación de aprisionamiento potencial.

El subsistema de visión, por un lado, aprovecha la característica rigidez y forma del cable/tubería para localizarlo en las imágenes que procesa. Múltiples secuencias de imágenes reales captadas con un ROV han sido utilizadas en su validación. Estas imágenes muestran cables parcialmente cubiertos por algas y arena estando a su vez rodeados por algas y rocas, lo que las hace altamente realistas. La tasa media de aciertos alcanzada ha sido de aproximadamente del 90% para una tasa de imágenes de más de 40 por segundo.

En cuanto a la arquitectura de control, siendo reactiva , está basada en comportamientos descritos como campos de potencial, todo ello con la intención de interactuar adecuadamente con un entorno dinámico y no estructurado como es el

submarino. Simplicidad, robustez y modularidad son las principales características de este enfoque. No obstante, de él también se derivan varios problemas entre los que destaca el de aprisionamiento o bloqueo debido a mínimos locales. Diferentes configuraciones de obstáculos pueden dirigir a esta situación, tal como el típico cañón en forma de U. Por esta razón, al sistema de control se le ha añadido en su etapa final un nuevo componente denominado *Random T²* que da solución al problema aplicando dos nuevos conceptos: *Traversabilidad* y *Tenacidad*. Básicamente, este componente, dependiendo de la configuración de obstáculos existente alrededor del vehículo, puede seleccionar como salida una dirección de movimiento diferente a la sugerida por las etapas previas del sistema. La estrategia ha sido comparada con otras aparecidas en la literatura que son habitualmente referenciadas: *Avoiding the Past*, *Learning Momentum* y *Micronavigation*. Para ello, se ha hecho uso de NEMO-CAT, un entorno de simulación 3D implementado con OpenGL que incorpora el modelo hidrodinámico de un vehículo real diseñado y construido por el grupo de investigación *Computer Vision and Robotics* de la Universidad de Gerona denominado GARBI.

CONCLUSIONES

El presente artículo presenta una novedosa arquitectura de control para el seguimiento de cables/tuberías submarinas utilizando retroalimentación visual. Ésta incorpora una estrategia específica para evitar el típico problema de aprisionamiento característico de todos aquellos sistemas de control reactivos basados en el principio de campos de potencial. Una solución tanto a nivel local como global ha sido aportada haciendo uso de una reducida cantidad de recursos computacionales y de memoria. A su vez, un estudio comparativo de la eficiencia de la estrategia desde el punto de vista de la longitud del camino recorrido por el vehículo hasta su objetivo ha sido llevado a cabo. Como resultado, nuestro algoritmo generó, en media, trayectorias 2.4 veces más cortas.

Journal of Maritime Research, Vol. II. No. 1, pp. 51-67, 2005

ISSN: 1697-4840

AN ANALYSIS OF MODELS IDENTIFICATION METHODS FOR HIGH SPEED CRAFTS

J. Aranda[1], R. Muñoz[2], S. Dormido Canto[3], J.M. Díaz[4] and S. Dormido Bencomo[5]

Abstract

Two different approaches of the system identification method have been proposed in order to estimate models for heave, pitch and roll dynamics of a high speed craft. Both of them resolve the identification subject as an optimization problem to fit the best model. The first approach uses genetic algorithms and nonlinear least squares with constraints methods applied in the frequency domain. The second one suggests a new parameterization which facilitates obtaining high quality starting values and avoids non-quadratic functions in the cost function. At last it is shown an example in which the two approximations are applied and compared.
Keywords: system identification, optimization problem, genetic algorithms, nonlinear least squares.

INTRODUCTION

The response of a ship advancing in a seaway is a complicated phenomenon involving the interactions between the vessel dynamics and several distinct hydrodynamic forces. All ship responses are non linear to some extent, but in many cases when nonlinearities are small a linear theory will yield good predictions.

[1] Profesor de la Universidad Nacional de Educación a Distancia (jaranda@dia.uned.es).C/ Juan del Rosal 16. 28040 Madrid. Spain
[2] Profesor Ayudante de la Universidad Nacional de Educación a Distancia (rmunoz@dia.uned.es).
[3] Profesor de la Universidadd Nacional de Educación a Distancia (sebas@dia.uned.es).
[4] Profesor Colaborador de la Universidad Nacional de Educación a Distancia (josema@dia.uned.es).
[5] Catedrático de la Universidad Nacional de Educación a Distancia. (sdormido@dia.uned.es).

The study is focused on a ship advancing at constant mean forward speed with arbitrary heading in a train of regular sinusoidal waves. Experimental and theoretical investigations have shown that a linear analysis of ship motions give excellent results over a wide variety of sea conditions.

The past decade has seen a growing interest on high speed crafts for both cargo and passenger transportation. Different designs have been considered, and a significant attention has been focused on fast mono-hull displacement ships. One of the objectives in the design is passenger comfort and vehicle safety. Vertical accelerations associated with roll, pitch and heave motions are the main cause of motion sickness. For that reason, a first goal is to damp these three movements.

Therefore, it is necessary to build a mathematical model of the dynamical system that permits the designing of a controller which achieves the reduction of the heave, pitch and roll motions, and consequently the reduction of the motion sickness index.

Thus, as an initial study, previous researches of the work group have studied the longitudinal and transversal dynamics separately. Firstly, it has been studied heaving and pitching motion for the case of head seas, (μ=180deg) (Aranda et al., 2004a), modeled actuators and designed different controllers, (Aranda et al., 2002a, 2002b), in order to achieve heave and pitch damping and with successful results. And secondly, it has been analyzed the rolling response for the case of lateral waves (μ=90deg) (Aranda et al., 2003) and in the same way, it has been carried out the actuators modeling and controller designing (Aranda et al., 2004b).

In the present work the study has been extended to an analysis of heave, pitch and roll dynamics with different incidence angles between 180 degrees and 90 degrees.

There are many publications related to the ships modelling (Fossen, 2002; Lewis, 1989). In this work modeling is obtained from system identification method (Söderström et al, 1989; Pintelon and Schoukens, 2004), which is based on the observed input output data.

This research presents two approaches for identifying continuous transfer functions of the vertical and transversal dynamics of a high speed craft. In the first one the problem is set out as a nonlinear optimization problem with nonlinear constraints (Aranda et al., 2004). There, the proposed solution is described with a hybrid optimization method (genetic algorithm + nonlinear optimization algorithm with constraints from the Matlab toolbox). In the second one a discussion on the first method is made (Pintelon and Shoukens, 2004) and some questions are raised, in order to obtain models more efficiently. There, these new improvements and their application are depicted.

Thus, this paper is organized as follows. Firstly it is presented the basic steps in systems identification, where the criterion of fitness is developed. Secondly, it is presented the discussion on identification and the new solution of the problem. Finally, an example is shown in order to compare the two approaches.

SYSTEM IDENTIFICATION

The system identification problem is to estimate a model of a system based on observed input-output data. This procedure involves three basic steps: the input-output data, a set of candidate models (the model structure), and a criterion to select a particular model in the set, based on the information in the data (the identification method).

In general terms, an identification experiment is performed by exciting the system and observing its input and output over a time interval. These signals are recorded. Then it is tried to fit a parametric model of the process to the recorded input and output sequences. The procedure is illustrated in Figure 1 (Söderström and Stoica, 1989).

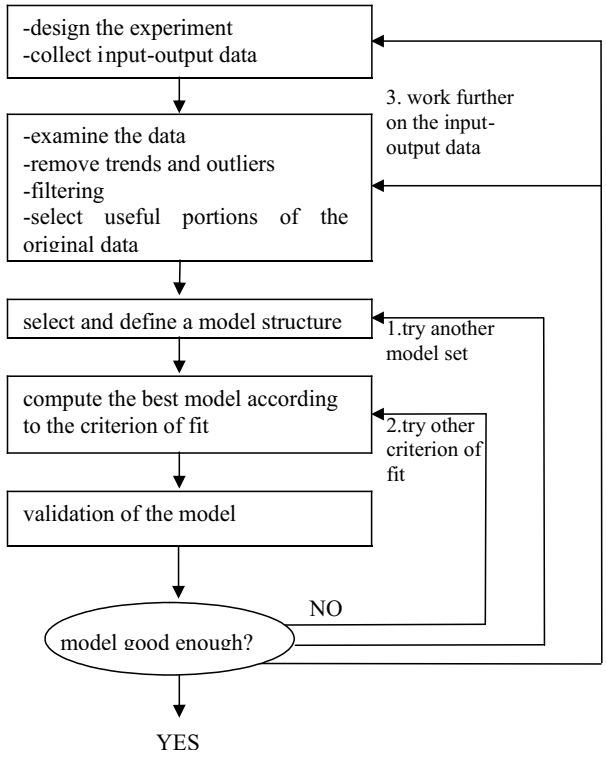

Figure 1. Identification procedure

Diverse experiments in CEHIPAR (El Pardo Model Basin, Spain) are made with a scaled down replica (1:25) of the TF120 ferry. Also there is a second self-propelled replica which is scaled (1:40).

In order to analyze the dynamic of the fast ferry, tests with diverse types of waves, ship speeds and different angles of incidence have been made. Also CEHIPAR has a program simulation PRECAL, which reproduces specified conditions and uses a geometrical model of the craft to predict its dynamic behavior. PRECAL solves the physical equations of the dynamic of a ship by using the Band Theory (Fossen, 2002). The program gives amplitude and phase data at different frequencies.

The experimental input- output data are generated by the program simulation PRECAL. Simulations are tried with regular waves, with the following characteristics,

— natural frequency between the rank [0.393,1.147] rad/s

— angles of incidence 90º, 105º, 120º, 135º, 150º, 165º, 180º

— ship speed 20, 30 and 40 knots.

Tests consist of excitation of the ship system by the sea wave (the input is the wave height (m)). For each type of wave, that is, wave frequency and angle of incidence, the ship responses are measured. In this case, the study is focused on heave, pitch and roll modes. Thus, the given outputs are the following (BAZAN, 1995): amplitude and phase of total the force of excitation heave, amplitude and phase of the total moments of excitation pitch and roll, amplitude and phase of the motion response heave, and amplitude and phase of the motion responses pitch and roll.

The block diagram of the system to identify is depicted in figure 2.

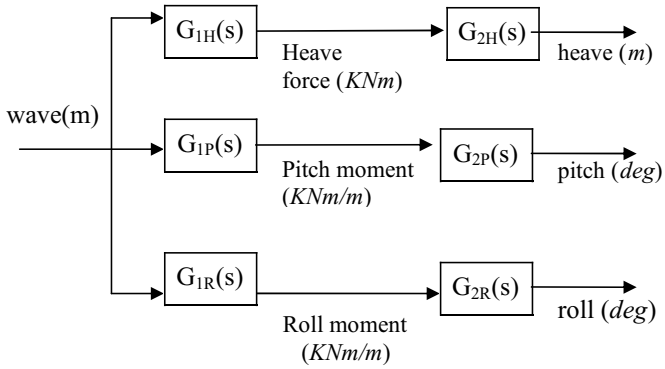

Figure 2. Block diagram of the system

Thus, the transfer functions to be modelled are the following

$G_{1H}(s)$: from wave height (m) to heave force (kN)

$G_{2H}(s)$: from heave force (kN) to heave motion (m)

$G_{1P}(s)$: from wave height (m) to pitch moment (kNm)

$G_{2P}(s)$: from pitch moment (kNm) to pitch motion (degrees)
$G_{1R}(s)$: from wave height(m) to roll moment (kNm)
$G_{2R}(s)$: from roll moment (kNm) to roll motion (degrees)
Based on the principle of linear superposition, it yields that

$$G_Z(s) = G_{1Z}(s) \cdot G_{2Z}(s), Z = H, P, R \tag{1}$$

Therefore, the given input output data are used to identify directly the transfer functions $G_Z(s)$ whose input is the wave height, and the outputs are the heave, pitch or roll motions, and similarly the transfer functions $G_{1Z}(s)$, whose input is the wave height, and the outputs are heave force, pitch moment, or roll moment. The identification of the transfer functions $G_{2Z}(s)$ are made indirectly, by using the relation (1).

Once the experiments with the system to model are designed, and the obtained input output data are examined, next step is to select and define a model structure and give a criterion of fit, so that it can be computed the best model that reproduces the dynamic of the ship system more suitably.

The system identification gives the mathematical model in the form of transfer function. Data given by the simulator PRECAL are in the frequency domain. Therefore, it will be carried out a parametric estimation of the transfer functions in the frequency domain.

In this way, consider the general parameterized transfer function (2). The estimation of the model consists of the fitness of the frequency response or Bode diagram of a transfer function with a fixed number of poles and zeros (model structure) to the actual measured data.

$$G(s,\theta) = \frac{B(s,\theta)}{A(s,\theta)} = \frac{b_{m+1}s^m + b_m s^{m-1} + ... + b_1}{s^n + a_n s^{n-1} + ... + a_1} \tag{2}$$

For the identification of the model it is employed a parametric method, characterized by the adjustment of the collected data to an estimated parameter vector θ,

$$\theta = (b_{m+1}, b_m, b_{m-1}, ..., b_1, a_n, a_{n-1}, ...a_1) \tag{3}$$

The parameter vector θ is determined as the vector that minimizes the sum of squared equation errors. Thus, it is defined the cost function J(θ):

$$J(\theta) = \sum_{i=1}^{N} \left| G(j\omega_i) - G(j\omega_i, \theta) \right|^2 \tag{4}$$

in this way, the parameter vector is obtained such

$$\hat{\theta} = \arg\min_{\theta} J(\theta) \tag{5}$$

In order to solve the minimization problem and therefore estimate a transfer function model, it must be considered the following factors

1. A physical insight of the dynamic of the system states that at low frequencies roll and pitch responses amplitudes must tend to zero, while the heave response amplitude must tend to one. That is

$$\begin{aligned} &\text{Heave: } G_{1H}(j\omega), G_{2H}(j\omega) \xrightarrow[\omega\to 0]{} 1 \\ &\text{Pitch: } G_{1P}(j\omega) \xrightarrow[\omega\to 0]{} 0 \\ &\text{Roll } G_{1R}(j\omega) \xrightarrow[\omega\to 0]{} 0 \end{aligned} \tag{6}$$

that it is translated for the parameter vector θ

$$\begin{aligned} &G_{1H}(s) \text{ y } G_{2H}(s) \rightarrow |a_1| = |b_1| \\ &G_{1P}(s) \rightarrow b_1 = 0 \\ &G_{1R}(s) \rightarrow b_1 = 0 \end{aligned} \tag{7}$$

2. The system must be stable. It is translated into the poles of the transfer function must belong to the left plane s. Thus, to ensure the stability of the estimated models the transfer functions are reparametrized as

$$G(s,x) = \frac{x_{n+m+1}s^m + x_{n+m}s^{m-1} + \ldots + x_{n+1}}{\prod_{i=1}^{npc}\left(s^2 + 2x_{2i-1}s + x_{2i-1}^2 + x_{2i}^2\right)\prod_{i=1}^{nps}\left(s + x_{npc+i}\right)} \tag{8}$$

with n = nps + npc and

$$\begin{cases} x_{2i-1} < -0.005 \text{ for i} = 1, 2, \ldots, \text{npc} \\ x_{npc+i} < -0.005 \text{ for i} = 1, 2, \ldots, \text{nps} \end{cases} \tag{9}$$

Then, the parameters x are obtained by minimizing

$$\sum_{i=1}^{N} \left| G(j\omega_i) - G(j\omega_i, x) \right|^2 \quad \text{subject to (7) and (9)} \tag{10}$$

It is important to note that the constraint $|a_1| = |b_1|$ is a strongly nonlinear function of x. This nonlinear minimization problem with nonlinear constraints is solved using the nonlinear optimization toolbox of Matlab.

Starting values are obtained via a genetic algorithm (Michalewicz, 1999) or generated at random. The solution of (10) is used as initial guess for a multistep procedure, also called alternating variables method (Fletcher, 1991).

The multistep procedure is motivated by the fact that direct measurements of the heave force to heave motion, pitch moment to pitch motion, and roll moment to roll motion dynamics are not available. Therefore, transfer functions $G_{1Z}(s)$ and $G_Z(s)$ (with Z = H, P or R) are directly estimated by minimizing (10). The solution given is used to identify the transfer function $G_{2Z}(s)$ (Z = H, P or R) by minimizing

$$\sum_{i=1}^{N} \left| G_Z(j\omega_i) - G_{1Z}(j\omega_i, x_a) G_{2Z}(j\omega_i, x_b) \right|^2 \text{ subject to (7) and (9)} \qquad (11)$$

successively x_a is determined for fixed x_b, and x_b is determined for fixed x_a, with $G_Z(j\omega_i)$ the simulated data and Z = H, P or R.

THE IDENTIFICATION METHOD

In this section some suggestions are made about the method described in the previous section. The fundamental questions are raised about: the excitation signal and plant model, the parametrization of the transfer functions, the choice of the starting values, and the multistep procedure.

Choice of the excitation signal and the plant model

Since the heave, pitch and roll dynamics of a ship are described by nonlinear differential equations (Kenevissi, 2003), it is important the choice of the excitation signal. It is shown that the frequency response of a system depends on the class of excitation signal used.

It is important that the type and power of the waves used for the linear identification experiment (linear approximation of the true nonlinear behaviour) coincides with the type and the power of the waves that the controller or actuators elements should compensate for in real life.

In this particular case the identification and validation are performed with respectively regular (single sines) and irregular (broadband signal) waves. Regular waves do not exist in nature, however they are very useful for the identification method and obtaining a linear model. The frequency rank and height of the sinusoidal signal used belong to the frequency spectral and amplitudes of the irregular waves, which are those that the real system could find.

In system identification the determination of model structure is an important aspect. And overparametrized model structure can lead to unnecessarily complicated computations for finding the parameter estimates and for using the estimated model. And underparametrized models may be very inaccurate. Therefore, it is necessary to employ methods to find an appropriate model structure. In practise identification often is performed for an increasing set of model orders. Then one must know when the model order is appropriate, i.e, when to stop. Needless to say, any real-life data ser cannot be modelled exactly by a linear finite-order model. However, the methods for finding the 'correct' model order are based on the statistical assumption that the data come from a true system within the model class considered.

Concerning the problem of choosing the model structure, the following question is raised: In the comparison between the frequency response or Bode diagram of the modelled transfer functions and the data (Aranda et al., 2004), it is observed that there is a discrepancy in the high frequency range. Thus one can wonder whether these differences are due to the intrinsic nonlinear behaviour of the heave, pitch and roll motions, or to a deliberate simplification of the linear dynamics.

For that reason, it is proposed that one way of guaranteeing that the best (in least square sense) linear approximation has been obtained, and therefore, that all the remaining errors are then due to nonlinear effects, is the utilization of classical model selection criteria such as the Akaike information criterion (AIC), and the whiteness test of the residual applied to the identification data (Ljung, 1999; Söderström et al., 1989).

Therefore, in the new approach of the identification method, these criterions are applied in order to ensure the best model structure and thus the best linearization.

Parameterization issues and starting values

Originally, in order to ensure the system stability, a re-parameterization of the transfer functions is carried out (8). Consequently the constraint (7) results in a cost function (10) that is strongly non-quadratic function of the model parameters. As a consequence of this parameterization, several disadvantages appear (Pintelon and Schoukens, 2004):

— Because of the nonlinear minimization and nonlinear constraints, the generation of starting values is non-trivial, especially for high order systems.

— The selection of the model is more complicated since the number of real nps and complex conjugate npc poles should be estimated. However, parameterization (2) only needs the number of total poles n.

— The classical derivative based nonlinear optimizers (Fletcher, 1991) will degenerate for multiplicities higher than one. On the other hand, parameterization (2) does not impose nor exclude particular pole positions and pole multiplicities.

These problems can be avoided as follows:
Using parameterization (2), cost function can be written as

$$\sum_{i=1}^{N}\left|G(j\omega_i)-\frac{B(j\omega_i,\theta)}{A(j\omega_i,\theta)}\right|^2 \quad \text{subjetc to (7) and (9)} \tag{12}$$

Thus, the nonlinear constraint $|a_1| = |b_1|$ can easily be satisfied by minimizing the cost function two times: first subject to $a_1=b_1$, next subject to $a_1 = -b_1$, and finally selecting the solution with the smallest cost function.

Applying the same trick, high quality starting values for (12) can be obtained via the linear least squares estimate

$$\sum_{i=1}^{N}\left|A(j\omega_i,\theta)G(j\omega_i)-B(j\omega_i,\theta)\right|^2 \quad \text{subjetc to (7)} \tag{13}$$

Concerning the stability constraint, two different approaches are possible for imposing it. Either the constraint is imposed during the minimization as proposed in the previous method and in Van Gestel et al. (2001), or first and unconstrained optimal noise removal problem is solved and next a stable approximation is calculated (Mari, 2000). In this case the first scheme is applied.

The Multistep procedure

As it is has been commented in previous sections, the input output data which are obtained from the simulations are the input wave and outputs forces or moments, and the input wave and outputs the movements. These data are used directly for the identification of the transfer functions $G_{1Z}(s)$ and $G_Z(s)$, with Z = H, P or R.

The alternating variables method or multistep procedure proposed to minimize (11) is usually inefficient and is not guaranteed to converge to a stationary point of (11).

Hence, another proposed approach is to minimize simultaneously x_a and x_b. If parameterization (2) is used, this scheme will be easier since high quality starting values are available via (13).

Once questions and how to solve them are set out, next section show the definitive approach for the identification problem.

RESOLUTION TO THE IDENTIFICATION PROBLEM

In this section it is described the procedure developed for the identification of the models, considering all the suggestions raised in previous sections.

Collecting input-output data

For each particular case of force, moment or motion of heave, pitch and roll responses, initially there are a set of N experimental points of amplitude $|G(j\omega_i)|$ and phase $arg(G(j\omega_i))$, for each type of wave, characterized by the natural frequency ω_{oi}, with i = 1..N.

It must be considered that the frequency of oscillation of a ship response when a wave with natural frequency ω_o reach the ship with an angle μ, is the frequency of encounter ω_e, which is determined by

$$\omega_e = \omega_0 - \frac{\omega_0^2}{g} U_0 \cos\mu \tag{14}$$

According to this, the starting point are the experimental data, $G(j\omega_{ei})$, i=1…N, that expressed in binomial form are

$$G(j\omega_{ei}) = |G(j\omega_{ei})|\cos(\arg(G(j\omega_{ei}))) + j|G(j\omega_{ei})|sen(\arg(G(j\omega_{ei}) \tag{15}$$

Criterion of fit.

According to what it has been already commented, the identification problem is solved as an optimization problem. The transfer function to be estimated, with m zeros and n poles is :

$$G(s,\theta) = \frac{B(s,\theta)}{A(s,\theta)} = \frac{b_{m+1}s^m + b_m s^{m-1} + ... + b_1}{s^n + a_n s^{n-1} + ... + a_1} \tag{16}$$

where the parameter vector θ is:

$$\theta = (a_1, a_2, ..., a_{n-1}, a_n, b_1, ..., b_{m-1}, b_m, b_{m+1}) \tag{17}$$

In order to facilitate calculations in the resolution of the optimization problem, the parameter vector is redefined in terms of the x variable:

$$x = (x_1, x_2, ..., x_n, x_{n+1}., , , , , x_{n+m}) \tag{18}$$

Thus, the transfer function is:

$$G(s,x) = \frac{B(s,x)}{A(s,x)} = \frac{x_{m+1}s^m + x_m s^{m-1} + ... + x_{n+1}}{s^n + x_n s^{n-1} + ... + x_1} \tag{19}$$

and then the cost function J(x) is

$$J(x) = \sum_{i=1}^{N} \left| G(j\omega_i) - G(j\omega_i, x) \right|^2 \tag{20}$$

The problem of obtaining the value of the parameters x that find the minimum of the multivariable function J(x) is solved with the Matlab optimization toolbox.

Constraints

The constraints of the problem are

i) $|b_1| = |a_1|$ for $G_{1H}(j\omega_e)$, $G_{2H}(j\omega_e)$

This condition is translated for the parameters vector x into:

$$\left| x_{n+1} \right| = \left| x_1 \right| \tag{21a}$$

ii) $|b_1| = 0$ for $G_{1P}(j\omega_e)$

In order to ensure that this constraint is satisfied in the identification of the model wave to pitch moment, it is necessary to impose in the parameter vector x that

$$x_{n+1} = 0 \tag{21b}$$

iii) System stability. This constraint forces the real part of the poles to be negative, that is, to be in the left hand on the s-plane.

Starting values.

High quality starting values, i.e, near to the global optimum, are basic to reach the convergence point. In [1], starting values are obtained via a genetic algorithm or generated at random. The trouble met in the identification of new models with different angles of incidence is that in many occasions, due that starting values were not adequate or distant from the minimum, the procedure of minimization was long and costly. This was intensified when genetic algorithms were used, since it is a method based on the heuristic that did not give good results in many cases. For that reason, it is developed a new method to obtain the starting values x_0. This method consists of a linear least square estimation. From the cost function J(x) expression:

$$J(x) = \sum_{i=1}^{N} \left| G(j\omega_{ei}) - G(j\omega_{ei}, x) \right|^2 = \sum_{i=1}^{N} \left| G(j\omega_{ei}) - \frac{B(j\omega_{ei}, x)}{A(j\omega_{ei}, x)} \right|^2 \tag{22}$$

it yields:

$$\sum_{i=1}^{N} \left| A(j\omega_{ei}, x) G(j\omega_{ei}) - B(j\omega_{ei}, x) \right|^2 \tag{23}$$

Therefore, a problem of least squares is set out. For each frequency value ω_{ei}, the denominator $A(j\omega_{ei},x)$ and numerator $B(j\omega_{ei}, x)$ are only function of the vector x, and $G(j\omega_{ei})$ is a complex value. Hence, rewriting the above expression leads to an equation of the type c * x – d = 0, where x is the parameters vector (the starting values) to estimate.

Next, considering all the points i = 1..N, that is, all the frequencies w_{ei}, one matrix C with N files and n+m columns, and one column vector with n+m size are given. Thus it is raised a least squares problem

$$C \cdot x - d = 0 \tag{24}$$

Multistep procedure. Identification of the transfer functions $G_{2Z}(s)$.

In this work, originally it is proposed the multistep procedure, where $G_{2Z}(s,x_b)$ is identified from the previously estimated transfer function $G_{1Z}(s,x_a)$ and the data $G_Z(s)$ (11). As an alternative to this procedure, it is suggested to solve simultaneously both transfer functions and estimate the parameters vector x_a and x_b at the same time.

Another approach for estimating $G_{2Z}(s)$ is to make a previous hypothesis of linearity and determine the points to fit the transfer function from the linear superposition principle. Thus, for each frequency of encounter of wave ω_{ei}, i =1..N:

$$|G_{2Z}(j\omega_{ei})| = \frac{|G_Z(j\omega_{ei})|}{|G_{1Z}(j\omega_{ei})|}; \qquad \arg(G_{2Z}(j\omega_{ei})) = \arg(G_Z(j\omega_{ei})) - \arg(G_{1Z}(j\omega_{ei})) \tag{25}$$

where Z = H, P, R.

AN EXAMPLE

The whole work tries to identify a continuous linear model of heaving, pitching and rolling dynamics. Specifically, models of G_{1H}, $G_{2H,}$ $G_{1P,}$ $G_{2P,}$ $G_{1R,}$ and G_{2R} are identified for incidence waves between 90 and 180 degrees. Each plant models set have the same number of poles and zeros.

In this section it is shown a practical case of application and comparison of the two approaches commented. Specifically, it is presented the identification of the model corresponding to the wave to heave force plant, for the incident angle 135º and ship speed 40 knots.

Thus, for each case, it is presented the transfer function model identified and the Bode diagram in which it is compared with the true data. Besides it is shown the temporal response of the final model identified, for the particular case of irregular waves SSN=5.

Wave to Heave Force $G_{1H}(s)$ Model:. First approach

As it has been noted in previous sections, first step is to select a set of candidate model structures. Table 1 shows two of these considered model structures (m,n,nps), and the value of the cost function *J* for speed 40 knots. Here, *m* is the number of zeros, *n* is the total number of poles, and *nps* is the number of simple poles. The parameter vector *q* and transfer function are determined for each model structure. These all models give very similar Bode plots in the frequency range of interest, so this is a proof that these must reflect features of the true system. Structure with minimum *J* is selected as the best model.

model structure (*m,n,nps*)	cost function J
(3,4,2)	0.51
(3,3,1)	0.79

Table 1. Model structures, cost function J and AIC

Finally, structure (3,4,2) is chosen, and the estimated transfer function is

$$G_{1H}(s) = 9333\frac{76.56s^3 - 22.21s^2 + 322.5s - 14.92}{s^4 + 21.26s^3 + 154.7s^2 + 289s + 14.92} \qquad (26)$$

Figure 3 shows the Bode plots of the estimated transfer function and the simulated true data. It can be seen that the model is quite capable of describing the system.

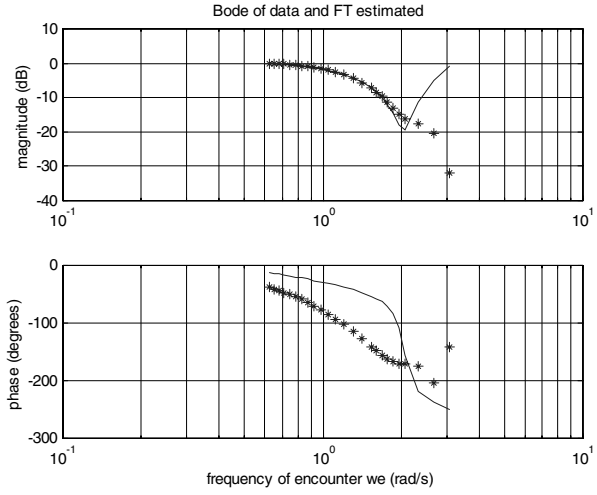

Figure 3.Bode plot of $G_{1H}(s)$ and experimental data

Finally, figure 4 shows the response in the temporal domain of the model identified.

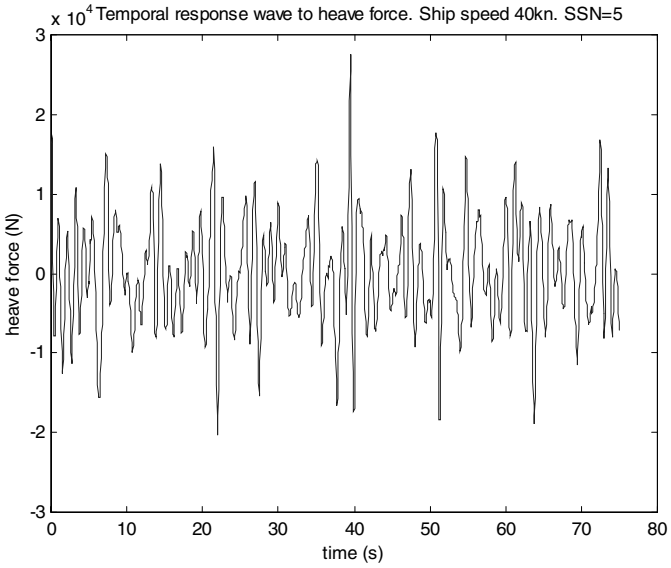

Figure 4.Temporal response $G_{1H}(s)$

Wave to Heave Force $G_{1H}(s)$ Mode: Second approach.

Table 2 shows two of the model structures (*m* is the number of zeros,and *n* the number of poles) that had been tried, and the respective values of AIC and cost function *J*. According to Akaike's theory, those with the lower value AIC is selected. In this case, structure (3,4), with *m* = 3 zeros and *n* = 4 poles gives the best result, so this structure is the chosen one.

model structure (m,n)	AIC	cost function J
(3,4)	-63.31	0.0347
(3,3)	-54.71	0.055

Table 2. Model structures, cost function J and AIC

Once model structure is fixed, the identification procedure is executed and the following transfer function is estimated:

$$G_{1H}(s) = 9333\,\frac{26.02s^3 - 22.13s^2 + 160.9s^1 + 0.9}{s^4 + 125.4s^3 + 149.1s^2 + 181.3s^1 + 0.9} \qquad (27)$$

Figure 5 shows the comparison between the Bode diagram of the transfer function identified and the actual data. It is shown that the model fits the data quiet good. Next, figure 6 shows the temporal response of the final estimated model.

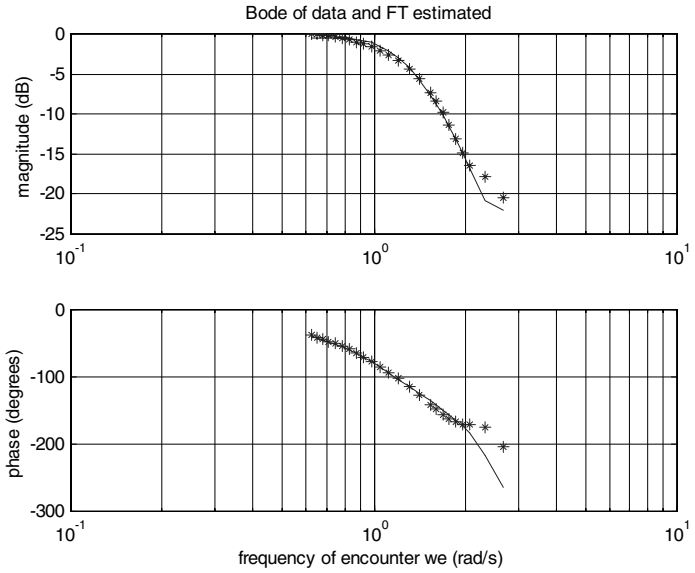

Figure 5. Bode plot of $G_{1H}(s)$ and data

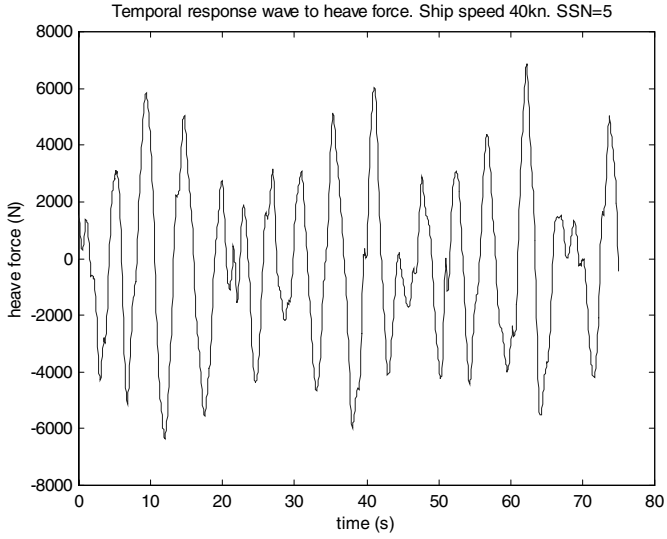

Figure 6. Temporal response $G_{1H}(s)$

Wave to Heave Force $G_{1H}(s)$ Model: Comparison.

Evaluating the results of the two implementations, it is seen in numerical results and graphics that the second approach estimates a transfer function model that fits the data more accurately. In addition, in the Bode diagram of the first $G_{1H}(s)$ it is observed that the amplitudes at high frequencies are too much large, which is translated into a very oscillatory and not proper behaviour in the temporal response.

CONCLUSIONS

In this paper two different approaches of the system identification method has been proposed in order to analyse and identify models for the heave, pitch and roll dynamics of a high speed craft.

The first approach uses genetic algorithms and non linear least squares with constraints methods applied in the frequency domain as a criterion of fit to compute the best model. This method has been employed to model the vertical dynamic (heave and pitch modes) for the particular case of waves from directly ahead. However, when the study is extended to the horizontal dynamic (roll mode) and in addition other angles of incidence, it is not obtained such good models. Furthermore, it is observed that the technique does not guarantee the best linear approximation, and involves a lot of computational load due to non quadratic functions.

For that reason it is suggested another procedure. The second approach changes the type of parameterization, in order to facilitate the model selection and avoid non-quadratic functions in the cost function. Moreover and most important, this new parameterization promotes obtaining high quality starting values via a linear least squares estimate.

The chapter is concluded with an example in which the two approximations are applied. The particular case is the wave to heave force plant, with incidence wave 135º and ship speed 40 knots. For each method, obtained model's properties are examined. Bode plots are computed, graphed and compared with experimental data. It is seen that estimated model describes data information. Models which best agree with the experimental data are selected. Temporal response is also depicted. Finally, it is shown that the second approach obtains more accurate models that the first one.

AKKNOLEDGMENTS

This development was supported by MCyT of Spain under contract DPI2003-09745-C04-01.

REFERENCES

Aranda, J., J.M. Díaz, P. Ruipérez, T.M. Rueda, E. López (2002a). Decreasing of the motion sickness incidence by a multivariable classic control for a high speed ferry. *CAMS ProceedingVolume*. Pergamon Press.

Aranda, J., J.M de la Cruz, J.M. Díaz, S. Dormido Canto (2002b) .QFT versus classical gain scheduling: study for a fast ferry. *15th IFAC World Congress b'02*.

Aranda, J, R. Muñoz, J.M Díaz (2003). Roll model for control of a fast ferry. *2nd International Conference on Maritime Transport and Maritime History.*

Aranda, J. Cruz, J.M de la, Díaz, J.M. (2004a) Identification of Multivariable Models of Fast Ferries. *European Journal of Control.* 10:1-12.

Aranda, J, R. Muñoz, J.M Díaz. (2004b). The problem of the coupling of the vertical movement control with roll movement in fast ferries. In:*CAMS 2004 Proceeding Volume. 239-244.*

Bazán. National Company (1995). *Sea behaviour tests of the Turbo Ferry TF-120*. OTI-2086-CM-1.

Fletcher, R., (1991) *Practical Methods of Optimization (2nd ed.).*Wiley, New York.

Fossen, T.I, (2002). *Marine control systems: guidance, navigation and control of ships, rigs and underwater vehicles*. Marine Cybernetics AS, Trondheim.

Kenevissi, F., Atlar, M., and Mesbahi, E., (2003) *A new-generation motion-control system for twin-hull vessels using a neural optimal controller.* Marine Technology and Sname News, vol.40. no 3, pp. 168-180.

Lewis, E.V, (1989), *Principles of Naval Architecture. Volume III*. Society of Naval Architects and Marine Engineers.

Ljung, L., (1999) *System Identification: Theory for the User*. Prentice Hall.

Lloyd ARJM.(1998) *Seakeeping: ship behaviour in rough water*. Ellis Horwood.

Mari, J. (2000) Modifications of rational transfer matrices to achieve positive realness, *Signal Processing*, vol. 80, pp. 615-635.

Michalewicz, Z. (1999) *Genetic Algorithms + Data Structure= Evolution Programs.* Third, revised and extender Edition. Springer.

Söderström, T. and P. Stoica.(1989) *System Identification*. Prentice Hall.

Pintelon, R. and Schoukens, J., (2001) *System Identification: A Frequency Domain Approach.* Piscataway, USA: IEEE Press.

Pintelon, R. and Schoukens, J. (2004). Discussion on "Identification of multivariable models of fast ferries"

Van Gestel, T., Suykens, J., Van Doore, P and De Moore, B., (2001) Identification of stable models in subspace identification by using regularization. *IEEE Trans. Autom. Contr.*, vol 46, no 9, pp 1416-1420.

Journal of Maritime Research, Vol. II. No. 1, pp. 69-86, 2005

ISSN: 1697-4840

APPLICATION OF A ROBUST QFT LINEAR CONTROL METHOD TO THE COURSE CHANGING MANOEUVRING OF A SHIP

T. M. Rueda[1], F. J. Velasco[1], E. Moyano[2], E. López[3], J.M. de la Cruz[4]

ABSTRACT

This paper describes in detail the design methodology of a robust QFT (Quantitative Feedback Theory) controller for the control of the course changing of a ship. A linear model is used with uncertainty in the parameters. The system is designed to fulfil the specifications of robust stability and robust tracking of a reference system.

Keywords: Ship control, ship autopilots, marine systems, control systems, ship model, course-changing control, plant templates, bounds, QFT control.

INTRODUCTION

If a control system were represented by a fixed, known mathematical model and, if this model were available even in the presence of disturbances, the design of the controller required to attain the desired behaviur specifications would be a relatively simple matter. However, the mathematical model of the system can present variations due, amongst other things, to modeling errors or to the effects of external disturbances. In order to reduce the sensitivity of the system to these uncertainties, a closed loop control system is required. The designed controller must also be robust in order to attain the required specifications, even when faced with uncertainty in the model and the presence of disturbances. The quantity of feedback required will be directly proportionate to the degree of uncertainty and to the desired reduction in sensitivity.

[1] Dept. Electronics Technology and Systems Engineering and Automatics. Univ. de Cantabria (ruedat@unican.es) (velascof@unican.es)
[2] Dept. of Applied Mathematics and Computation Sciences. Univ. de Cantabria. (moyanoe@unican.es)
[3] Dept. of Sciences & Techniques of Navig., Marine Engines and Ship Cons. UPV. (cnplogae@lg.ehu.es)
[4] Dept. of Computer Science and Systems Engineering. Univ. Complutense (jmcruz@dacya.ucm.es)

In the 1960s, Isaac Horowitz (1963) introduced an efficient robust control design technique in the frequency domain, known as the "Quantitative Feedback Theory" or QFT. This technique considers a priori the uncertainty that may be present in the process and its environment and establishes a balance between the quantity of feedback required and the design complexity. The controller designed with this method is of minimum cost, does not have a large gain and minimises the control effort. Moreover, it has a smaller bandwidth than that obtained using any other design technique dealing with special structures and their uncertainties, disturbances and/or specifications.

The QFT method has already been applied in the design of different types of control systems for, for example, flight control (Houpis et al., 1994), control of an activated sludge wastewater treatment plant (Ostolaza and García Sanz, 1997), robot control systems (Yaniv and Horowitz, 1990; Kelemen and Bagchi, 1993; Piedmonte et al., 1998; Choi et al., 1999), stabilisation of the vertical movement of a ship (Aranda et al., 2002; Velasco et al., 2004).

This paper presents the application of this method to the control of the course changing manoeuvring for a ship (Rueda and Velasco, 2000 and Rueda, T.M. 2005). Course control is of special interest for joint operations between ships such as assistance to a damaged ship, towing manoeuvres and going along side or two ships sailing close to each other. A Matlab QFT toolbox (Borguesani, 1995) is used for the design and analysis of the control system.

METHODOLOGY. QFT DESIGN TECHNIQUE FOR LINEAR SYSTEMS

The QFT design technique is characterised mainly by its consideration a priori of the uncertainty of the process, caused by the variations in the parameters of the equipment to be controlled and by external disturbances and takes into account in the controller design process both the gain and its phase. It attempts to minimise the control effort in order to avoid saturations in the actuators or in the plant, which can be caused by the amplification of the sensor noise required to reach the desired specifications with a minimum bandwidth. With this method, a robust controller is obtained which is insensitive to the uncertainties of the process. The system model may be given as a transfer function or using experimental data. The representation in state variables is not normally used, since it is rather more complex. This technique makes it possible to predict quite simply whether some desired behaviour specification will not be fulfilled and to rectify the design accordingly without using complex mathematical tools. With this design method, a controller can be selected in graph form in the frequency domain.

The QFT method proposes as a general control strategy the two degrees of freedom structure presented in Figure 1, in which both compensators (F(s) and G(s)) are LTI, linear and time invariant.

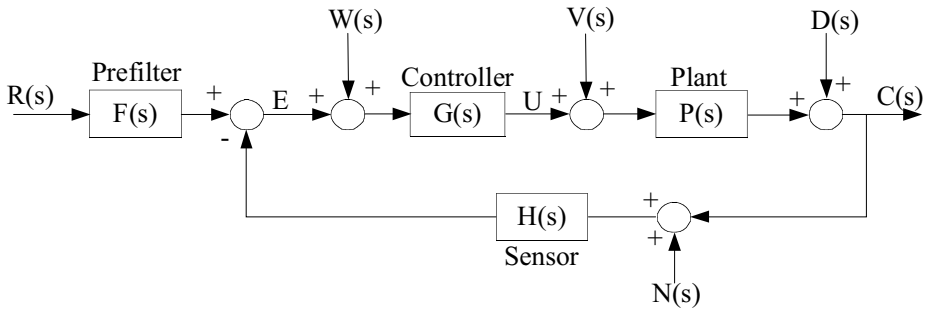

Figure 1: Two degrees of freedom control structure

Below, we will applied the QFT technique to the design of the control system for the course changing manoeuvre for a Mariner class cargo ship (Rueda and Velasco, 2000).

DEVELOPMENT

Mathematical Model for Course Control of a Ship

In the literature (Fossen, 1994), linear and non-linear techniques are proposed which describe the basic dynamics for the course control on the horizontal plane. Figure 2 shows the block diagram of a ship's steering system.

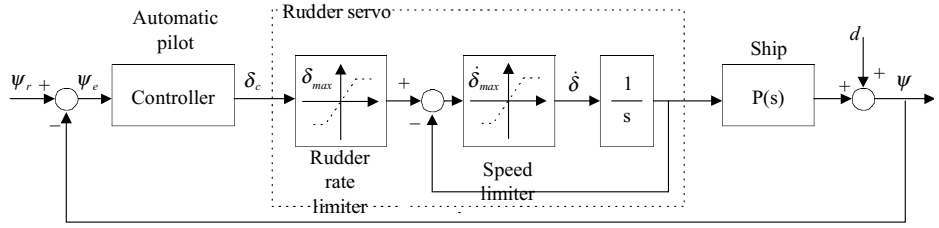

Figure 2: Ship's steering system

The command applied is ψ_r, which represents the desired course, ψ_e is the error in the course; the control signal which acts as the command on the rudder servomotor is δ_c, and represents the rudder angle required to correct the course deviation. The actual value of the ru dder angle is δ, and ψ is the ship's course. The effects of saturation are considered both in the rudder angle and in the speed of change of this angle.

Control Problem

The objectives to be performed by an automatic pilot are:

Course-keeping: Maintain the heading of a ship following a given course ($\psi(t)$ = constant).

Course changing: This manoeuvre must be performed in the minimum time possible, without overshoots at the beginning and end of the operation, to show clearly to the other ships the intentions of the manoeuvre. This can be achieved by using a second order reference model to determine the trajectory (Fossen, 1994):

$$\ddot{\psi}(t)+2\zeta\omega_n\dot{\psi}(t)+\omega_n^2\psi(t)=\omega_n^2\psi_r \tag{1}$$

where ζ ($0{,}8 \le \zeta \le 1$) is the desired closed loop damping ratio, and ω_n is the natural frequency, whose value depends on the the ship's dynamics.

In both situations, the system must work efficiently, independently of the disturbances caused by the wind, waves and currents.

APPLICATION: COURSE CONTROL FOR A SHIP WITH A LINEAR MATHEMATICAL MODEL

Definition of Design Problem

Nomoto et al. (1957) propose, for the analysis of ship stability and the design of automatic pilots, an approximate first order model:

$$\frac{\psi}{\delta}(s)=\frac{K}{s(1+sT)} \tag{2}$$

where T is the value of an effective time constant *($T=T_1+T_2-T_3$)*

The parameters K, T_1, T_2 y T_3 represent the ship's dynamics. These are determined by the dimensions and forms of the ship, depending also on operating conditions, such as speed, load, ballast, draft, trim and depth of water.

One ship represented by the above mathematical model is the Mariner class cargo ship, (Fossen, 1994) with:

$$K = \text{-}0.185\ \text{s}^{-1} \qquad \left.\begin{array}{l} T_1 = 118\ \text{s} \\ T_2 = 7.8\ \text{s} \\ T_3 = 18.5\ \text{s} \end{array}\right| T = 107.3\ \text{s} \tag{3}$$

The ship model to carry out the design of a QFT controller, assuming that the K and T parameters show uncertainty, is:

$$P(s)=\frac{\psi}{\delta}(s)=\frac{K}{s(1+sT)} \text{ with } \left|\begin{array}{l} K \in [\text{-}0.135,\ \text{-}0.235] \\ T \in [80.3,\ 134.3] \end{array}\right. \tag{4}$$

The system should fulfil the following specifications:

1. Robust stability:Phase margin of at least 45º, gain margin of 2 dB

2. Robust tracking of reference signal, desired course: the course changing manoeuvre must be defined within an acceptable range of variation with respect to a reference signal. The lower bound will be a course change which is slower than the reference. The upper bound will be a master course-change than the reference. Figure 3 shows the specified bounds.

These bounds correspond to the trajectory defined by the response to the step input of the following A(s) and B(s) functions:

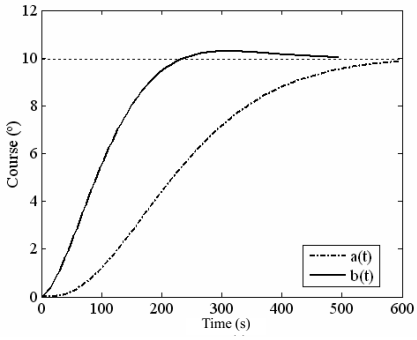

Figure 3: Bounds in the time domain

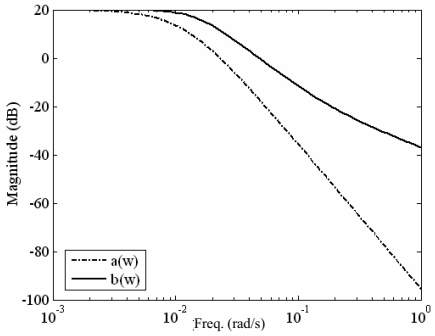

Figura 4: Bounds in the frequency domain

$$A(s)=\frac{168*10^{-8}}{s^3+0.03424s^2+40.3366*10^{-5}s+168*10^{-8}}$$
$$B(s)=\frac{14.0625*10^{-4}s+225*10^{-6}}{s^2+0.0225s+225*10^{-6}} \quad (5)$$

To apply the QFT design technique, the specifications need to be defined in the frequency domain. Thus, for the case under study:

$$a(\omega)\le T(j\omega)\le b(\omega) \quad (6)$$

where T is the closed loop reference transfer function.

Figure 4 shows the representation in frequency domain of the established tolerances.

In order to fulfil both specifications, a QFT controller will be designed made up of the compensator G(s) and the pre-filter F(s) of the two degrees of freedom system of Fig. 5.

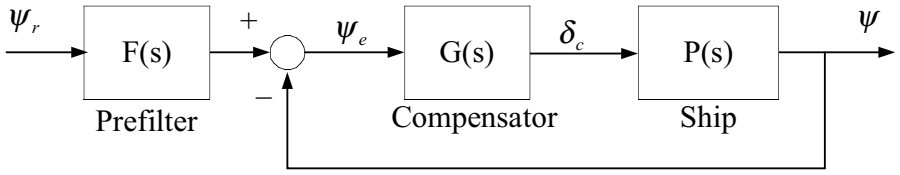

Figure 5: QFT control of course changing

Selection of Design Parameters

The second step in the design process is to select a nominal plant $P_0(s)$ from among the family of plants $\boldsymbol{P}(s)$. An adequate and finite set of frequencies Ω must also be selected. This set is determined by the bandwidth of the system and by the frequencies of interest, for which the different desired behaviour specifications are defined. In this case, the nominal plant selected is:

$$P_0(s) = \frac{-0.135}{s(107.3s+1)} \tag{7}$$

Taking into account the frequency response bounds permitted, Figure 5, it choose as a set of design frequencies:

$$\Omega = \{0.003,\ 0.007,\ 0.01,\ 0.02,\ 0.05,\ 0.1\}\text{rad/s} \tag{8}$$

Design

The third step in the design process is to represent as accurately as posible the uncertainty of the system. When the system is not defined by a single model, but rather has several due to the parametric uncertainty, the frequency response of the system for a given frequency is represented by a set of points, as many as there are different models. All of these points define a region of uncertainty known as template. There will be as many templates as frequencies in the set Ω.

The most common way to calculate a template is to perform a sweep of the values that the model parameters can take. In this study case, a sweep is made of the values that can be taken by the parameters K and T. The extremes of the uncertainty intervals are taken as references, and these values have been selected:

K = {-0.135, -0.16, -0.185, -0.235}

T = {80.3, 95.3, 107.3, 122.3, 134.3}

In order to perform the control system design, it suffices to consider the contour of a template, since if this contour respects the regions forbidden by the specifications, the rest of the templates will do too (García-Sanz and Vital, 1999).

The templates obtained for the family of plants ***P(s)*** and for the set of frequencies **Ω** are as shown in Figure 6.

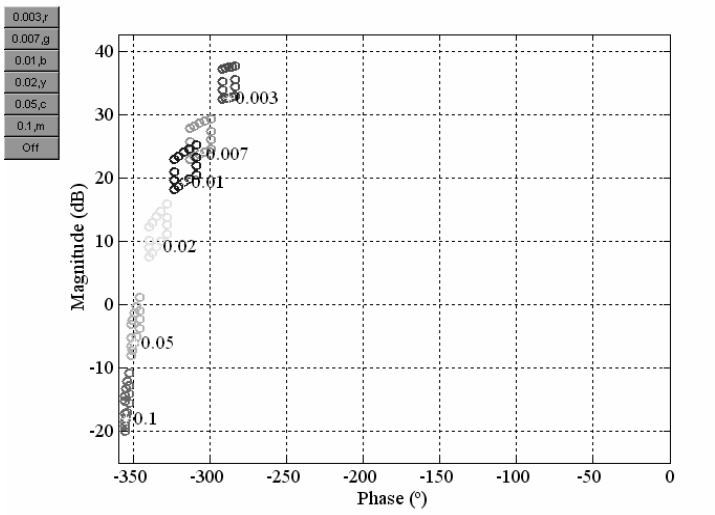

Figure 6: Templates

Each point represents the frequency response of one plant of the family and each colour distinguishes the response for each value of the frequency range. The shape of the templates varies with the frequency and its size decreases when the frequency increases.

Obtaining the Bounds

The fourth step in the design is to define, in QFT terminology, the desired behaviour restrictions. The specifications given, combined with the uncertainty of the system, form what are termed bounds. They are represented on the magnitude$_{dB}$-phase plane, and there is one for each frequency and specification; they are denoted as *B(w)*.

These curves are the objects which define the bounds of the regions prohibited for the adjustment of the controller. If the transfer function of the controller is denoted as *G(jw)* and the transfer function of the nominal plant as $P_0(jw)$, the bounds are those regions that the open loop function frequency response $L_0(jw)$ ($L_0(jw) = G(jw)P_0(jw)$) must avoid in order to guarantee the fulfilment of the design specifications for the whole set of plants ***P(jw)***. In order to use the QFT method, the bounds need to be defined in the frequency range.

The procedure for obtaining in graph form the bound for each frequency and each specification is immediately available through the Matlab QFT toolbox.

Robust Stability

Relative stability is normally expressed in terms of certain desired gain margins and phases. These are related with a value in decibels δ, known as the M-circle because it takes this shape if represented in a magnitude$_{dB}$-phase diagram. This circle identifies an exclusion zone around the point [-180º, 0dB], which the loop function must not cross ($\forall \omega \in \Omega, \forall P \in \boldsymbol{P}$) in order to ensure the margin of minimum stability. The specification of robust stability is written as:

$$\left| \frac{P(j\omega)G(j\omega)H(j\omega)}{1+P(j\omega)G(j\omega)H(j\omega)} \right| \leq W_{S_1} = \delta \tag{9}$$

relating it with the gain margin (GM) and phase (PM) as follows:

$$GM = 1 + \frac{1}{\delta}$$
$$PM = 180 - \cos^{-1}\left(\frac{0.5}{\delta^2} - 1 \right) \tag{10}$$

For the example proposed, a phase margin of at least 45º and a gain margin of 2 dB were specified.

Thus, the following should be fulfilled:

$$\left| \frac{P_0(j\grave{u})G(j\grave{u})}{1+P_0(j\grave{u})G(j\grave{u})} \right| \leq \delta = 1.2 \tag{11}$$

Taking into account the specifications imposed and the uncertainty of the model, the bounds for robust stability are as shown in Figure 7.

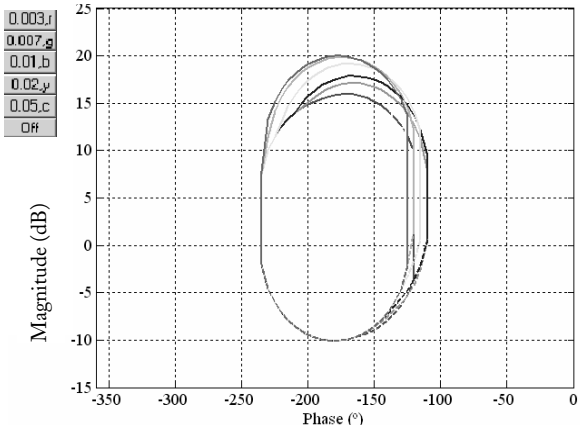

The bounds for the frequency range Ω are represented by the following colour code: ω = 0.003 rad/s in red, 0.007 rad/s in green, 0.01 rad/s in blue, 0.02 rad/s in yellow, 0.05 rad/s in light blue and 0.1 rad/s in magenta. This will apply to all of the bounds graphs.

Figure 7:
Robust stability bounds

When the bounds are represented by a continuous line and are closed, the specification is verified if the frequency response of the loop function for each frequency is outside the curve corresponding to the same frequency.

Robust tracking of a reference signal

The tracking specification is established by means of lower, a(t), and upper, b(t), bounds in the system response. It is considered that both functions have Laplace transform A(s) and B(s). For the example used, it was specified that the response to a course changing should be kept within the bounds given in Figure 5. In order to apply the QFT technique, this specification is defined in the frequency domain as follows

$$a(\omega) \le 20\log\left|T(j\omega)\right| \le b(\omega), \quad \forall\omega \in \Omega, \forall P(s) \in \boldsymbol{P}(s) \tag{12}$$

where *T(jw)* is the closed loop transfer function of the system.
For the QFT design, the specification is established as follows:

$$W_{S_{7a}} \le \left|\frac{P(j\omega)G(j\omega)}{1+P(j\omega)G(j\omega)H(j\omega)}\right| \le W_{S_{7b}} \tag{13}$$

where:

$$\begin{aligned} W_{S_{7a}} &= \left|a(\omega)\right| \\ W_{S_{7b}} &= \left|b(\omega)\right| \end{aligned} \tag{14}$$

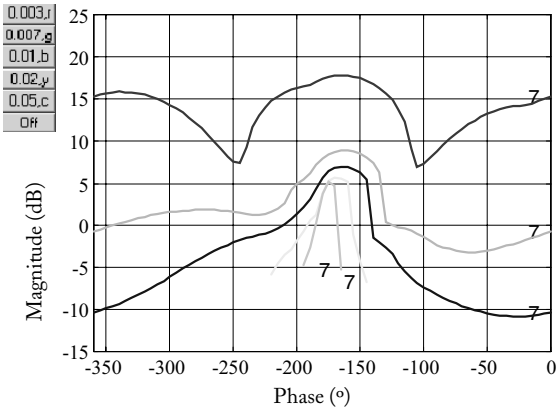

Figure 8: Robust tracking bounds

In the example, in order to obtain robust tracking bounds, a subset of Ω is considered, and it is required that the specification is verified only for frequencies lower than 0.05 rad/s. Combining the specification and the uncertainty, the robust tracking bounds of Figure 8 are obtained.

The robust tracking bounds are open and have a continuous line. Thus, the open loop response, *L(jw)* , for each

frequency must be adjusted so that this point is located above the bound corresponding to this same frequency. Thus, it is ensured that the specification is fulfilled.

Tuning of the Controller

The fifth step in the design of the control system consists in finding a controller with which all of the desired specifications are fulfilled. It is also known as the synthesis or "loop-shaping" phase.

The method consists in assuming an initial value of the controller function $G_0(jw)$, and adjusting the loop function $L_0(jw)$ which verifies the imposed restrictions and minimises the control effort. The adjustment is made using the Matlab QFT Toolbox, shifting the loop curve vertically and horizontally on the magnitude$_{dB}$-phase plane, until it is situated in such a way as to not violate the bounds and as to have the lowest gain possible.

For the example of the Mariner class cargo ship, and assuming an initial controller of a constant value, $G_0(s)=1$.

The representation of the loop function is a curve with several points marked in colours. These points correspond to the response of the loop for the various frequencies defined in **Ω**, following the same colour code as in the bounds. The loop adjustment must be done in such a way that each coloured point is close to the bound of the same colour, and same frequency. It must also be taken into account whether the bound is a continuous line or not. If they are all continuous, the point must be above for open curves (ω = 0.003, 0.007, 0.01 rad/s) and outside for closed curves (ω = 0.02, 0.05, 0.1 rad/s).

This part of the design process is not automated in the Matlab toolbox; obtaining a good design with little overdesign depends greatly on the skill of the designer. There is no single or perfect solution.

The controller is related with the loop function as follows:

$$L_0(j\omega) = G(j\omega)P_0(j\omega) \tag{15}$$

In this way, once the loop is adjusted, it is simple to obtain the transfer function of the compensator. The controller obtained is robust, that is, it provides good results for all of the family of plants defined by the uncertainty, not only for the nominal plant used in the loop-shaping stage.

It is recommended, in this loop-shaping stage, to always begin by adjusting the point corresponding to the lowest frequency, continuing upwards and modifying the function progressively.

For the example of the course changing manoeuvre, the terms included are:

1.- Reduce the system gain to adjust the frequency w = 0.003 rad/s. The loop function point for this same frequency, in red, must be above the bound at this

frequency, also in red, and as near as possible, so that there is as little as possible overdesign. For the compensator $G_1(s)$, this condition is fulfilled, as can be seen in Figure 9.

$$G_1(s) = -0.0692 * G_0(s)$$
$$L_1(j\omega) = G_1(j\omega) P_0(j\omega) \tag{16}$$

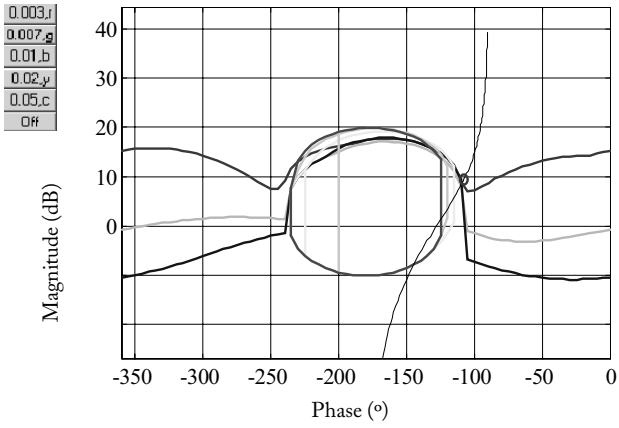

Figure 9: Loop function L1 and bounds

2- Add phase-lead, a real zero. This achieves the adjustment of the conditions for the frequencies 0.007 rad/s, green, and 0.01 rad/s, blue. The position of the loop at these frequencies must follow the same criteria as that of step 1. Figure 10 shows that the conditions are verified for the following $G_2(s)$ controller:

$$G_2(s) = G_1(s) * \left(\frac{s}{0.01585} + 1 \right)$$
$$L_2(j\omega) = G_2(j\omega) P_0(j\omega) \tag{17}$$

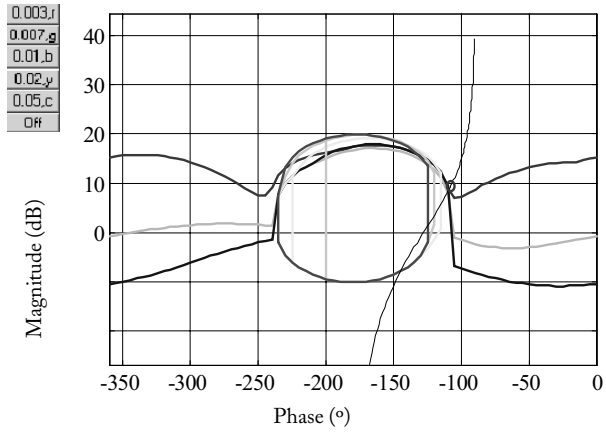

Figure 10: Loop function L2 and bounds

3º- There are also bounds for the frequencies of 0.02 rad/s, yellow, 0.05 rad/s, light blue, and 0.1 rad/s, magenta. In these cases, the point corresponding to the loop must be outside the oval. This is fulfilled, so that it will not be necessary to modify the obtained compensator. However, the closer the corresponding bound

points, the lower the feedback cost. A certain improvement is observed in Figure 11; this is achieved by adding two complex poles conjugated with the natural frequency ω_n = 0.1783 rad/s and damping ratio δ = 0.1099, obtaining the controller $G_3(s)$.

$$G_3(s) = G_2(s) * \frac{1}{\left(\frac{s^2}{0.1783^2} + \frac{2*0.1099}{0.1783}s + 1\right)}$$
$$L_3(j\omega) = G_3(j\omega) P_0(j\omega) \tag{18}$$

The compensator $G(s)$ obtained finally is:

$$G(s) = \frac{-0.1388s - 0.0022}{s^2 + 0.0392s + 0.0318} \tag{19}$$

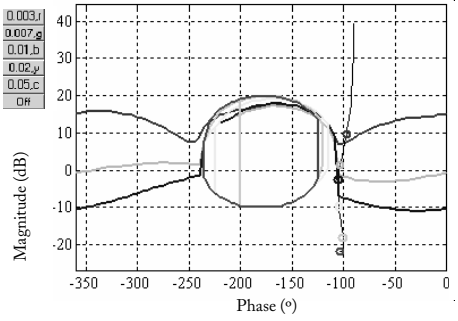

Figure 11: Loop function L3 and bounds

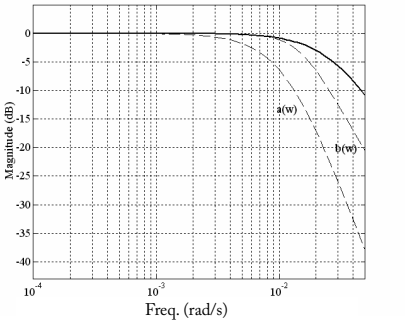

Figure 12: Robust tracking

The design of the controller with which the robust tracking bounds are respected in the loop function frequency response is performed in two stages. The uncertainty of the system means that there is a maximum and a minimum response. The first step in the design is to tune the compensator $G(s)$, so as to reduce the difference between the two responses. The second step consists in adjusting a pre-filter $F(s)$, which transfers the variations obtained with the above design to the zone defined by the tolerances $b(w)$ and $a(w)$. That is, the definition of equation 6 can be written as:

$$a(\omega) \le \left|F(j\omega)\right|_{dB} + \left|T_l(j\omega)\right|_{dB} \le b(\omega)$$
$$T_l(j\omega) = \frac{L(j\omega)}{1 + L(j\omega)}$$
$$T(j\omega) = F(j\omega) T_l(j\omega) \tag{20}$$

Figure 12 shows the frequency response of the system with the controller Q but, without the prefilter F, it is not within the bounds

The adjustment of the prefilter is performed graphically by shifting the system response curve using the mouse, so that it is within the required tolerances. In this case, we get:

$$F(s)=\frac{1}{104.51s+1} \tag{21}$$

Design Validation

As the last step in the design process, a validation of the obtained results should be made, graphically checking the specifications in the frequency and time domains.

Moreover, this validation is essential, since the design has been made only for a finite set of frequencies and hence it cannot be ensured, a priori, that it will be fulfilled for any other frequency, inside or outside this range. Thus, it needs to be checked for a higher number of frequencies.

For the proposed example, it is verified whether the specifications are fulfilled for a new range of frequencies Ω_v, for 100 values logarithmically spaced between 10^{-4} and 0.1 rad/s.

Figure 13 shows with a dotted line the desired stability value (δ = 1.2 = 1.58 dB) and with a continuous line the system response. As this latter value is below the specification line, the required robust stability condition is fulfilled.

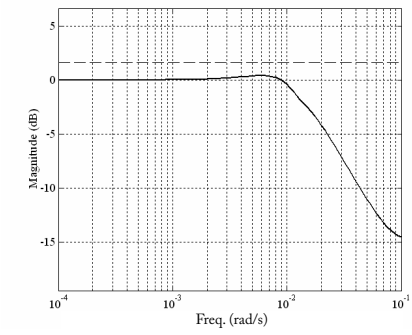

Figure 13: Robust Stability

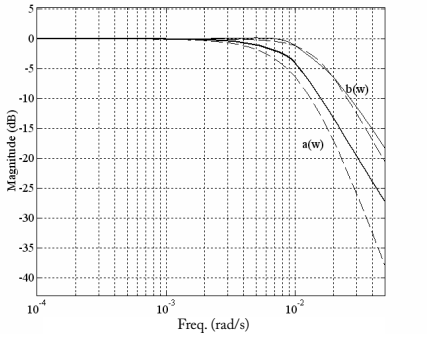

Figure 14: Robust tracking with compensator and prefilter

Figure 14 shows that the conditions of robust tracking are fulfilled for the course changing manoeuvre in the frequency domain; the system response, in a continuous line, is within the permitted tolerance, in the dotted line.

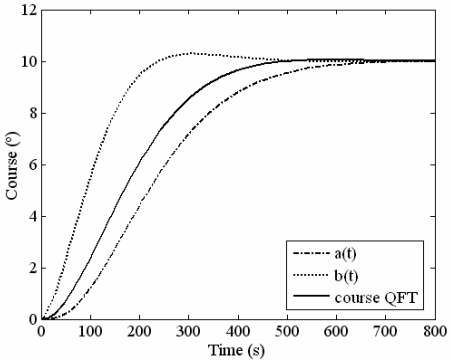

Figure 15.a: Course changing manoeuvre

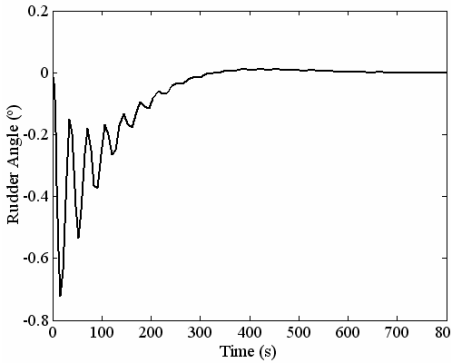

Figure 15.b: Rudder angle

Course changing manoeuvre in the time domain

The course changing manoeuvre must be within the permitted tolerantes a(t) and b(t). Figure 15.a shows that this is fulfilled. Figure 15.b shows the rudder angle required to carry out this manoeuvre.

CONCLUSIONS

A linear QFT robust control methodology has been applied to the course changing manoeuvre for a ship. It has been demonstrated that this technique is suitable for application in this case, which presents uncertainties in the parameters.

It has been verified, by means of simulation, that the required specifications of robust stability and robust tracking are fulfilled.

Another important factor is the small control effort required to perform this course changing manoeuvre.

ACKNOWLEDGEMENTS

This work has been partially financed by the MCYT through project DPI2003-09745-C04-03.

REFERENCES

Aranda, J., De la Cruz, J. M., Díaz, J. M. and Dormido Canto, S. (2002) QFT Versus Classical Gain Scheduling: Study for a Fast Ferry. *Control 15th IFAC World Conference*.

Borguesani, C., Chait, Y. and Yaniv, O. 1995. *Quantitative Feedback Theory Toolbox – For use with MATLAB*. The MathWorks Inc.

Choi, S. B., Cho, S. S. and Park, Y. P. (1999) Vibration and Position Tracking Control of Piezoceramic-based Smart Structures via QFT. *ASME Journal of Dynamic Systems, Measurement and Control* (121), 27-33.

Fossen, T. I. (1994). Guidance and Control of Ocean Vehicles. John Wiley and Sons Ltd., England.

García-Sanz, M. and Vital, P. (1999) Efficient Computation of the Frequency Representation of Uncertain Systems. *Proceedings 4th International Symposium on QFT and Robust Frequency Domain Methods*. Durban, South Africa.

Horowitz, I. M. (1963) *Synthesis of Feedback Systems*. Academic Press. New York.

Houpis, C. H., Sating, R. R., Rasmussen, S. and Sheldon, S. (1994) Quantitative Feedback Theory Technique and Applications. *International Journal of Control* 59, 3970.

Kelemen, M. and Bagchi, A. (1993) Modelling and Feedback Control of a Flexible Arm of a Robot for Prescribed Frequency Domain Tolerances. *Automatica* (29), 899-909.

Nomoto, K., Taguchi, T., Honda, K. and Hirano S. (1957). On the steering qualities of Ships. International Shipbuilding. Progrees (4).

Ostolaza, J. X. and García-Sanz, M. (1997) Control of an Activated Sludge Wastewater Treatment Plant with Nitrification-Denitrification Configuration using QFT Technique. *Proceedings of Symposium on Quantitative Feedback Theory and Other Frequency Domain Methods and Applications*, University of Strathclyde, Glasgow, Scotland.

Piedmonte, M. D., Mechl, P. H., Nwokah, O. D. and Francheck, M. A. (1998) Multivariable Vibration Control of a Coupled Flexible Structure using QFT. *International Journal of Control* (69) 475-498.

Rueda, T. M. and Velasco, F. J. (2000) Robust Course-Changing Controller for a Ship using QFT Design Technique. 2nd International Congress on Maritime Technological Innovations and Research. Cádiz.

Rueda, T.M. (2005). *Metodología de reducción de modelos y control robusto QFT para el gobierno y estabilización de buques*. Tesis doctoral. Departamento de Tecnología Electrónica e Ingeniería de Sistemas y Automática. Santander.

Velasco, F. J., Rueda, T. M. López, E. and Moyano, E. (2004) Pitch Movement QFT Control to Reduce the MSI of a Turbo Ferry. *IFAC Conference CAMS 2004, Control Applications in Marine Systems*. Ancona, Italy 345-350.

Yaniv, O. and Horowitz, I. (1990) Quantitative Feedback Theory for Active Vibration Control Synthesis. *International Journal of Control* (51), 1251-1258.

APLICACIÓN DEL MÉTODO DE CONTROL ROBUSTO QFT LINEAL A LA MANIOBRA DE CAMBIO DE RUMBO DE UN BUQUE

RESUMEN

En este artículo se describe detalladamente la metología de diseño de un controlador robusto QFT (Quantitative Feedback Theory) para el control de cambio de rumbo de un barco. Para ello se utiliza un modelo lineal con incertidumbre en los parámetros. Se desea que el sistema cumpla especificaciones de estabilidad robusta, y de seguimiento robusto de un sistema de referencia.

INTRODUCCIÓN

Si un sistema de control estuviera representado por un modelo matemático conocido y fijo y, aunque existiesen perturbaciones se pudiera disponer de un modelo, el diseño del controlador necesario para alcanzar las especificaciones de comportamiento deseadas, no sería demasiado complicado. Sin embargo, el modelo matemático del sistema puede presentar variaciones debidas, entre otras causas, a errores de modelado o al efecto de perturbaciones externas desconocidas. Para reducir la sensibilidad del sistema ante dichas incertidumbres, es necesario un sistema de control en lazo cerrado. Además, el controlador diseñado deberá ser robusto para poder alcanzar las especificaciones deseadas, a pesar de la incertidumbre del modelo y de la presencia de perturbaciones. La cantidad de realimentación necesaria será directamente proporcional a la cantidad de incertidumbre y a la reducción de la sensibilidad deseada.

En la década de los 60, Isaac Horowitz (1963) introduce una potente técnica de diseño de control robusto en el dominio frecuencial, la teoría de la realimentación cuantitativa, "Quantitative Feedback Theory" o QFT. Esta técnica considera a priori la incertidumbre que puede presentarse en el proceso y su entorno, y establece un equilibrio entre la cantidad de realimentación necesaria y la complejidad del diseño. El controlador diseñado con este método es de coste mínimo, no tiene ganancia grande y minimiza el esfuerzo de control. Además tiene ancho de banda más pequeño que el que se obtiene con cualquier otra técnica de diseño que considere estructuras especiales para las incertidumbres de la planta, perturbaciones y/o especificaciones.

En este artículo se presenta su aplicación al control de la maniobra de cambio de rumbo de un buque. El control de rumbo es de especial interés para actuaciones en cooperación entre buques como, por ejemplo, auxilio de un buque averiado,

maniobra de remolque, y abarloamiento o navegación en proximidad.

METODOLOGÍA:

La técnica de diseño QFT se caracteriza principalmente porque considera a priori la incertidumbre del proceso, debida a variaciones en los parámetros de la planta a controlar o a perturbaciones externas, y tiene en cuenta en el proceso de diseño del controlador tanto la ganancia como la fase del mismo, intentando minimizar el esfuerzo de control. Con este método se obtiene un controlador robusto, insensible a incertidumbres en el proceso. El modelo del sistema puede venir dado como función de transferencia o mediante datos experimentales. Esta técnica permite anticipar de forma sencilla si alguna especificación de comportamiento deseada no se va a cumplir, y rectificar el diseño en función de esos datos. El método QFT propone como estrategia general de control la estructura de dos grados de libertad.

El modelo del buque para realizar el diseño de un controlador QFT, es:

$$P(s)=\frac{\psi}{\delta}(s)=\frac{K}{s(1+sT)} \quad \text{with} \quad \begin{vmatrix} K \in [-0.135, \ -0.235] \\ T \in [80.3, \ 134.3] \end{vmatrix}$$

Los parámetros K, T representan la dinámica del buque.

Se desea que el sistema cumpla las especificaciones siguientes:

1.- Estabilidad robusta: Margen de fase de al menos 45º, margen de ganancia de 2 dB

2.- Seguimiento robusto de señal de rumbo deseado: La maniobra de cambio de rumbo debe estar definida dentro de un rango de variación respecto a una señal de referencia. La frontera inferior será un cambio de rumbo más lento que el de referencia. La frontera superior será un cambio de rumbo más rápido que el de referencia.

Se ha utilizado como planta nominal:

$$P_0(s)=\frac{-0.135}{s(107.3s+1)}$$

y como conjunto de frecuencias para el diseño:Ω={0.003, 0.007, 0.01, 0.02, 0.05, 0.1}

El controlador se ha validado para un nuevo rango de frecuencias , 100 valores logarítmicamente espaciados entre 10^{-4} y 0.1 rad/s., comprobándose que se verifica la condición de estabilidad robusta exigida. Igualmente se comprueba que se cumplen las condiciones de seguimiento robusto de la maniobra de cambio de rumbo

CONCLUSIONES

Se ha introducido la metología de control robusto QFT lineal para la maniobra de cambio de rumbo de un buque y se ha mostrado que esta técnica es adecuada en este caso, que presenta incertidumbre en los parámetros.

Además se ha comprobado mediante simulación, que se cumplen las especificaciones requeridas de estabilidad robusta y seguimiento robusto.

Es de destacar el pequeño esfuerzo de control necesario para realizar esta maniobra de cambio de rumbo, lo que permite no tener que realizar continuas demandas en el timón.

Journal of Maritime Research, Vol. II. No. 1, pp. 87-104, 2005

ISSN: 1697-4840

TRENDS ON MODELLING TECHNIQUES APPLIED ON SHIP'S PROPULSION SYSTEM MONITORING

R Ferreiro[1], M. Haro[2] and F.J. Velasco[3]

Abstract

The aim of the work deals with some aspects regarding modelling techniques using analytical redundancy usually applied in fault detection, fault isolation, decision making and system recovery when monitoring severe or critic control systems such as ship propulsion systems, in order to achieve fault tolerant control systems. To get such modelling objectives, back-propagation neural networks are used as universal functional approximation devices or soft sensors whose outputs are compared with real-time data to achieve residuals.

Keywords: Neural networks, Back propagation, Residual generation, Functional redundancy.

INTRODUCTION TO THE STRUCTURE OF THE SHIP PROPULSION SYSTEM

Low performance of ship propulsion system associated to automation system can cause a relevant reduction in the ship's ability to propel and manoeuvre itself, which requires effective means to prevent faults, avoiding to develop into a failure. Several algorithms and methods from different research areas can be used to analyse the system and subsequently detect, isolate, and decide about the faults to recover the system. The ship propulsion system described was presented as an international benchmark by (M. Blanke, et al. 2003), (D. Herrmann, 2000) and was used as a platform for development of new ideas and comparison of methods.

The topics treated in this paper are based in the increasing demand of modeling strategies focused on structural analysis. It is shown how residual generators

[1] Profesor de la Universidad de la Coruña. (ferreiro@udc.es). Spain

[2] Profesor de la Universidad de Cádiz. Fac. Ciencias Náuticas. (manuel.haro@uca.es). Spain

[3] Profesor de la Universidad de Cantabria. E.T.C de Náutica (velasco@inican.es). Spain

are directly deduced from analysis of structure and how functional redundancy can be obtained. The dynamics of the propulsion system is non-linear. Furthermore, some essential faults are non-additive. The implication is that some residual generators become nonlinear. This work illustrates how such real-life phenomena can be handled in the general framework at modeling level. Detailed modeling and data recorded from maneuvering trials with the ferry give a realistic scenario for test of diagnostic methods and techniques to obtain fault tolerance.

Ship propulsion system

An outline of the propulsion system chosen for the benchmark is shown in figure 1 (of table 1 for a list of symbols) (R. Izadi-Zamanabadi and M. Blanke, 1998,1999).

The main components are described by the following blocks:

— *Diesel dynamics* gives engine torque to drive the propeller shaft.
— *Shaft dynamics* provides shaft speed given diesel and propeller torques.
— *Propeller characteristics* provide propeller thrust and load torque from shaft speed *n*, propeller pitch ϑ and water speed V_a (speed of advance).
— *Ship speed dynamics* determines ship speed from propeller thrust and external forces.
— *Propeller pitch and shaft speed controllers* (governor) control the propeller pitch and shaft speed.

The coordinated control level calculates set-points for shaft speed and propeller pitch controllers.

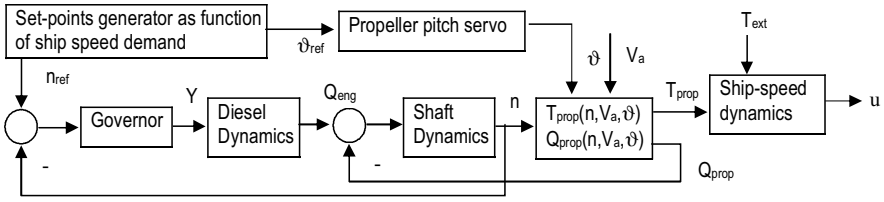

Fig. 1. Block diagram of the generic ship propulsion system

Symbol	Unit	Explanation
I_t	Kgm^2	Total inertia I
K_y	Nm	Torque coefficient
n	$rads^{-1}$	Shaft speed
R(u)	N	Hull resistance
T_{prop}	N	Propeller thrust
T_{ext}	N	External force
1 - t	-	Thrust deduction factor

Symbol	Unit	Explanation
u	ms^{-1}	Ship speed
V_a	ms^{-1}	Water velocity
$1 - w$	-	Wake fraction
Q_{eng}	Nm	Diesel torque
Q_f	Nm	Shaft friction torque
Q_{prop}	Nm	Propeller torque
Y_d	0...1	Fuel index
ϑ	-1...1	Propeller pitch

Table 1. List of symbols used in the ship propulsion system

MODELS OF THE PROPULSION SYSTEM: CONVENTIONAL APPROACH

The overall function of the propulsion system is to maintain the ship's ability to propel itself and to manoeuvre. Propulsion requires thrust ahead whereas manoeuvres require ahead and astern thrust ability. With a positive shaft speed n, this is obtained by an appropriate change of the propeller pitch ϑ, which is the angle that the propeller blades are twisted.

The component hierarchy is treated as belonging to two levels. Lower level components are the diesel engine with shaft speed controller, the propeller with the pitch controller, and the ship's speed dynamics. The upper level comprises coordinated control for the lower level components and overall command to the propulsion system. Reconfiguration will take place at the upper level, but lower-level controllers should be fault-tolerant, if possible, to maintain their primary services.

Upper-level components.

Upper level components are the following:

— *Command handle:* A command handle's position constitutes the main man-machine interface (MMI).

— *Combinator:* Use-modes with different interpretations of handle position are available:

-Manoeuvring: Handle position determines n and ϑ;

-Economy: Handle position determines n_{com} and ϑ_{com};

-Set speed: Maintain a set ship speed using measured ship speed U.

— *Efficiency optimiser:* The efficiency optimiser determines the set of n and ϑ that achieves the desired ship speed $U_{ref} = f_{sc}(h)$ as determined by the handle position, without ship speed feedback.

— *Ship speed control*: Ship speed control aims at maintaining a set ship speed within a narrow margin. This component uses measured ship speed as one of its input variables.

— *Diesel overload control*: Overload is avoided by reducing the propeller pitch if diesel torque is close to maximum at a given shaft speed.

Lower-level components.

The lower level consists of the shaft speed and the propeller-pitch controllers and the physical components of the propulsion system. In a component-based analysis, the physical components related to the pitch control function are lumped together to a new entity called propeller pitch control.

Propeller pitch control.

The pitch control is an aggregated component that comprises a large hydraulic actuator turning the propeller blades, the feedback from a pitch sensor, a controller and the drive electronics. In its original implementation, this component has only one version of the usemode um_1, which denotes the automatic mode. In order to obtain fault tolerant properties, other versions are added. The math model for physical parts of the component is composed of the following equations:

$$\vartheta_m = \vartheta + \nu_\vartheta + \Delta\vartheta \tag{1}$$

$$\vartheta = max(\vartheta_{min}, min(\vartheta, \vartheta_{max})) \tag{2}$$

$$\dot{\vartheta} = max(\dot{\vartheta}_{min}, min(u_\vartheta, \dot{\vartheta}_{max})) + \Delta\dot{\vartheta}_{inc} \tag{3}$$

The control signal is generated according

$$u_\vartheta = k_t(\vartheta_{ref} - \vartheta_m)$$

Here, ϑ_m is the measured propeller pitch, $d/dt[\vartheta_{min}, \vartheta_{max}]$ the rate interval set by the hydraulic pump capacity and geometry, and $[\vartheta_{min}, \vartheta_{max}]$ is the physical interval for propeller-blade travel. n_ϑ is the measurement noise. Two faults are included in the model: leakage $\Delta\vartheta'_{inc}$, and pitch sensor fault $\Delta\vartheta$.

Shaft speed control.

The input to the shaft speed controller, which is called the governor, is given by the shaft speed reference n_{ref} and the measured shaft speed n_m . The output is the throttle of the diesel engine, which is proportional to the fuel index *Y*. The governor is a PI controller. Anti-windup is part of the integrating action, and *K* is the anti-windup gain. The controller is given by

$$n_m = n + \nu_n + \Delta n \tag{4}$$

$$\dot{Y}_i = \frac{k_r}{\tau_i}((m_{ref} - n_m) - K(Y_{PIb} - Y_{PI})) \tag{5}$$

$$Y_{PIb} = Y_i + k_r \cdot (n_{ref} - n_m) \tag{6}$$

$$Y_{PI} = \min(\max(Y_{PIb}, Y_{Ib}), Y_{ub}) \tag{7}$$

Y_{lb} and Y_{ub} are the lower and upper bounds for the integrator part of the governor, and Δn the measurement fault. The governor comprises fuel index limits to keep the diesel engine within its allowed envelope of operation.

A similar formal description can be made for each physical component, but this is omitted for brevity.

Diesel engine.

The diesel engine generates a torque Q_{eng}, which is controlled by its fuel index Y, to drive the shaft (M. Blank and J. S. Andersen, 1984). The diesel engine dynamics can be divided into two parts. The first part describes the relation between the generated torque and the fuel index. It is given by the transfer function

$$\frac{Q_{eng}(s)}{Y(s)} = \frac{K_y}{\tau_c s + 1} \tag{8}$$

where K_y is the gain constant and τ_c, is the time constant corresponding to torque build-up from cylinder firings (M. Blanke, 1981).

The second part expresses the torque balance of the shaft:

$$I_m \dot{n} = Q_{eng} - Q_{prop} - Q_f \tag{9}$$

Q_{eng} is the torque developed by the diesel engine, Q_{prop} is the torque developed from the propeller, and Q_f is the friction torque.

Propeller thrust and torque.

A controllable pitch propeller (CP) has blades that can be turned by means of a hydraulic mechanism. The propeller pitch ϑ can be changed from 100 % (full ahead) to -100 % (full astern) with asymmetric or different thrust efficiency.

The propeller thrust and torque are determined by the following bilinear relations:

$$T_{prop} = T_{|n|n}(\vartheta)|n|n + T_{|n|V_a}(\vartheta)|n|V_a \tag{10}$$

$$Q_{prop} = Q_{|n|n}(\vartheta)|n|n + Q_{|n|V_a}(\vartheta)|n|V_a \tag{11}$$

V_a is the velocity of the water passing through the propeller disc (speed of advance)

$$V_a = (1-w)U \tag{12}$$

where w is a hull-dependent parameter or wake fraction. The coefficients $T_{|n|n}, T_{|n|V_a}, Q_{|n|n}$ and $Q_{|n|V_a}$ are complex functions of the pitch ϑ. T_{prop} and Q_{prop} are calculated by interpolating between tables of data measured in model propeller tests. K_T and K_Q, denote thrust and torque coefficients in (13) and (14), which depends on advance number J defined in table 2, and propeller pitch.

$$T_{prop} = K_T \rho D^4 |n|n \tag{13}$$

$$Q_{prop} = K_Q \rho D^5 |n|n \tag{14}$$

where D is the propeller diameter and r the mass density of water.

Velocities		*Power*	
Ship's speed	u	Effective towing power	$P_E = R_{(U)} \cdot u$
Arriving water velocity to propeller (speed of advance)	u_A	Thrust power delivered by propeller to water	$P_T = \frac{P_E}{\eta_H}$
Effective wake velocity	$u_w = u - u_A$	Power delivered to propeller	$P_D = \frac{P_T}{\eta_B}$
Wake fraction coefficient	$W = \frac{u-u_A}{u}$	Power of main engine (brake power)	$P_B = \frac{P_D}{\eta_S}$
Advance number	$J = \frac{u_A}{n \cdot D}$		
Resistance		*Efficiencies*	
Towing resistance	$R_{(U)}$	Hull efficiency	$\eta_H = \frac{1-t}{1-W}$
Thrust force developed by the propeller	T_{prop}	Prop. effic.(open waters) " " (behind hull)	η_0 $\eta_B = \eta_H \cdot \eta_R$
Thrust deduction factor	$F = T_{prop} - R_{(U)}$	Propulsion efficiency	$\eta_D = \eta_H \cdot \eta_B$
Thrust deduction coefficient	$t = \frac{T_{prop} - R_{(U)}}{T_{prop}}$	Shaft efficiency	η_S
		Total efficiency	$\eta_T = \frac{P_E}{P_B} = \eta_H \cdot \eta_B \cdot \eta_S$

Table 2. Conventional parameters involved on ship dynamics

Ship speed dynamics.

The following non-linear differential equation approximates the ship speed dynamics:

$$(m - X_{\dot{U}})\dot{u} = R(u) + (1 - t_T)T_{prop} + T_{ext} \tag{15}$$

$$u_m = u + v_U$$

The term R(u) describes the resistance of the ship in the water. It is a negative quantity. $X_{\dot{U}}$ represents the added mass in surge, which is negative. The thrust deduction ($1-t_T$) represents the net thrust lost due to the propeller-generated flow at the ship's stern. T_{ext} is the external force brought about by the wind and the waves. v_U is the measurement noise.

Some scenarios for fault diagnosis

The faults considered relevant in this system are summarized in table 3.

Fault	Symbol	Type
sensor faults	$\Delta\vartheta$	additive - abrupt
hydraulic leak	$\Delta\vartheta'_{inc}$	additive - incipient
sensor faults	Δn	additive - abrupt
diesel fault	ΔK_y	multiplicative - abrupt

Table 3. Faults considered

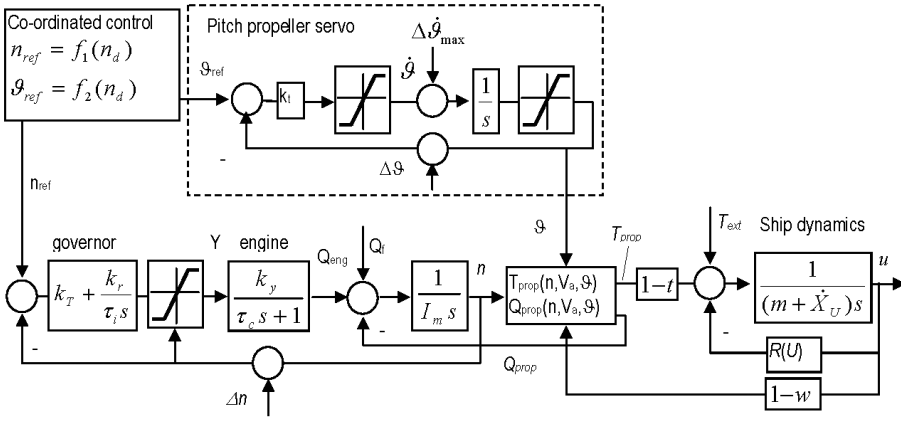

Fig. 2 Propulsion system with saturation phenomena shown for shaft speed and pitch controller.

A formal analysis of fault propagation shows that they have different degrees of severity. Some are very serious and need rapid fault detection and accommodation to avoid serious accidents if the component failure occurs during a critical manoeuvre. The time to detect and reconfigure is hence essential. Some of the faults are based on actual events that have caused serious damage due to the lack of fault-tolerant features in existing propulsion control systems. Figure 2 locates the generic blocks with possible faults of the benchmark in the system block diagram.

MODELS OF THE PROPULSION SYSTEM: PROPOSED APPROACH

Introduction

Described conventional approach exhibits some linear transfer functions combined with non-linear function models in which non linear and time-variant coefficients coexists. An alternative approach to the conventional modeling method described in last section (M. Blanke et al., 2003), can be achieved by modeling the propulsion system by means functional approximation devices in those cases where non-linear and time variant coefficients are present. Necessary data to achieve the proper functions has been acquired from maneuvering trials (R. Izadi-Zamanabadi and M. Blanke, 1999).

Neural Network based functional approximation

Neural Networks (NN) are essentially nonlinear function approximators that utilize process inputs to predict process output. The technical promise of neural-network technology comes from the fact that universal approximators are created using a multi-layer network with a single hidden layer that can approximate any continuous function to any desired degree of accuracy. Soft sensors that utilize NNs must be adapted to the special requirements of the process industry. In particular, it is necessary to compensate for the delay in the process output for changes in upstream conditions. Thus, a NN typically has one output (the predicted variable) and any number of upstream measurements as inputs with compensation of process delay. Figure 3 shows a three-layer feedforward NN.

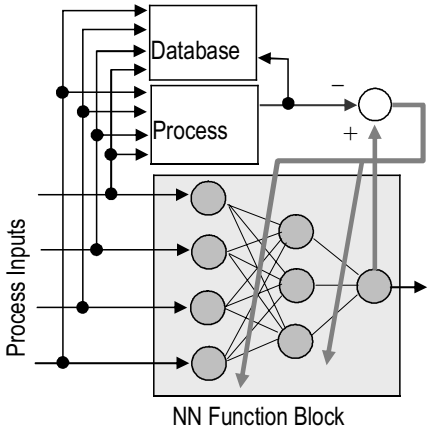

Fig. 3. Structure of a NN Function Block for on-line training.

An object oriented tool provides easy-to-use means for developing and training the NN model. This tool gives us a practical way to create virtual sen-

sors for measurements previously available only through the use of lab analysis or online analysers. Such tools are configured in a way easy to understand and use, allowing process engineers to produce extremely accurate results even without prior deep knowledge of NN theory. In figure 3 it is shown the structure of a NN Function Block connected to operate in an on-line training phase.

Alternative approach to monitoring system

A ship's resistance is particularly influenced by its speed, displacement, hull form and hull conditions. The total resistance R_T consists of many source-resistance R which may be classified into three main groups: frictional resistance, residual resistance and air resistance.

Hull resistance R due to hydrodynamic forces in surge motion is a nonlinear function of the ship velocity and wet surface which is associated to ship mass at constant trim. So that, using experimental data from towing tank tests, following function describes the total hull resistance as

$$R_{(u,m)} = f(u,m),\ \frac{du}{dt} = 0 \tag{16}$$

By means of sea trials the effective brake power of main engine P_B and effective towing power P_E may be associated to the hull resistance and external forces. Considering the influence of external forces the effective towing power is,

$$P_E = P_B \cdot \eta_T = (R_{(u,m)} + T_{ext}) \cdot u \tag{17}$$

With data achieved from steady state sea trials, a database with a set of brake powers, ship velocities, ship displacements, and hull resistances in absence of external forces, can be associated by means of functional approximation procedures under nominal hull conditions. So that, if such conditions change, the differences must be achieved by comparing nominal with actual conditions (parity relations). To do that, a virtual sensor consisting in a back propagation feedforward neural network (BPNN) properly trained and structured as a set of inputs and an output, can approximate the hull resistance into the range of possible displacements and velocities of the ship. Figure 4 shows the virtual sensors for brake power and hull resistance achieved by applying functional approximation by means of BPNNs.

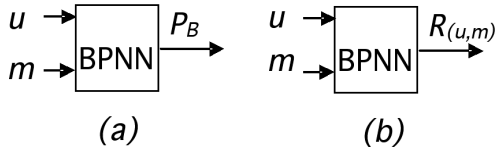

Fig. 4. Functional approximation. (a), brake power. (b), hull resistance.

Functional approximation by means of (16) is an alternative to conventional observers applied in solving FDI tasks in (M. Blanke, et al. 2003), (J. P. Gauthier, 1992)

The total efficiency under sea going conditions is then achieved by using (17) as shown in figure 5. If the difference between actual total efficiency and nominal efficiency estimated by functional approximation is greater than a proposed threshold *Thr2*, then a prejudicial force related with hull resistance is present. Such unwanted force or added resistance may be due to a problem on the propeller or to the increase of resistance of ship's hull. In the same way, the nominal associated brake power ca be compared with actual *Thr1*, to alert of a problem related with propulsion efficiency.

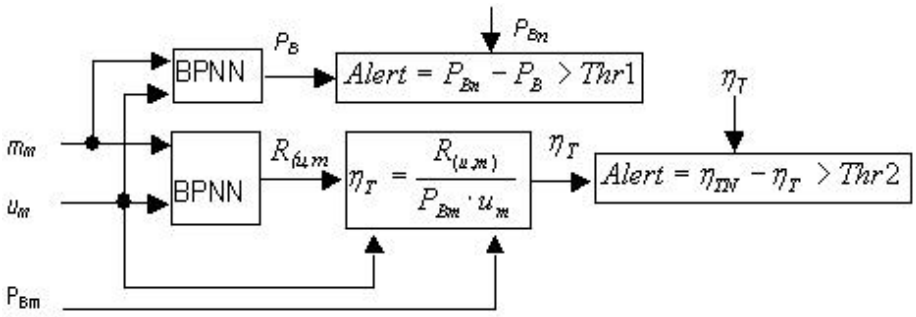

Fig. 5. Diagnosing the hull resistance and propulsion efficiency

As is well-known, the effective brake power P_B of a Diesel engine is proportional to the mean effective pressure (mep) P_e and engine speed n, that is

$$P_B = C \cdot P_e \cdot n \tag{18}$$

Functional redundancy can be applied by using (18) against P_B achieved by functional approximation as described in figure 4(b). If abnormal differences exists, then it is highly probably the presence of a fault in the P_B measuring device or in the device responsible for P_B generation, that means the propulsion engine. In order to avoid ambiguity with regard to measuring device, then triple redundancy is proposed. Then function to be applied could be achieved as follows: The operating curves for an engine indicate that the load torque Q is a nonlinear function of both the fuel flow rate F and the output shaft speed n. Consequently, the steady state dynamic behavior of the engine may be approximated by a BPNN structured as two inputs (F, n)and an output Q. Given the actual load torque, then, brake power is obviously achieved as described by (19). Figure 6 shows the BPNN necessary to approximate the function given by (19).

$$Q = f(F, n)$$
$$P_B = Q \cdot n \tag{19}$$

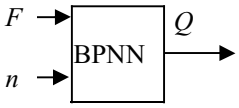

Fig.6. Load torque achieved by functional approximation with BPNN as function of fuel flow rate and engine speed.

Discussion of results

A conventional modeling technique proposed as an international Benchmark in propulsion system monitoring is compared with the proposed modeling technique based in functional approximation by means of massive application of virtual sensors based in conjugate-gradient back propagation neural networks.

Results shown in mentioned benchmark were compared with results achieved by applying proposed models described by (16), (17), (18) and (19).

The hull resistance as function of ship speed and ship cargo conditions at constant trim is shown in figure 7.

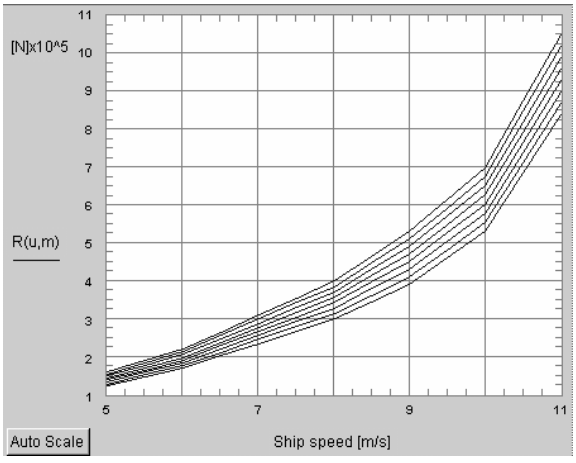

Fig. 7. Ship hull resistance as function of ship speed and ship loading conditions for different velocities.

The lower line belongs to a 16500 tons displacement and the upper line to the 23500 ton displacement. Intermediate lines belongs to 1000 tons difference between each other. Mentioned line functions are very different from those of conventional hull resistance coefficients mainly when ship speed is greater than 7-8 m/s..

Figure 8 shows the ship estimated speed due to propulsion system activity in which a step input in speed demand was applied. Two lines (dashed and continuous) are shown in each graph. Dashed lines belongs to proposed model while continuous line represents the conventional model used in benchmark. Left hand graph shows the ship speed as function of time and right hand graph shows the hull resistance as function of time.

As proposed modeling technique is experimental instead of empiric, it reflects virtually the real scenario. Slightly differences are observed after some reasonable time. Such differences are interpreted as modeling error which are prejudicial when processed as parity relations in searching for residuals.

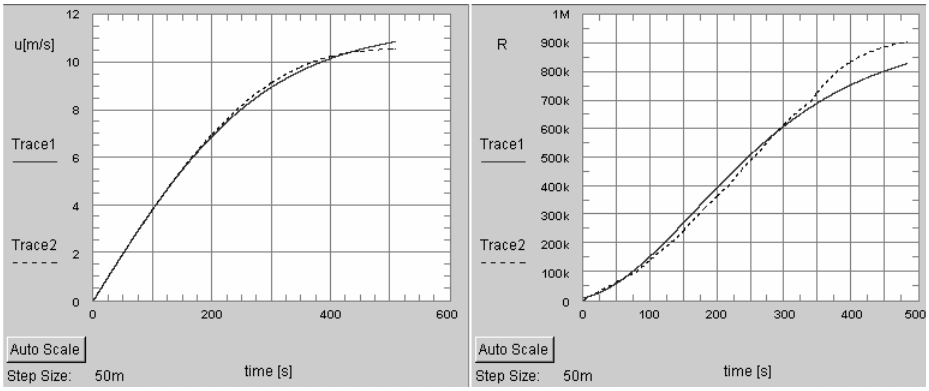

Fig. 8. Comparison of model results. Dashed line, functional approximation model. Continuous line, conventional model used in benchmark. Ship full loaded conditions (23500 Tons)

Nevertheless, in figure 9 there are shown the same curves for ship unloaded (ballast). The differences are much more relevant. It means that modeling errors are greater when ship is unloaded. It is due to ship nominal conditions which belongs to the conditions of full loaded ship. From the point of view of residuals generation,. mentioned differences are very important because they introduce an important degree of error in the residuals and an important lost of precision when malfunction detection is to be carried out.

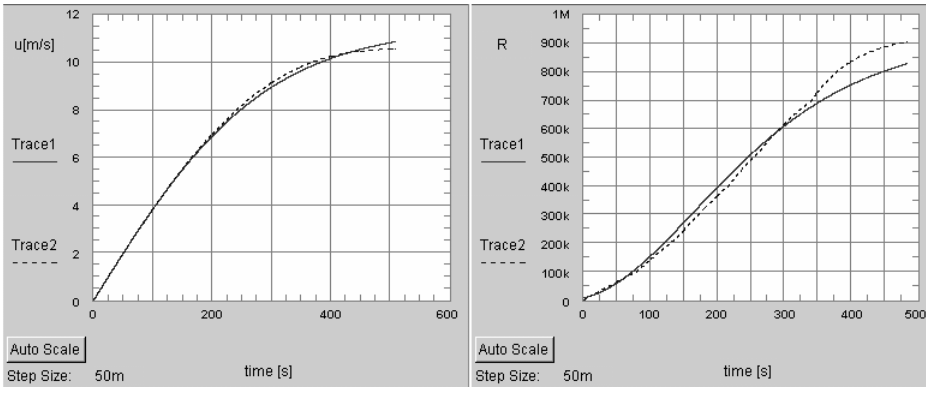

Fig. 9. Comparison of model results. Dashed line, functional approximation model. Continuous line, conventional model used in benchmark. Ship ballast loaded (16500 Tons)

The main drawbacks of using conventional modeling techniques with regard to proposed, are:

- The exaggerated deviations of ship parameters from nominal cargo conditions (ballast or full loaded conditions) are responsible for very different dynamic behaviors.
- The determination of coefficients used in (13) and (14) which depends on the advance number *J*, is a tedious task.
- The advance number depends on the speed of advance V_a and ship speed *u*, which depends on wake fraction. Wake fraction is affected of uncertainty because of variations in nominal conditions (speed and mass variation).
- The variation of ship mass at least in a 50% of total mass, and consequently the added mass and hull resistance contribute also to large modeling errors.

SOME CONCLUSIONS

By comparing simulation results achieved from the benchmark with those achieved by applying proposed functional approximation based models, different responses has been found, which used by means of parity relation, provides precisely and useful residuals when focused on fault detection tasks.

The fact of using functional approximation to describe nonlinear functions, reduce drastically the possibility of modeling errors, which makes the nonlinear residual generators sufficiently precise and flexible in a wide range of dynamic situations.

It has been shown that mentioned drawbacks disappear by applying neural network based modeling as virtual sensors and observers. As results of proposed enhancements due to different modeling techniques, ship speed, hull resistance and total mass (ship mass plus added mass) are easily predicted, providing relevant data in monitoring the propulsion system.

Acknowledgement

The author wishes to acknowledge the financial support of the Spanish MICYT and FEDER Founding at DPI2003-00512 project

References

M. Blanke, M. Kinnaert, J. Lunze, M. Staroswiecki. Diagnosis and Fault-Tolerant Control. Springer-Verlag, Berlin. Heidelberg, 2003 pp 469-496

R. Izadi-Zamanabadi and M. Blanke. A ship propulsion system as a benchmark for fault tolerant control. Technical report, Control Engineering dept.,Aalborg University, Denmark 1998.

R. Izadi-Zamanabadi and M. Blanke. A ship propulsion system as a benchmark for fault tolerant control. *Control Engineering Practice,* 7(2):277-239, 1999

M. Blanke. *Ship Propulsion Loses Related to Automatic Steering and Prime Mover Control*. PhD Thesis, Technical University of Denmark (DTU) 1981.

M. Blank and J. S. Andersen. On dynamics of large two stroke diesel engines: New results from identification. *Proceedings 9th IFAC World Conference*, Budapest 1984.

J. P. Gauthier, H. Hammouri and S. Othman. A simple observer for non linear systems applications to bioreactors. *IEEE Trans.* AC-37:875-880, 1992

D. Herrmann. *Qualitative Fehlerdiagnose im Automatennetz am COSY Ship Propulsion Benchmark*. Diploma RBEIT, tu Hamburg-Hamburg 2000.

TENDENCIA EN LAS TÉCNICAS DE MODELIZACIÓN APLICADA A LA MONITORIZACIÓN DE SISTEMAS DE PROPULSION DE BUQUES

Resumen

Los objetivos del artículo apuntan a varios aspectos relacionados con técnicas de modelización que utilizan redundancia analítica aplicada a la detección de fallos, su aislamiento y toma de decisiones sobre estrategias de recuperación en tareas de monitorización de sistemas de propulsión de buques, para conseguir tolerancia a fallos. Tales objetivos de modelización son llevados a cabo mediante la aplicación masiva de aproximadores funcionales basados en redes de neuronas artificiales, cuyas salidas son utilizadas como generadores de residuos mediante ecuaciones de paridad

INTRODUCCIÓN A LA ESTRUCTURA DEL SISTEMA DE PROPULSIÓN

El bajo rendimiento de los sistemas de propulsión asociado con los sistemas de automatización originan una reducción importante en la habilidad del buque para maniobrar en condiciones de seguridad aceptables, lo que requiere medios efectivos para prevenir fallos, evitando así la evolución hacia averías graves. Se pueden utilizar varios algoritmos y métodos desde diferentes áreas de investigación para analizar los sistemas y consecuentemente, detectar, aislar y decidir la estrategia de reconfiguración del sistema. El sistema de propulsión del buque descrito ha sido presentado como un marco de referencia "benchmark" de rango internacional por (M. Blanke, et al. 2003), (D. Herrmann, 2000) y ha sido utilizado como una plataforma de desarrollo de nuevas ideas y métodos de comparación.

Los aspectos tratados en este artículo están basados en la creciente demanda de estrategias de modelización en base tanto al análisis estructural como a aproximación funcional con datos experimentales. Se muestra como son directamente deducidos los generadores de residuos a partir del análisis estructural y como se puede obtener redundancia funcional mediante modelización basada en aproximación funcional. La dinámica del sistema de propulsión es fuertemente no lineal. Además, algunos fallos esenciales son no aditivos. Esto implica que algunos generadores de residuos son no lineales. Este trabajo ilustra como pueden ser manejados estos fenómenos de la vida real en un marco general a nivel de modelización. La modelización al detalle y la adquisición de información experimental a partir de pruebas de mar con el ferry referenciado en la bibliografía de referencia, proporcionan un escenario realista para el estudio de métodos de diagnóstico y técnicas para obtener tolerancia a fallos.

Sistema de propulsión del buque

El esquema del sistema de propulsión elegido para el benchmark se muestra en la figura 1 (tabla1 para la lista de símbolos) (R. Izadi-Zamanabadi and M. Blanke, 1998,1999).

Los componentes principales del sistema de propulsión se describen mediante una serie de bloques:

- — *Dinámica del motor Diesel*, proporciona el par motor que actúa sobre la hélice a través del eje propulsor.
- — *Dinámica del eje*, proporciona *Shaft dynamics* provides el par de rotación a la hélice a determinada velocidad de rotación.
- — *Características del propulsor*, proporciona el empuje en función del paso de la hélice ϑ, su velocidad de rotación n, y la velocidad de avance V_a .
- — *Dinámica del buque*, determina la velocidad del buque a partir del empuje del propulsory las fuerzas externas.
- — *Controladores de paso de hélice y velocidad del motor*, regulan respectivamente el paso de hélice y velocidad del eje en función de la demanda de velocidad del buque.

El bloque de cálculo de los valores de referencia de velocidad y paso de hélice está realizado por un controlador coordinado bajo criterios de eficiencia

Modelo del sistema de propulsión:

MODELO DEL SISTEMA DE PROPULSIÓN PROPUESTO

Introduction

El modelo convencional está basado en funciones de transferencia lineales combinadas con modelos no lineales en los cuales coexisten coeficientes variantes en el tiempo y pronunciadas no linealidades. Una alternativa al método de modelización convencional (M. Blanke et al., 2003), consiste en modelizar el sistema de propulsión por medio de aproximación funcional en base a la aplicación masiva de redes neuronales artificiales sobre todo en sub-modelos no lineales con parámetros tiempo variantes. Los datos necesarios para la modelización por el método propuesto proceden de pruebas de mar (R. Izadi-Zamanabadi and M. Blanke, 1999).

Aproximación funcional basada en redes neuronales artificiales

Las redes de neuronas artificiales (NN) son esencialmente aproximadores universales de funciones que utilizan las entradas del proceso para predecir la salida del mismo. La razón de la utilización de tecnologías basadas en NNs obedece a al hecho de ser implementados mediante software y capacitado para aproximar b cualquier función continua bajo cualquier grado de precisión. Los sensores virtuales que utilizan NNs son implementados mediante herramientas de soft orientadas a

objetos capaces de realizar las fases de captura y procesado de información, el entrenamiento y la aplicación posterior al proceso en cuestión.

Sistema de monitorización alternativo

La resistencia al avance del buque está particularmente influenciada por la velocidad, el desplazamiento, la forma del casco y las condiciones dinámicas del mismo la resistencia total al avance R_T consiste en varias Fuentes de resistencia R las cuales pueden ser clasificadas en tres grupos prncipales: resistancia friccional, resistencia residual y resistancia al aire.

La resistencia al avance R debida a las fuerzas hidrodinámicas en la dirección de avance (popa-proa) es una función no lineal de la velocidad del buque y la superficie mojada, la cual está asociada al desplazamiento del buque a asiento constante. Mediante aproximación funcional se consigue la modelización precisa de la resistencia al avance como alternativa a la modelización convencional con observadores aplicada para resolver el problema de detección de fallos y aislamiento en sistemas de propulsión ensayada en (M. Blanke, et al. 2003), (J. P. Gauthier, 1992)

DISCUSIÓN DE LOS RESULTADOS

Se ha comparado una técnica convencional de modelización propuesta como un "benchmark" internacional para sistemas de propulsión de buque con una técnica de modelización basada en la aplicación masiva de aproximadores funcionales con técnicas neuronales para la monitorización, lo cual incluye detección temprana de fallos, aislamiento toma de decisiones y recuperación, esto es, tolerancia a fallos. Los inconvenientes hallados cuando se aplican las técnicas tradicionales son:

- variaciones exageradas de los parámetros del buque a partir de valores nominales de operación (condiciones de carga y velocidad)
- la determinación de los coeficientes descritos y utilizados en (13) y (14), los cuales dependen del factor de avance J, y del paso de hélice.
- el factor de avance depende de la velocidad de avance y de la velocidad del buque, y ésta depende del factor de estela. A su vez el factor de estela está afectado por incertidumbre a causa de las variaciones en las condiciones nominales de navegación(variación de masa y velocidad)
- la variación de masa del buque que conlleva la masa hidrodinámica añadida a diferentes velocidades contribuye a una fuente de error de modelado importante.

CONCLUSIONES

Mediante la comparación de los resultados obtenidos a partir del benchmark con los resultados obtenidos al aplicar los métodos de modelización basados en la aproximación funcional, se observan diferencias esenciales, las cuales al ser utilizadas

por los generadores de residuos mediante ecuaciones de paridad, proporcionan resultados de detección de anomalías con baja precisión. Tal aseveración se basa en el hecho de que las diferencias observadas obedecen al error de modelado de los modelos convencionales, puesto que la modelización propuesta refleja el comportamiento dinámico con suficiente precisión.

Se ha mostrado que los inconvenientes citados desaparecen aplicando aproximadores funcionales de modo masivo para la modelización. Como resultado de ello, entre los objetivos de detección de anomalías se hallan otras ventajas como la de predecir la masa añadida, la velocidad y resistencia al avance, lo que produce información relevante en las tareas de monitorización a modo de sensores virtuales.

Journal of Maritime Research, Vol. II. No. 1, pp. 105-125, 2005

ISSN: 1697-4840

SIMULATION OF PASSENGERS MOVEMENT ON SHIP EMERGENCIES. TOOLS FOR IMO REGULATIONS FULFILMENT

A. López Piñeiro[1], F. Pérez Arribas[2], R. Donoso[3], R. Torres[3]

ABSTRACT

The main objective of this paper is to present the conceptual design, models and user oriented software tools developed to apply the IMO passengers evacuation rules in an automatic way. A summary of the main ship evacuation problems, underlining the differences between land and ship emergency situation are presented. Also we present the related IMO regulations with an historic and present rules review. We show the different numerical model types used for the study of pedestrian movement and its evolution towards cellular agents models. Also we present an historic overview of the work made in this area by our Spanish research group. Finally the results inside the SIFBUP research project are presented. Its main aim is the analysis and simulation of the passengers flow aboard ships, specially focused in the resolution of problems related with ship evacuation in emergency situations.

Key Words: Ship evacuation, pedestrian movement, cellular agents model.

INTRODUCTION. THE SHIP EVACUATION PROBLEM.

The well-known disasters of the Herald of Free Enterprise, Scandinavian Star and the Estonia have set a new regulation about passengers safety and crew training of passengers ships that include ship evacuation and evacuation aids.

[1] Dr. Ingeniero Naval. Catedrático de Universidad Director del Laboratorio de Electrotecnia, Electrónica y Sistemas. (amable.lopez@upm.es). Dpto. Sistemas Oceánicos y Navales. Escuela Técnica Superior de Ingenieros Navales. Universidad Politécnica de Madrid.

[2] Dr. Ingeniero Naval. Profesor Asociado. Dpto. Enseñanzas Básicas de la Ingeniería Naval. Escuela Técnica Superior de Ingenieros Navales. (fperez@etsin.upm.es) . Universidad Politécnica de Madrid.

[3] Ingeniero Naval. Aula Izar

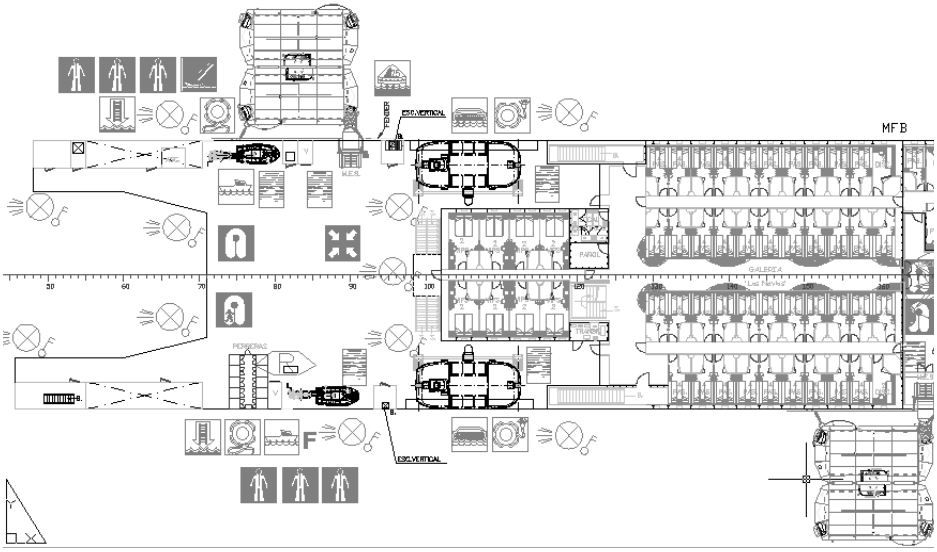

Figure 1. Partial view of ship evacuation facilities

In all transport and public building it is compulsory to have a scheduled evacuation plan and during an emergency situation all people must follow it. From the post-catastrophic analysis of significant events, the experts underline the following people behaviour:

— Most of people do not start walking the emergency alarm sounds. There is an important delay to react to the alarm indication, known as "awareness time".
— People usually follow a known route better than follow the emergency exit symbols.
— In general, people move with a strong influence of their relatives behaviour.
— Evacuation symbols are not followed, especially if they are text ones.
— Physical and psychological constraints are very important, with significant variation between different people types.
— People can go through a smoky area of reduced visibility, especially if they know well the place or if someone acting as a leader guides them.
— In crowded situations, it is not common the generation of a panic situation.

But also there are big differences between land emergency situations and ship evacuation (Lopez, 2002). The environment and the human behaviour are quite different due to:

— Distribution and evacuation aids that are unknown for the normal passenger.
— Different crisis origin.
— Movements are difficult in a non-horizontal and unsteady platform.

— The ship is isolated and frequently in a "rough sea".
— People (passengers and crew) with multilingual and multicultural origin.
— Different ship operation situations.

Due to the mentioned reasons, passenger ship evacuation is a complex process (figure 1). According to IMO regulations (MSC, 2002) it must be scheduled in mustering and abandon phases (M&A). The first is an uncontrolled movement of people from the initial places to assembly stations. In the second stage the passengers have to be guided (controlled) by crewmembers that develop a supervised plan avoiding unnecessary crowds and queues.

Evacuation may happen at any time while sailing. So, facilities for it must be always ready. The crew must be trained with frequent aboard exercises. They will know the evacuation ways and their duties at these situations. Maintenance of the evacuation ways and lifesaving systems is also an important matter.

According to IMO, the main part of the Ship Evacuation Plan (SEP) is: "an operating guide, either printed or in computer format, where missions and duties of the crew, basic operations sequence and operating criteria (with examples, if possible) are indicated". The main interfaces of the SEP with passengers' evacuation are the information sings in the escaping routes and the instructions in the case of ship evacuation. A good SEP must:

— Be easily managed; with a clear abandon group definition and their travel schedule (without crossing or overlapping between groups).
— Calculate, with a suitable reliability level, the arrival time to the mustering stations for the different passengers groups.
— Calculate and minimise the time between the ship abandon command and the moment that the last person abandons the ship.

During emergency stage, the situation must be managed according to the SEP through appropriate decisions and commands according the two phases of the M&A process. From the start of the emergency signal and during the mustering phase there will be few control (formally there will be uncontrolled passenger movement). Passengers go to the assembly stations following the main or the secondary evacuation plan and signals.

Then, the crew verify passenger's number and their lifejackets use. When the Master give the "ship abandon" order, the crew lead the passengers towards the embarkation points (evacuation stations) in "controlled groups" through the ship evacuation routes, moving at a near-optimal speed and flow. For this controlled passenger' flow, there are two different options: one member of the crew acts as a "leader" for a group of passengers, or different crewmembers are placed in critical points of the evacuation route in order to guide the passengers and regulate their flow.

As a consequence of the mentioned above, the need of specific models and tools for the ship evacuation analysis is clear.

IMO REGULATIONS

IMO (International Maritime Organisation) from a long time has published an extensive normative about ship evacuation, meanly in SOLAS regulation (IMO, 1973), mainly defining the safety boats and rafts number and characteristics. Until the last century end, the main regulation about inside ship design related with evacuation was the Amendment 757 that regulates the stair wide. This situation has changed by mean of the work of the IMO MSC (Maritime Safety Committee).

In 1999 the MSC published the Circular 909 tilted "Interim guidelines for a simplified evacuation analysis of ro-ro passenger ships" (MSC, 1999) that was the first attempt to have a whole analysis about the passenger movement inside ship during emergency situation. Other IMO regulations have been publishes in order to improve the evacuation process on different passenger ships (Ro-pax, HSC, large passenger ships, etc.).

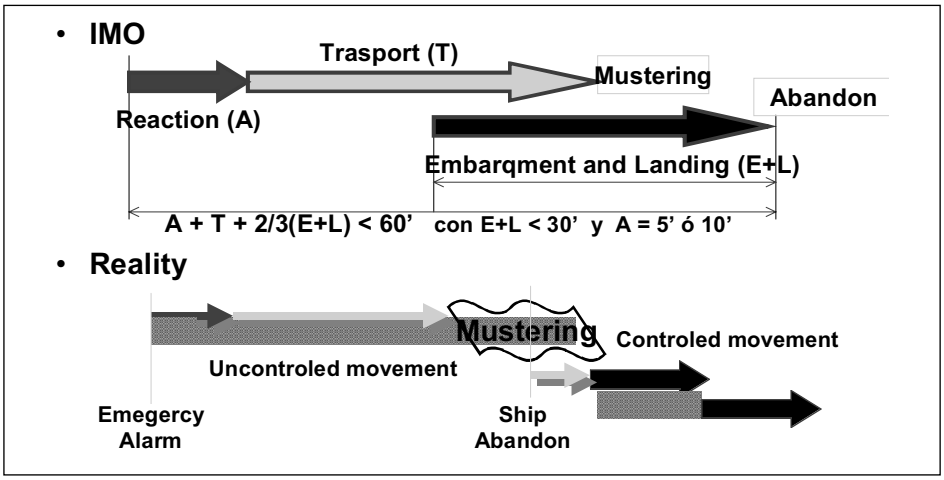

Figure 2. Comparison between IMO SEP and real situations.

Finally the MSC has published in June 2002 a document (MS-c1033) titled "Interim guidelines for evacuation analysis for new and existing passenger ships" (MSC, 2002), that includes two analysis methods. This guide mentions that further investigations and developments are necessary. It offers the possibility of using two different methods:

— A simplified evacuation analysis.

— An advanced evacuation analysis.

The Committee, as far as both methods need to be extensively validated, agreed that the Guidelines would have an interim nature and that the evacuation analysis methods should be reviewed in the future with the light of the results of experience using the present Guidelines, ongoing research and development aiming

at applying only the advanced evacuation method and, when available, analyses of actual events utilizing it.

The **simplified analysis** is based in a macro-model adapted from the buildings evacuation method (Perez, 2003). For the calculation of the evacuation time, the following components are considered:

— The awareness time (A) is the one that people need to react to an emergency situation.

— The travel time (T) is defined as the time it takes people to move, to the assembly stations and the embarkation stations. For its calculations, a hydraulic macro-model is used, based on a speed-density function modelled with data of table 1.

— The embarkation and launching time (E+L) is the sum of the time required to provide ship abandonment.

The evacuation process, as illustrated in figure 2, should be complied with:

— Calculated total evacuation time: $A + T + 2/3 (E + L) \leq n\ E + L \leq 30'$ For Ro-Ro passenger ships, n = 60. For passenger ships other than Ro-Ro passenger ships, n = 60 if the ship has no more than 3 main vertical zones; and 80, if the ship has more than 3 main vertical zones.

With the **advanced evacuation analysis** each occupant is studied as an individual that has a detailed representation of the layout of a ship and simulates the interaction between people and the ship environment.

Type of facility	Initial density D (p/m2)	Initial specific flow Fs (p/(ms))	Initial speed of persons S (m/s)
Corridors	0	0	1.2
	0.5	0.65	1.2
	1.9	1.3	0.67
	3.2	0.65	0.20
	≥3.5	0.32	0.10

Table 1. Values of initial specific flow and initial speed as a function of density.

This method of estimating the evacuation time is based on several idealized benchmark scenarios and the following assumptions are considered:

— Passengers and crew are represented as unique individuals with specified individual abilities and different response times.

— Passengers and crew will evacuate via the main escape routes.

— Passenger load and initial distribution is based on chapter 13 of the FSS Code.

— Full availability of escape routes is considered unless otherwise is stated.

At least, four scenarios should be considered for the analysis. Two scenarios, namely night (case 1) and day (case 2) and, two further scenarios (case 3 and case 4) based on reduced escape route availability are considered for the day and night case.

The Guide permits a big freedom in the model choice with the following limits:

— Each person is represented in the model individually.
— The abilities of each person are determined by a set of parameters, some of which are probabilistic as show in table 2.
— The movement of each person is recorded.
— The parameters should vary among the individuals of the population.
— The basic rules for personal decisions and movements are the same for everyone, described by a universal algorithm.
— The time difference between the actions of any two persons in the simulation should be not more than one second of simulated time, e.g. all persons proceed with their action in one second (a parallel update is necessary).

Also the Guide explain a validation procedure with 11 test designed to check that pax moves:

— With speed, flow and reaction times corrects.
— In a logical mode against obstacles and counter-flow.
— With whole results in complex scenarios consistent whit changes in the flow parameters.

Population groups - passengers	Walking speed on flat terrain (e.g. corridors)		
	Minimum (m/s)	Mean (m/s)	Maximum (m/s)
Females younger than 30 years	0.93	1.24	1.55
Females 30-50 years old	0.71	0.95	1.19
Females older than 50 years	0.56	0.75	0.94
Females older than 50, mobility impaired (1)	0.43	0.57	0.71
Females older than 50, mobility impaired (2)	0.37	0.49	0.61
Males younger than 30 years	1.11	1.48	1.85
Males 30-50 years old	0.97	1.3	1.62
Males older than 50 years	0.84	1.12	1.4
Males older than 50, mobility impaired (1)	0.64	0.85	1.06
Males older than 50, mobility impaired (2)	0.55	0.73	0.91
Population groups - crew	**Walking speed on flat terrain (e.g. corridors)**		
	Minimum (m/s)	**Mean (m/s)**	**Maximum (m/s)**
Crew females	0.93	1.24	1.55
Crew males	1.11	1.48	1.85

Table 2. Example of population data.

The travel time, both that predicted by models and as measured in reality, is a random quantity due to the probabilistic nature of the evacuation process. In total, a minimum of 50 different simulations should be carried out for each of the four-benchmark cases. A safety margin is added to account for the assumptions. It is 600 s for cases 1 and 2 and 200 s for cases 3 and 4

Finally the Guide reflects the documentation of the algorithms should and that the results of the analysis should be documented by means of:

The travel time, both that predicted by models and as measured in reality, is a random quantity due to the probabilistic nature of the evacuation process. In total, a minimum of 50 different simulations should be carried out for each of the four-benchmark cases. A safety margin is added to account for the assumptions. It is 600 s for cases 1 and 2 and 200 s for cases 3 and 4

Finally the Guide reflects the documentation of the algorithms should and that the results of the analysis should be documented by means of:

— Details of the calculations.
— The total evacuation time.
— The identified congestion points.

PEDESTRIAN MOVEMENT MODELS

If we study the different approaches to pedestrian movement analysis, that is the base for aboard evacuation study, we can classify the used models in tree groups: macro-models, micro-models and meso-models.

Macro-models consider the behaviour of people movement analysing the global response of a group that occupies a local or sector. The main parameters are speed, maximum flow and passengers' density. From land evacuation studies, different functions have been proposed for the curve speed vs. density (figure 3). In optimal path analysis it is normal to consider constant speed and maximum flow.

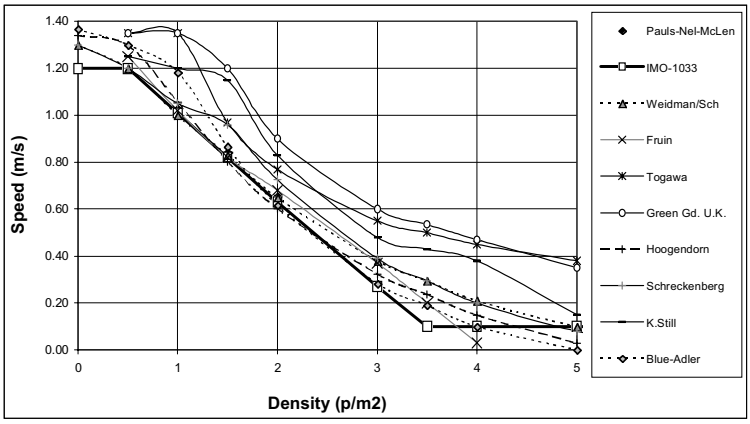

Figure 3. Speed vs. pax density.

In any case, the most important simplification is the modelling of people as a compressible fluid, with a maximum flow and density. Any situation that tries to overpass it, produces a "catastrophic" response (queue formation), This methodology is known as "hydraulic model".

Micro-model approach presents the movement of every person. There are three main approaches: linear, corpuscular and the cellular ones (Perez, 2001). At the moment the last one is the most popular on technical developments (Lopez, 2003). It is based in the division of the available space for motion in squared cells that can be occupied (or not) by a person.

The movement of every person is influenced by its objectives (direction, attraction, etc.) and by the occupation of the near cells (people, walls,). It is a discrete model (in space and time) well adapted for programming with "agent modelling" techniques. The Meso-model makes a mixture of previous models (Letizia, 2000), (Lopez, 2002). Generally it uses the macro for calculus and the micro for presentation.

One important modelling aspect is the variability of human behaviour. Data of figure 3 are mean values, but people speed can be a function of: age, gender, health, platform stability, etc. (Brumley, 200). Due to this reason, input data for the micro-models must be heuristic and tools based in it must use Monte-Carlo simulation methodology or other similar ones to obtain reliable statistical results.

In this moment the most advanced pedestrian movement simulation tools are based on cellular models. In it the space is divided is squared cells, and passengers are studied individually like. One person thereby occupies one cell and two different passengers cannot occupy the same cell. Other cells contain different information, depending on the way it influences the person standing on it. If it is not accessible, it represents an obstacle like a wall or furniture.

The individual behaviour of every passenger when going from cell to cell is studied by mean of an "agent model". Passenger's speed is influenced by passengers' density around, and by the number of cells in the advance direction that the person can move. One passenger cannot jump others to move forward them, and must go through left or right, if possible. If not, he must wait or move laterally in some cases.

SESAMO AND SIFBUP MODELS AND TOOLS

Since long time ago, Izar shipyards and the ETSIN R&D Group on Aboard Human Factors have a close collaboration in the study of ship evacuation problems. The first attempt start in 1997 with the B-09 Project, developed under the Astilleros Españoles (today integrated in Izar) direction. Its aim was to develop a new type of ro-pax ship, including the developing of tools for its evacuation analysis.

In this time there was no definitive method for studying the evacuation of a ship, so, the ETSIN evacuation research team developed a detailed study on advantages and disadvantages of different methods and their usage in practice. Based on this work some methods and tools have been developed for qualitative and quantitative analysis for ship evacuation. The acronym of these methods is SESAMO (Ship Evacuation Simulation and Analysis, Madrid Original). Their common model is a network inside the general arrangement for the study of the passengers flows follow-

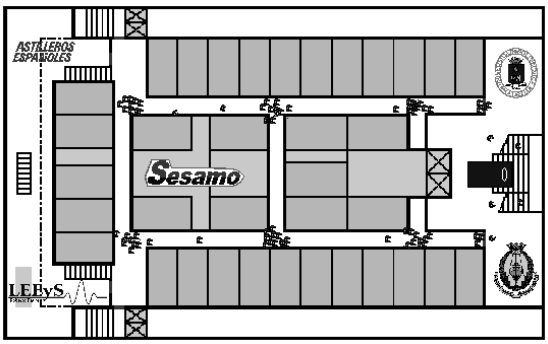

Figure 4. Graphical output of Sesamo-S program

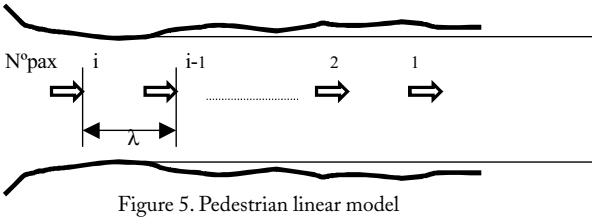

Figure 5. Pedestrian linear model

ing the hydraulic methodology with macro- and meso-models use. There are different versions with different in complexity (Lopez, 1999):

— P (Preliminary) A manual method that allows to check the evacuation plan and its devices in a few hours and see the critic points of the arrangement.

— M (Manual) The agreement with the MSCc909 normative of the evacuation plan is checked and specially the total time of evacuation. Excel ® support is used for the calculations.

— T (Temporal) Like M bu with a specific treatment of the beginning and disappearing of queues.

— S (Simulation) Based on useful tools for the study of the evacuation plan, evacuation routes and salvage devices. Arena support is used for the simulation, as show in figure 4.

When the B-09 was finishes the ETSIN R&D group study the feasibility of a micro-model based in the representation of individual passenger movement in corridors (figure 5). The model core was that the speed of a pax was function of the separation (l) with the previous one (Perez, 2001). The developing of MSC circular 10033 shows us that we must move toward cellular models.

Based in this previous experience, under the support of the Spanish R&D Program for the Shipyard Industry, sponsored by the Ministry of Science and Technology and controlled by the "Gerencia del Sector Naval", we started in 2002 the Sifbup project (DINN-17) with a team composed by:

— Izar, the Spanish main group of shipyards, as main partner with expert knowledge in ship design.

— The ETSIN as scientific partner and responsible of the development of the software tools.

— Trasmediterranea, the main Spanish company of passenger ships, with direct experience on passenger ship operation.

— Next Limit Company, experts on 3D simulation. Incorporated in the middle of the project life.

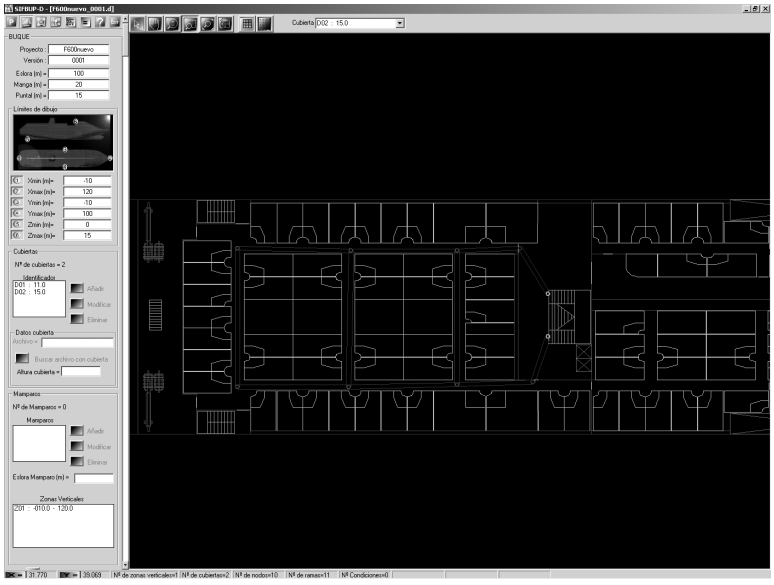

Figure 6. Sifbup-D user Interface.

The main project objective is to develop a family of tools designed to aid the study of aboard people and vehicles flow. We have developed different tools oriented to the various necessities along the ship' life, such us:

— The Sifbup-D, for the evacuation study in the first phases of the ship project.
— The Sifbup-S, a 2D simulation of people movement in normal aboard operation and in emergency situations.
— The Sifbup-S3D, to see the people movement in a "virtual reality" environment.
— The Sifbup-V, to analyse the load and unload operations of trucks, cars and other vehicles inside ferries and other Ro-Ro ships.

The Sifbup-D has been designed to fulfil with the MSC-c1033 simplified evacuation analysis with a design (figure 6) specially oriented to de preliminary ship design phase. It is based in a macro-model that could be of easy use and have a quick response. It uses an initial model of the evacuation network with nodes (gates, cross-points, etc.) and branches (corridors, stairs, etc.), like is showed in figure 7.

The macro-model computes the passenger evolution calculating the initial and final passing time of every passengers group through all the nodes that the group follows. It also includes the checking of possible interaction between groups in every node and the detection of queues.

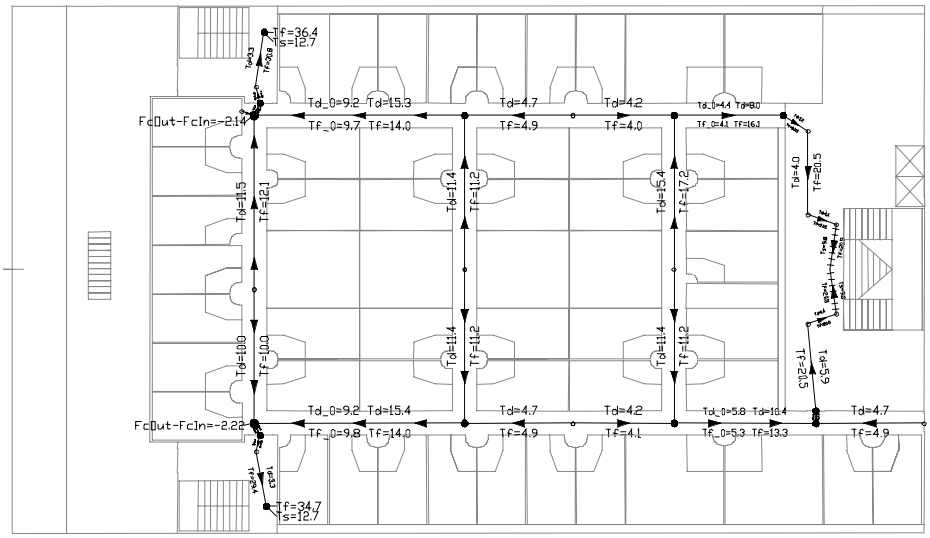

Figure 7 Sifbup-D Evacuation draw

THE SIFBUP-S MODEL

For the design of the Sifbup-S model we need to adapt the cellular model for complex spaces. The general arrangement of the ship or a part of it, with cabins, corridors and public spaces is imported (via a .dxf file normally) and floor is divided in squared cells of 0.4 by 0.4 meters (figure 8, left). This is a standard value in evacuation studies (Koning, 2001) that derives from the maximum density in crows when the movement reaches a stop.

This discreetization and the cell size could be an important error source. The main argument against the use of cells is the exclusion of small variations in the width of corridors or doors. In our design this problem is overcome with a coefficient that affects the speed and it is a function of the corridor or door with where the passenger is moving.

The next important design concept is that the ship and evacuation modelling is divided in these stages: Strategic, tactical and operative levels.

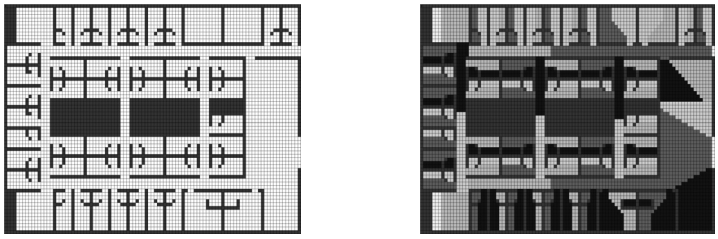

Figure 8. Discreetization in cells and tactical level.

The strategic level

In this stage we define the scenario layout and solve the problem concerning with orientation of a person is the global route choice. How a person evades obstacles and other passengers is considered in the operative level as is described forward, but the way that a person chooses where to go and to get there is the decisive problem. In the case of evacuation, this is called the evacuation plan that can be the main evacuation plan or secondary evacuation plan if the main is not possible because of fire or flooding for example.

Our cellular model can works with the information generated by the Sifbup-D, with branches and nodes in specific points. In this strategic level, decisions about the destiny points of the passengers (mustering and embarkment stations) are made. So, this strategic level is quite related with macro-models.

The tactical level

The main objective of this stage is to solve the direction in which passengers have to move in order to reach their goal (figure 8, right). So, a person knows where to move in the next time step and these motions will lead the final goal (mustering or embarkation stations). Crewmembers and passengers could have different routes towards the mentioned stations according their duty schedule at emergency, and sometimes, practically ever, there are encountered flows between crew and passengers. That is the reason because the model must solve encountered flows as it will be seen in the point IMO requirements, and every cell can have stored more than one route.

In our approach route information in given through potentials. This means that only goal cells have to be marked, and the potential will automatically spreads the directions from one accessible cell to the following and by this throughout the whole structure. When passengers reach the mustering stations, they wait in their cells until they can go to the different embarkation stations, as long as the lifeboat or other devices are being prepared.

Environmental conditions could be considered in this tactical level. If the ship is heeled port board during evacuation, the directions of the cells can be changed, "pushing" or changing the tendency of motion port board. Rolling motion can be also considered, by doing a periodical change of the tactical level (meanly in the speed effect) with the modal period of the Sea State where evacuation occurs. The effect of the environment can also affect speed in the operative level.

The operative level

Form the model work; this is the most important level. Every passenger is represented by an "agent" with interact with two cell matrixes at every moment: A sight matrix and a motion matrix. These have studied dimensions in order to have an

optimal point between precision and computer time. In figure 9 on show different situations for a pedestrian reserved cells are presented as arcs and selected path for advance with an arrow.

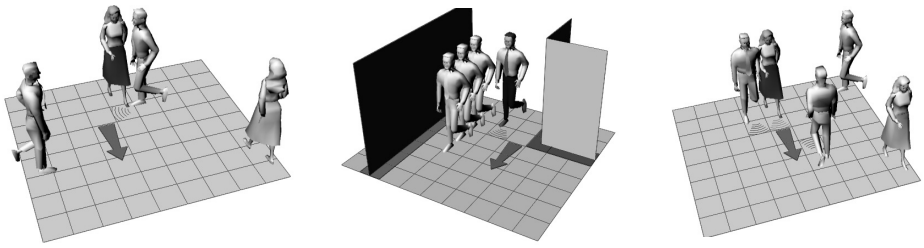

Figure 9. Examples of the operative level.

Passengers' density is calculated in a cell matrix that surrounds the passengers (sight matrix). With this passenger's density, speed can be obtained through an expression based in experimental results. According table 1 we use the following:

$$\begin{aligned} &S = S0 \cdot 1 \; ; D \;\; 0.5 \text{ pax/m2} \quad [1] \\ &S = S0 \cdot (1.153 - 0.306 \cdot D); 0.5 < D \;\; 3.5 \text{ pax/m2} \\ &S = S0 \cdot 0.082; 3.5 < D \text{ pax/m2} \end{aligned} \qquad (1)$$

Where S0 is a probabilistic function of the passenger type (crew, age, gender,) and MSC-c1033 Annex 2 also provides the values and D is the passengers density measured in the sight matrix. As far as the advance is a multiple of the cells length, sometimes a passenger will advance more than the exact value assigned by the speed function, and other times less. This lack or excess in the advance distance should be taken into account to correct the advance in the next time steep.

But a passenger can advance only the number of free cells in the direction of motion which is assigned in the tactical level, so this calculation is made in the motion matrix, and the lower of these two values (cells assigned by the speed function and free cells) is the number of cells that a passenger advances in this time step. So, a passenger can choose advance through the column or row of cells (path) of the centre, left, or right, chosen with an optimum path algorithm.

Every passenger reserves also one cell just in front of her for the next time step (arcs in figure 9), and this cell cannot be occupied or crossed by other passenger. This is a polite behaviour, trying not to disturb the advance of the rest of the passengers crossing their way, and in case of encountered flows, trying not to be face to face of other passenger.

THE SIFBUP-S APPLICATION

Once we developed the cellular model for the movement of persons in complex geometry environments, we made its implementation in a computer application (the Sifbup-S), using Visual-Basic programming language

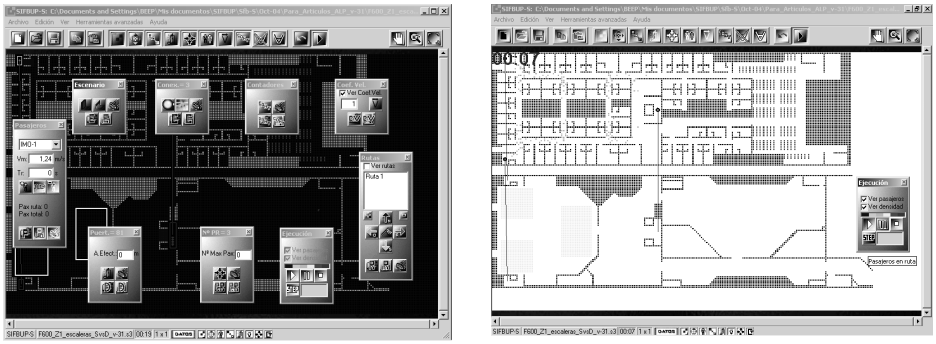

Figure 10. Sifbup-S edition an execution interfaces.

Our objective was to develop a flexible application, modular, integrated and oriented to the user (Lopez, 2003). The participation in the project of a shipyard, a ship owner and a company leader in visualization software were fundamental for its practical aspects. As a specification summary, the Sifbup-S has been designed to solve the following objectives:

- It fulfils with the advanced method of the MSC-c1033.
- Its concept design is opened, allowing the simulation of the movement of persons in 2D in complex stages.
- For the definition of the case and its analysis, it uses a modular structure with several data files that allow the use of previous work to modify or expand the present project.
- This structure allows to be integrated with other applications, such us CAD ones importing design in .dxf format, and the Sifbup-D and Sifbup-S3D.
- The user can start with a general analysis of the ship zones, using quick input data and then the user can improve the model, working with greater precision (doors, speed coefficients, etc.) at the critical zones.
- The 2D simulation allows a global and detailed vision of the evolution of a situation.
- The graphic interface design is highly ergonomic with Windows structure and an extensive mouse use.

In figure 10 we see the application general aspect in the edition and calculation modes.

The edition process can also be accomplished in manual form, if we have not any previous data files, or in an automated way if we have previous studies from other applications. In the first case it is compulsory to provide the following data:

— Layout representation.
— Routes definition (field of directions)
— Pax placement in theirs start points
— Connections (staircases) between decks or floors.

When the project definition is finished, we can start the simulation. We will see in the screen all pax movements (figure 11). In order to make easy this graphic analysis the application has several usual post-process facilities (Scroll and zoom; Stop (pause) and step-by-step execution; Image capturing; etc...) and each pax has a triple symbol tag:

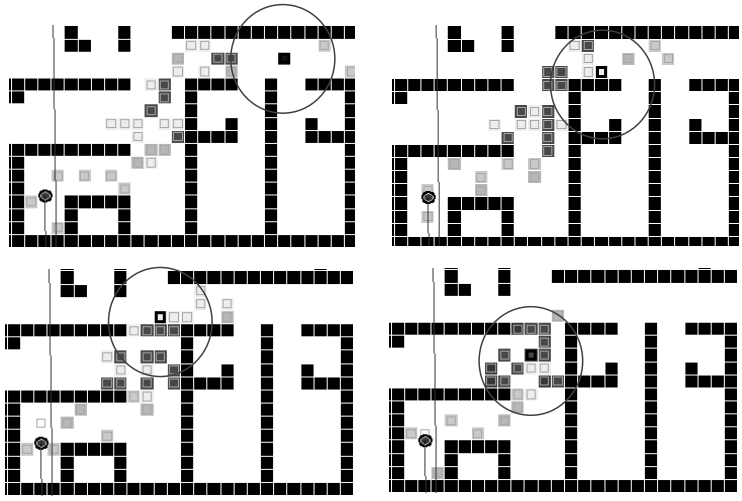

Figure 11. Advance images of a tagged pax.

— The symbol shape: represents the pax type, which is related to his maximum speed.
— The symbol colour: shows the pax origin (route).
—The cell background: informs about the density around a cell.

When calculation phase is finished, a special mark appears on all the cells which density have overcomes a threshold limit during a significant period of time. By this way is easy to identify the crowded zones that will affect seriously to the evacuation process.

By default the calculation mode works with a deterministic method. This helps the post-process and initial analysis. According to the advanced methodology indicated by the regulation MSC-c1033, the application has also a random analysis

mode. This randomises automatically the properties of each pax and allows a statistic analysis of the total time of the evacuation, with multiple speed and awareness time distribution for a given study.

The program also exports the following information:

— Evolution of the pax number along time in the points were counters are placed.
— Multiple "photos" of the process.
— Video image of all the evacuation process (using external tools).
— Statistic results.
— Final pax position.
— Path of every single pax during the simulation. Starting with this data file we can work with the application Sifbup-3D to generate a simulation in 3D, as shown in figure 12 with the scene visualization controlled by the user (virtual reality).

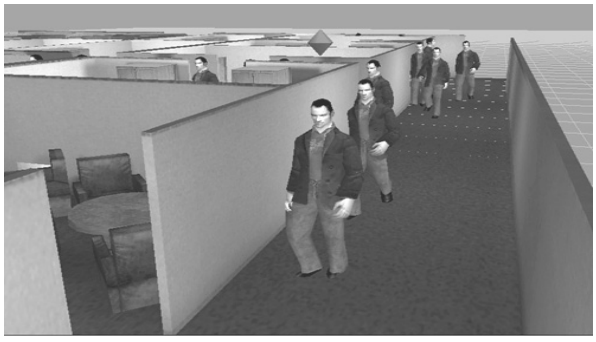

Figure 12. 3D evacuation simulation.

CONCLUSIONS

The evolution on maritime regulations on people onboard behaviour during emergency situation has been presented, showing the trend to the use of simulation tools, Also, the necessity of special models to study the movement of people on complex and size limited scenarios has been showed, with the special requirements to use them on ship emergency evacuation simulations.

The accomplishment of the existing regulation has to be implemented with a family of models and modular tools in order to make easy the designers work. For the first steps a macro-model will be the optimal solution if it can be connected with more advanced model

Our approach to solve the simulation approach, was based on an improved cellular agent model; it is a good solution, not only on the theoretical face, but also on their easiness to use it to develop a used oriented application for the pedestrian flow aboard simulation.

REFERENCES

Brumley A. and Koss L. (2000): The influence of human factors on the motor ability of passenger during the evacuation of ferries and cruise ships, *Conference on Human Factors in Ship Design and Operation, London.*

IMO (1973) Security Of Life At Sea Regulation (SOLAS), ed. *International Maritime Organization London.*

Konig T. et al. (2001): Assessment of Evacuation of Processes on Passenger Ships by Microscopic simulation In: Schermberk, A. ed. *Pedestrian and Evacuation Dynamics*. Ed. Sharma, London.

Letizia, L. (2000): Developments in Evacuation Systems and Techniques", *Safer-Eurororo Workshop, Madrid,.*

López, A.; Robledo, F. et al. (1999): Investigación multi-institucional sobre ferry de alta velocidad,. *36 Sesiones Técnicas de Ingeniería Naval. AINE, Cartagena*.

López, A. (2002): Simulación del movimiento de las personas a bordo. Aplicación a la evacuación en situaciones de emergencia". X *Jornadas Universidad Politécnica de Madrid – Fuerzas Armadas, Madrid.*

López, A. and Pérez, F. (2002): Models and tools for the ship evacuation simulation, *3rd. International Congress on Maritime Technological Innovations and Research, Bilbao.,*

López, A. and Pérez, F. (2003): Ship evacuation optimisation. Tools for master an designer aid, *2nd International Conference in Pedestrian and Evacuation Dynamics (PED'03), London.*

López, A. and Pérez, F. (2003): Designer and master aids to improve the evacuation of passenger ships, *World Maritime Technical Conference. S. Francisco*.

MSC (1999) "Interim guidelines for a simplified evacuation analysis of ro-ro passenger ships"

MSC (2002): Maritime Safety Committee Circ. 1033. IMO, London.

Pauls, J. (1993). *SFPE on fire protection engineering handbook. Chapter 13: movement of people*. New York: NFPA.

Pérez, F.and López, A. (2001): A 2D model to study the evacuation of ship passengers, *Second International Conference "Navy ands Shipbuilding Nowadays" NSN'2002, St. Petersburg.*

Pérez, F and López, A. (2003): Cellular models applied to the evacuation of ship passengers, *International Congress on Ship and Shipping Research, Palermo.*

SIMULACIÓN DEL MOVIMIENTO DE LOS PASAJEROS A BORDO DURANTE EMERGENCIAS. HERRAMIENTAS PARA EL CUMPLIMIENTO DE LA NORMATIVA DE LA OMI

RESUMEN.

El objetivo principal de este artículo es presentar el diseño conceptual, los modelos y las aplicaciones informáticas desarrollados para cumplir con la normativa de la OMI sobre evacuación de pasajeros. Se presenta un resumen de los principales problemas relacionados con la evacuación de un buque, resaltando las diferencias entre las situaciones en tierra y a bordo, completándose con una visión general de la evolución de la normativa de la OMI. Tras revisar los distintos tipos de modelos utilizados para el estudio del movimiento de peatones se presenta la evolución de los trabajos en esta área realizados por nuestro grupo de I+D. Finalmente se presentan los resultados del Proyecto Sifbup, haciendo un especial énfasis en los aspectos de modelado y simulación del movimiento de personas en 2D.

NORMATIVA Y TIPOS DE MODELOS.

La principal diferencia entre un buque y un edificio, cuando se desencadena un proceso de evacuación, ocasionado por una emergencia, es el entorno circundante. En tierra lo más seguro es salir cuanto antes a la calle, pero el mar es un entorno incómodo y peligroso, por lo que la decisión de abandono del buque debe ser tomada solo en casos extremos.

Por ello, la reglamentación de la OMI indica que ante la aparición de una situación de emergencia a bordo, el proceso de evacuación debe realizarse en dos fases:

- Una primera de "reunión" en la que los pasajeros (y parte de los tripulantes) deben ir hasta los puestos de reunión, en donde son informados y controlados. Estos puestos deben tener unas condiciones de seguridad y confort para poder ser utilizados durante un tiempo prolongado.
- Una segunda de "abandono" en la que son conducidos desde los puestos de reunión a los de embarque, en grupos ordenados, donde acceden a los botes y balsas salvavidas.

Además de las situaciones usuales en tierra (retardo en el inicio de la evacuación, uso de los caminos conocidos, apreciables diferencias en las velocidades de desplazamiento, etc.), a bordo existen unas características especiales, que deben consideradas en el diseño, simulación y análisis de los planes de evacuación. Entre otras, podemos destacar:

— Distribución en planta compleja y desconocida.
— Movimientos de la plataforma.
— Personas de orígenes e idiomas muy diversos.

Para atender a esta situación, la OMI, además de la normativa clásica (fundamentalmente el reglamento del SEVIMAR) sobre medios de salvamento, en los últimos años ha desarrollado una serie de normativa sobre el proceso de evacuación dentro del buque en la que existen tres hitos importantes:

— La resolución 737, sobre ancho de escaleras.
— La circular 909 del MSC, con una guía inicial para el cálculo del tiempo de evacuación.
— La circular 1033 del MSC, en la que se mejora el método de la anterior y se planten los principios y datos básicos para el desarrollo de herramientas de análisis y simulación detallados.

Los distintos grupos de investigación que estudian el movimiento de las personas como peatones, tanto en situaciones de emergencia como de uso de distintos espacios han trabajado con muchos tipos de modelos, entre los que podemos destacar:

— Los macro-modelos de tipo hidráulico, en los que las personas se representan por grupos en los que la velocidad y flujo son función de la densidad, pudiendo estudiarse con herramientas relativamente simples, los puntos de formación de colas y el tiempo total de desplazamiento.
— Los micro-modelos de tipo celular, en los que el escenario de análisis se divide en una serie de celdas cuadradas iguales, que pueden estar: libres, ocupadas por una persona o bloqueadas por un obstáculo.

La forma de reacción de cada individuo se modela por medio de un "agente" que tiene en cuenta su comportamiento en función de sus objetivos (dirección de marcha) y del entorno que le rodea.

La interacción entre el comportamiento de todos los agentes da como resultado la simulación del movimiento de las personas en la situación analizada.

LOS DESARROLLOS SESAMO Y SIFBUP.

Dentro de la E.T.S.I.N, desde el año 1997 existe un grupo de I+D en Factores humanos a bordo. De su colaboración con distintas empresas del sector (especialmente Astilleros Españoles y en la actualidad Izar), han surgido una serie de proyectos de I+D que han dado como resultado un amplio conjunto de modelos y herramientas para la simulación de movimientos a bordo. Dentro de este trabajo, podemos destacar dos familias (la SESAMO y la SIFBUP) en las que se han desarrollado en el pasdo las siguientes herramientas:

— El Sésamo-P (preliminar). Método muy sencillo, que permite una valoración (muy rápida, con un cálculo manual) de un "segmento" del plan de evacuación de un buque.

— El Sésamo-M (MSC-c909). Se basa en la circular 909 y utiliza como base hojas de cálculo en Excel.
— El Sésamo-T (temporal). Es un refinamiento del M, que tiene en cuenta el cronograma (tiempos de paso) de los pasajeros en distintos puntos críticos.
— El Sésamo-S (simulación). Esta herramienta se base en el código de simulación de procesos discretos Arena e incluye una visualización del movimiento de los pax.

En la actualidad se han completado una serie de herramientas, basadas en aplicaciones informáticas propias, en las que se han cuidado especialmente los aspectos de ergonomía:

— El Sifbup-D, para el análisis simplificado según la circular 1033 , orientado a las fases de diseño inicial del buque.
— El Sifbup-S, una simulación digital orientada tanto al estudio de evacuaciones como de movimientos de grandes conjuntos de personas
— El Sifbup-S3D, para permitir ver los resultados de la anterior en 3 dimensiones en un "entorno virtual"
— El Sifbup-V, para analizar los procesos de carga y descarga de vehículos.

MODELO Y APLICACIÓN PARA SIMULACIÓN.

Entre todas las herramientas anteriores destaca el Sifbup-S, diseñado para la simulación en 2 dimensiones con un modelo celular con agentes, cumpliendo los principios del método avanzado de la circular 1033. El modelo se implementa sobre tres niveles:

— El estratégico, en el que se define el escenario y los objetivos globales de origen y destino.
— El táctico, en el que se completan las direcciones de movimiento para las distintas posiciones y rutas y se establecen los coeficientes de corrección para espacios especiales.
— El operativo en el que se materializa el comportamiento de los agentes con el análisis de las celdas próximas a través de dos matrices de visión y de operación.

Este modelo se ha implementado en una aplicación informática, desarrollada sobre Visual-Basic, modular e interconectable con las otras aplicaciones Sifbup, en la que se han desarrollado diversos métodos para la introducción de los datos y unas herramientas de postprocesado avanzadas que permiten:

— Una visión dinámica del proceso de evacuación tanto en su conjunto como en los detalles de cada persona, a través de una simbología dinámica muy potente.
— La salida de los resultados numéricos más significativos en forma de tablas y gráficos.

— La simulación aleatoria de un conjunto de casos, analizando estadísticamente sus resultados.

CONCLUSIONES.

Para cumplir con la evolución de la normativa de la OMI sobre evacuación en buques de pasaje, y que los diseñadores y operados cuenten con una serie de herramientas adecuadas, se necesitan distintos tipos de modelos y herramientas, siendo lo ideal que sean de tipo modular.

Para los primeros pasos del diseño lo ideal son los macro-modelos, pero para un análisis más detallados lo más adecuado son los micro-modelos basados en "agentes celulares". Las herramientas desarrolladas muestras la idoneidad de este enfoque, con aplicaciones de una gran potencia y versatilidad para el usuario.

INSTRUCTIONS FOR AUTHORS

http://www.jmr.unican.es

Description

Journal of Maritime Research (JMR) publishes original research papers in English analysing the maritime sector international, national, regional or local. JMR is published quarterly and the issues—whether ordinary or monographic—include both theoretical and empirical approaches to topics of current interest in line with the editorial aims and scope of the journal.

The objective of JMR is to contribute to the progress, development and diffusion of research on the maritime sector. The aim is to provide a multidisciplinary forum for studies of the sector from the perspective of all four of the following broad areas of scientific knowledge: experimental sciences, nautical sciences, engineering and social sciences.

The manuscripts presented must be unpublished works which have not been approved for publication in other journals. They must also fulfil all the requirements indicated in the 'Technical specifications' section. The quality of the papers is guaranteed by means of a process of blind review by two scientific referees and one linguistic reviewer. Although the journal is published in print format, the processes of submission and reception of manuscripts, as well as revision and correction of proofs are all done electronically.

The publication process

Submission and acceptance of manuscripts

Papers should be sent via the journal's web site at http://www.jmr.unican.es, following the guidelines indicated for the submission of manuscripts by authors. Submitting the manuscript involves sending electronically via the web site three different types of information: general information about the article and the authors, an abstract and the complete paper.

The general information about the article and the authors, as well as the acknowledgements, is to be introduced by means of an electronic form, in which the following data are requested:

- Title of the paper. Subtitle.
- Field of the manuscript presented (Experimental Sciences, Engineering, Nautical Sciences or Social Sciences) and sub-field.
- E-mail of the author to whom correspondence should be addressed.
- Personal data of each author including name, professional category or position, institution or organisation, postal address and e-mail.
- Acknowledgements, if included, should be no longer than 150 words without spaces between paragraphs.

The manuscripts submitted which are in line with the aims and scope of JMR will be submitted to a blind review process. The objective is to assess the scientific quality (two referees) and ensure that the text is linguistically acceptable (one reviewer). Only those works which are considered adequate from a scientific point of view will be reviewed linguistically. Manuscripts which do not pass the linguistic filter will be admitted with the condition that the author make linguistic and stylistic modifications as indicated.

Authors will be informed of the acceptance, rejection and/or modifications required no later than four months after the receipt of the manuscript. Once the paper has been accepted, authors can check on the status of their article via the web site. Any doubts or questions should be addressed to the Editor at jmr@unican.es

Copyright

After manuscripts have been definitively accepted, the authors must complete the copyright agreement assigning the copyright to JMR so that it can be published.

Proofs

Once the copyright transfer agreement has been completed, the Editors will assign the paper to an upcoming issue of JMR and proofs will be sent as a PDF file to the author who has corresponded with JMR throughout the reviewing process. The corrected proofs must be returned by e-mail to the Editor of JMR within 96 hours of receipt.

Reprints

Once the paper has been published, the authors will be sent a total of 12 free reprints, which will be sent the postal address of the corresponding author. Authors may also request, via the JMR web site http://www.jmr.unican.es, a maximum of 10 complete journals at 50% of the cover price.

Style and technical specifications

Manuscripts should be sent to JMR's web site in a format that is recognisable to Microsoft Word (.doc) in any of its versions for Windows. The maximum length of manuscripts is 23 double-spaced pages (approximately 7000 words) including the abstract, references and appendices. Manuscripts will be submitted using a specific application of the electronic form used to send personal data. The page layout should follow these guidelines:

- Size: DIN A4 (29 cm by 21 cm)
- Margins, 3 cm: top, bottom, left, and right.
- Font: Times New Roman, normal style, 12-point type.
- Double spacing should be used for all the paper except for the references which are to be single-spaced.
- Notes, when necessary, are to be placed at the end of the paper and numbered in their order of appearance in the text. Mathematical derivations should not be included in these endnotes.

The abstract is to be presented on one page and should include the following information:

- Title and subtitle of the paper
- Field and sub-field of the work presented.
- Abstract, which is to be no longer than 200 words, and should have no spaces between paragraphs.

- Key words (between 3 and 5) which will be used for computerised indexing of the work, in both Spanish and English.
- The complete work should be no longer than 23 pages (about 7000 words) and should be structured as is shown below.

The first page will contain the same information as the summary:

- Title of the paper, as specific and brief as possible, and subtitle if desired.
- Field and sub-field of the work presented.
- Abstract of 200 words.
- Key words.

The rest of the article:

- Introduction or Problem
- Methods
- Development (application and results)
- Conclusions
- Endnotes
- References. Only those included in the article in alphabetical order.
- Appendix containing a condensed version of the article in Spanish. This is to be 3 or at most 4 pages in length (approximately 1000-1200 words) with the following sections: abstract, methods and conclusions.

The body of the article is to be divided into sections (bold, upper-case), subsections (bold, italics) and optionally into sub-subsections (italics), none of which are to be numbered. Insert line spaces before and after the title of each section, subsection and sub-subsection. Symbols, units and other nomenclature should be in accordance with international standards.

References

The Harvard System is to be used, following the guidelines indicated below.

The way in which *bibliographic citations* are included in the text will depend on the context and the composition of the paragraph and will have one of the following forms:

- One author: Farthing (1987); (Farthing, 1987); (Farthing, 1987 pp. 182-5)
- Several authors: Goodwin and Kemp (1979); Ihere, Gorton y Sandevar (1984); Ihere et al.(1984); (Ihere et al., 1984)

The *bibliographic references* are to be arranged in alphabetical order (and chronologically in the case of several works by the same author), as is indicated in the following examples:

Books

Farthing, B. (1987) *International Shipping.* London: Lloyd´s of London Press Ltd.

Chapters of books

Bantz, C.R. (1995): Social dimensions of software development. In: Anderson, J.A. ed. *Annual review of software management and development*. Newbury Park, CA: Sage, 502-510.

Journal articles

Srivastava, S. K. and Ganapathy, C. (1997) Experimental investigations on loop-manoeuvre of underwater towed cable-array system. *Ocean Engineering* 25 (1), 85-102.

Conference papers and communications

Kroneberg, A. (1999) Preparing for the future by the use of scenarios: innovation shortsea shipping, *Proceedings of the 1st International Congress on Maritime Technological Innovations and Research,* 21-23 April, Barcelona, Spain, pp. 745-754.

Technical Reports

American Trucking Association (2000) *Motor Carrier Annual Report*. Alexandria, VA.

Doctoral theses

Aguter, A. (1995) *The linguistic significance of current British slang*. Thesis (PhD).Edinburgh University.

Patents

Philip Morris Inc., (1981). *Optical perforating apparatus and system.* European patent application 0021165 A1. 1981-01-07.

Web pages and electronic books

Holland, M. (2003). *Guide to citing Internet sources* [online]. Poole,
Bournemouth University. Available from:
http://www.bournemouth.ac.uk/library/using/guide_to_citing_internet_sourc.html
[Accessed 1 November 2003]

Electronic journals

Storchmann, K.H. (2001) The impact of fuel taxes on public transport — an empirical assessment for Germany. *Transport Policy* [online], 8 (1), pp. 19-28 . Available from:
http://www.sciencedirect.com/science/journal/0967070X
[Accessed 3 November 2003]

Equations, tables, Illustrations.

Equations are to be written with the Microsoft Word Equation Editor using right-justified alignment. They should be numbered consecutively using Arabic numerals within parentheses.

Tables should be inserted in the appropriate point in the text using Microsoft Word. They should be numbered consecutively with Arabic numerals and a concise title should be centred at the top of the table. The source is to be indicated at the bottom on the left. Any symbols used should be explained.

Illustrations are to be inserted in the appropriate point in the text using Microsoft Word. All illustrations (graphs, diagrams, sketches, photographs, etc.) will be denominated generically Figures and are to be numbered consecutively using Arabic numerals with the title centred at the top. The source is to be indicated at the bottom on the left. Photographs must be in black and white with a quality of at least 300 ppp.